이학박사 학위논문

Synthesis and Application of Pyrimidine-Embedded Polyheterocycles

피리미딘이 포함된 다중고리골격 화합물들의 합성 및 응용

2016 년 8 월

서울대학교 대학원

화학부 유기화학전공

김 희 준

Abstract

Identification of new small-molecule modulators is an indispensable research objective in chemical biology and drug discovery. Organic small-molecule library is an inevitable resource in terms of performing the research. To satisfy the unmet need, diversity-oriented synthesis (DOS) has been emerged to maximize skeletal and stereo-chemical diversity of small-molecule library that have high potential to find various functional molecules. On the continuation of DOS strategy research, since 2006 privileged substructure-based DOS (pDOS) strategy has been developed to synthesize privileged structure-containing polyheterocycles with high biological relevancy. Privileged structure is defined as a single molecular framework able to provide high-affinity ligands for more than one type of receptors. Thus, privileged structural motifs have been frequently observed in bioactive natural products and synthetic medicines. Based on the empirical definition, we hypothesized that privileged substructure containing unique and diverse molecular framework serves powerful chemical tools for the identification of new small-molecule modulators. As the beginning of pDOS study, benzopyran embedded pDOS pathway was developed. For last decade, novel bioactive small-molecules have been discovered from the benzopyran pDOS library through a variety of screening campaigns and target identifications. We confirmed the high efficiency of pDOS strategy for identifying new bioactive compounds through the incredible results. In this thesis, development of new pDOS pathways for constructing pyrimidine-containing unprecedented polyheterocycles and their bio-applications toward unexplored biological systems are described.

In **Part 1**, new synthetic pathways of pyrimidine-containing unprecedented polyheterocycles are introduced. A new diversity-oriented synthesis pathway for the fabrication of a pyrimidine-embedded polyheterocycles library was developed for potential interactions with diverse biopolymers. Five different pyrimidine-embedded molecular frameworks were synthesized from highly

functionalized *ortho*-alkynylpyrimidine carbaldehydes by a silver- or iodine-mediated tandem cyclization strategy. The resulting polyheterocycles possess diverse fused ring sizes and positions with potential functionalities for further modification.

In **Part 2**, discovery of a new small-molecule to control cellular lipid droplets (LDs) using pyrmidine-containing new aza-tricyclic compounds is described. A series of pyrimidine-embedded polyheterocycles was synthesized using silver-promoted cascade cyclization in a facile manner. The resulting core skeletons containing a unique aza-tricyclic framework allowed for diverse display of non-covalent interacting elements, which probably serve as essentials for perturbing specific non-covalent interactions between various biopolymers. A new small-molecule that decreases the LDs without autophagic activity was discovered by using the unique chemical library.

In **Part 3**, discovery of new fluorophore and its bioapplication are described. A new fluorescent core skeleton containing pyrazolo[1,5-*a*]pyridine-fused pyrimidine, named Fluoremidine (FD), was discovered. FD analogues were prepared via a one-pot silver-catalyzed domino cyclization. An *N*,*N*-dimethylamino group at the R^1- and R^2-positions plays important roles in controlling fluorescent brightness and emission wavelength. An *N*-acetyl group at the R^3 position contributes to red shifting of the emission wavelength. FD shows excellent solvatochromism with turn-on fluorescence in the lipophilic environment, which was utilized to design a fluorescent probe, FD13, for visualizing lipid droplets in living cells.

Keywords: pyrimidine, pDOS, polyheterocycle, non-covalent interaction, phenotype-based screening, lipid droplet modulator, fluorophore, lipid droplet sensor.

Student number: 2011-30904

Table of Contents

Part 1. Privileged Substructure-Based Diversity-Oriented Synthesis Pathway for Diverse Pyrimidine-Embedded Polyheterocycles

Org. Lett. **2013**, *15*, 5814–5817.

1-1. Introduction

Facile fabrication of a structurally diverse small-molecule library plays a crucial role in drug discovery and chemical biology.[1] In particular, the unbiased collection of drug-like small molecules has become an inevitable resource[2] because it can provide a unique opportunity for the identification of novel chemical entities from phenotype-based screening, which is the leading approach for the development of first-in-class drugs.[3] Therefore, an efficient strategy for the expansion of molecular diversity is in great demand in the scientific community. Among the various approaches, diversity-oriented synthesis (DOS)[4] access the unexplored molecular frameworks with maximum structural and stereochemical diversity.[5] Along with this endeavor, we proposed a privileged substructure-based DOS (pDOS) approach for the efficient generation of distinct polyheterocyclic core skeletons embedded with privileged substructures.[6] We believe that the reconstruction of polyheterocycles decorated around privileged substructures harnesses the high biological relevance of the newly constructed molecular frameworks, which has been demonstrated by the discovery of novel bioactive compounds in diverse therapeutic fields such as cancer,[7] osteoporosis,[8] plays an indispensable role to inflammation,[9] and type II diabetes[10] from a benzopyran-embedded pDOS library. As a continuation of our work on the development of novel pDOS pathways, we choose pyrimidine as the key privileged substructure. Pyrimidine has been extensively explored in synthetic and medicinal chemistry owing to its unique mimicking of nucleosides and hydrogen bonding ability with nucleic acids in biological systems. In fact,

the pyrimidine ring system is common in various bioactive small molecules such as anti-bacterial agents,[11] cannabinoid receptor 2 agonists,[12] adenosine A3 receptor antagonists,[13] and dipeptidyl peptidase-4 inhibitors[14] (**Figure 1-1**).

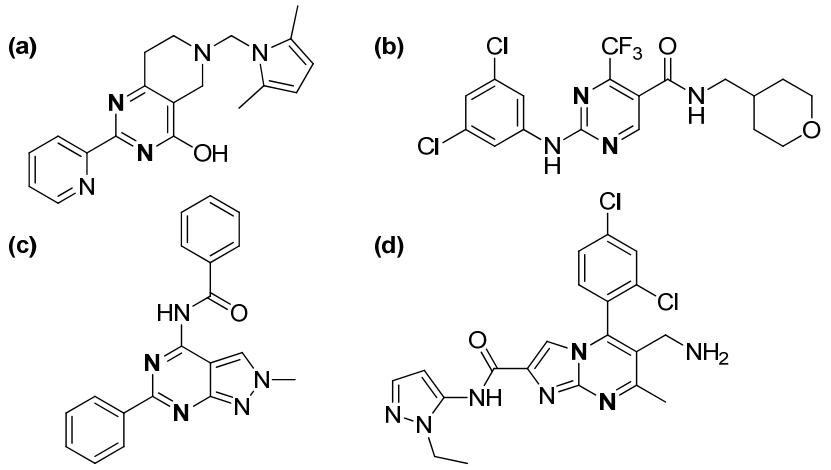

Figure 1-1. Pyrimidine-containing known bioactive small molecules (a) Bacterial protein synthesis inhibitor. (b) Cannabinoid receptor 2 selective agonist. (c) Adenosine A_3 receptor antagonist. (d) Dipeptidiyl peptidase-4 (DPP4) inhibitor.

Many Pyrimidine-containing polyheterocycles might function as small-molecule modulators that perturb unexplored biological systems, particularly protein-protein interaction. Although a vast number of pyrimidine-containing bioactive compounds are known, their structural frameworks are mainly limited to monocyclic or bicyclic skeletons, probably because of the usual design strategy of pyrimidine as nucleoside analogs. Herein, we describe a new pDOS strategy for the systematic fabrication of polyheterocyclic molecular frameworks around a pyrimidine ring to expand the molecular diversity beyond monocyclic and bicyclic pyrimidine skeletons.

1-2. Results and discussion

For the efficient fabrication of pyrimidine-containing polyheterocycles, we first designed and synthesized a key substrate, *ortho*-alkynylpyrimidine carbaldehyde **1**,[15] which can be easily converted to imines or hydrazones, followed by coinage-metal-catalyzed or halogen-promoted 6-*endo* cyclization process to afford bicyclic iminiums[16–19] as the key intermediate.

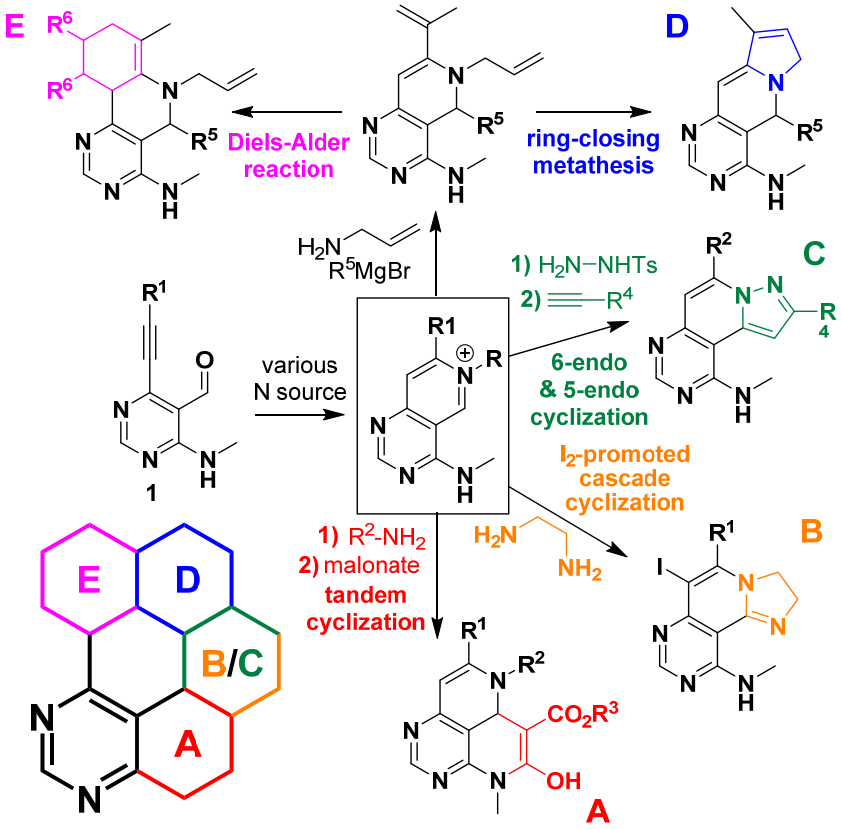

Figure 1-2. Diversity-oriented synthesis pathways for preparation of pyrimidine-embedded polyheterocycles.

This key intermediate can be transformed into five different pyrimidine-containing polyheterocycles (A–E) under different reaction conditions (**Figure 1-2**). Malonates (scaffold A), diaminoalkanes (scaffold B), and terminal alkynes (scaffold C) were separately reacted with each iminium intermediate, which allows the subsequent tandem cyclization via amide formation, iodine-promoted

cyclization,[18] and Ag-mediated 5-*endo* cyclization,[19] respectively. In order to obtain different orientations and ring topology of the pyrimidine-containing polyheterocycles (scaffolds D and E) obtained from the above-mentioned scaffolds, we introduced R^1 and R^2 substituents as the biasing elements in the bicyclic intermediates prepared via Ag-catalyzed 6-*endo* cyclization followed by the nucleophilic addition of Grignard reagents. The resulting bicyclic intermediates can be transformed to scaffolds D and E via ring-closing metathesis using second-generation Grubb's catalyst and Diels-Alder reaction with dienophiles, respectively.

Table 1-1. Exploration of Scaffold A[a]

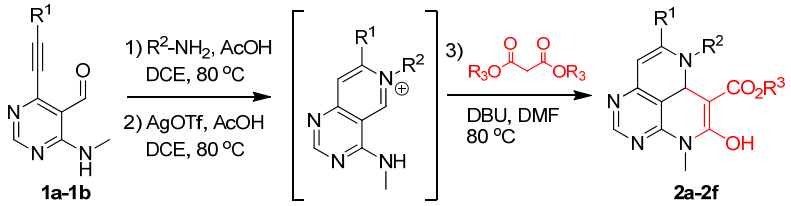

product	R^1	R^2	R^3	yield (%)[b]
2a	phenyl	4-MeO-Ph	ethyl	74
2b	phenyl	4-MeO-Ph	methyl	70
2c	phenyl	2-methoxyethyl	methyl	97
2d	*n*-propyl	4-MeO-Ph	ethyl	84
2e	*n*-propyl	4-MeO-Ph	methyl	83
2f	*n*-propyl	2-methoxyethyl	methyl	77

[a]See the Supporting Information for detailed experimental procedures. [b]Isolated two-step yields from imines (**1d**–**1g**).

For the preparation of scaffold A, key substrates **1a** and **1b** were reacted with various amines to afford the *ortho*-alkynylpyrimidyl aldimines, followed by Ag-mediated 6-*endo* cyclization of the imines with the internal alkyne to generate the pyridinium intermediates.[16] Next, the nucleophilic addition of dialkylmalonates with the pyridinium intermediate and subsequent lactamization of the esters with the methylamine moiety at the C-4 position of the pyrimidine afforded the pyrimidine-containing tricyclic cores (**Table 1-1**).

The resulting tricyclic cores spontaneously underwent keto-enol tautomerism to afford **2a**–**2f** because of the conjugation effect from ester group and the additional stabilization by intramolecular hydrogen bonding. The resulting hydroxyl group may be more useful than an amide group for rapid expansion of molecular diversity. This tandem cyclization procedure afforded six tricyclic compounds **2a**–**2f** with different substituents in good to excellent yields.

Scheme 1-1. Exploration of Scaffold B[a,b]

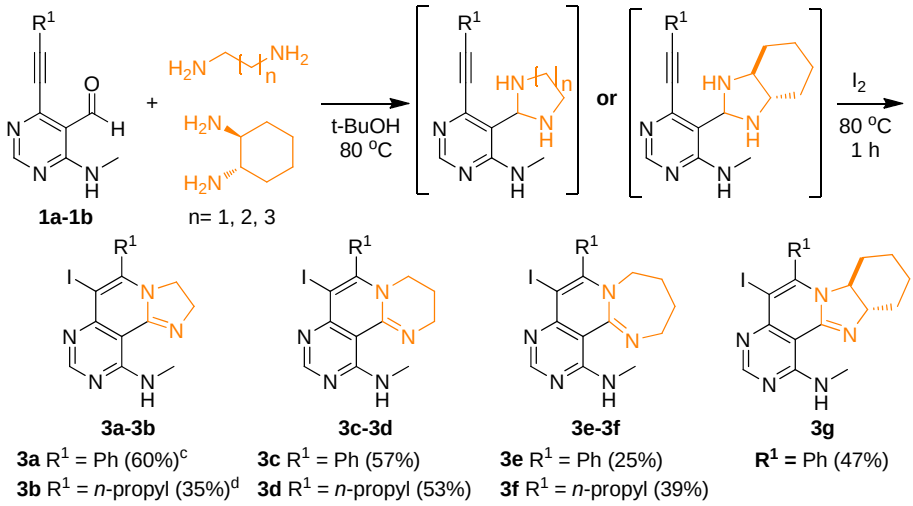

3a R^1 = Ph (60%)[c] **3c** R^1 = Ph (57%) **3e** R^1 = Ph (25%) **R^1 =** Ph (47%)

3b R^1 = *n*-propyl (35%)[d] **3d** R^1 = *n*-propyl (53%) **3f** R^1 = *n*-propyl (39%)

[a]See the Supporting Information for detailed experimental procedures. [b]Isolated yields.
[c]Fully aromatized product **3h** was obtained in 10% yield. [d]Fully aromatized product **3i** was obatined as 34% yield.

The reactions of electrophilic *ortho*-alkynylaldehyde **1a** and **1b** with diaminoalkanes afforded the cyclic aminal intermediates,[17] which were transformed into scaffold B via iodine-mediated tandem cyclization (**Scheme 1-1**).[18] In this one-pot procedure, iodine not only functioned as the oxidizing agent for the imidazolidine ring formation, but also activated the internal alkyne for the 6-*endo* cyclization process. Pyrimidine-containing polyhetero-cycles (**3a**–**3g**, scaffold B) with different ring sizes and additional fused rings were simply prepared by changing the length or the substituents of the diaminoalkanes (**Scheme 1-1**). To further expand the molecular diversity, the vinyl iodide group in scaffold B can be functionalized via palladium-mediated cross-coupling reactions, which has not been explored in this study.

Table 1-2. Exploration of Scaffold C[a]

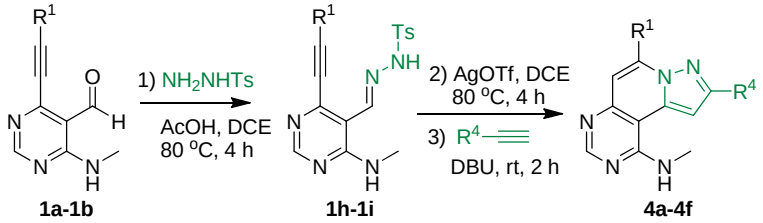

1a-1b **1h-1i** **4a-4f**

Product	R^1	R^4	yield(%)[b]
4a	phenyl	phenyl	64
4b	phenyl	cyclopropyl	72
4c	phenyl	1-methylethenyl	51
4d	*n*-propyl	phenyl	70
4e	*n*-propyl	cyclopropyl	69
4f	*n*-propyl	1-methylethenyl	69

[a]See the Supporting Information for detailed experimental procedures. [b]Isolated two-step yields from hydrazones.

For the preparation of scaffold C, a tosylhydrazine group was introduced to *ortho*-alkynylaldehyde in **1a** and **1b**, and the resulting hydrazone intermediates **1h**–**1i** were converted to pyrazolopyrido[4,3-*d*]pyrimidines via Ag-catalyzed 6-*endo* tandem cyclization with the internal alkyne to afford isoquinolinium intermediates, followed by 1,8-diazabicyclo[5.4.0]undec-7-ene (DBU)-catalyzed nucleophilic addition of R_4-containing terminal alkynes. Subsequent intramolecular 5-*endo* cyclization and aromatization[19] afforded scaffold C (**Table 1-2**). The substrate scope of this cascade cyclization was demonstrated to be very diverse because it could accommodate alkyl, aryl, and vinyl acetylenes at the R^4 position to afford pyrimidine-containing tricycles **4a**–**4f** in moderate to good yields (**Table 1-2**).

Table 1-3. Exploration of Scaffold D and E[a]

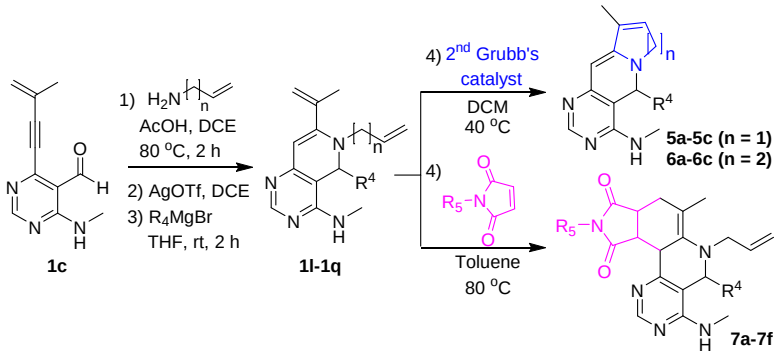

product	SM[b]	n	R^4	R^5	yield(%)[c]
5a	**1l**	1	methyl	–	50
5b	**1m**	1	phenyl	—	48
5c	**1n**	1	4-MeO-Ph	–	48
6a	**1o**	2	methyl	–	48
6b	**1p**	2	phenyl	–	60
6c	**1q**	2	4-MeO-Ph	–	52
7a	**1l**	1	methyl	phenyl	36
7b	**1m**	1	phenyl	phenyl	32
7c	**1n**	1	4-MeO-Ph	phenyl	42
7d	**1l**	1	methyl	4-MeO-Ph	34
7e	**1m**	1	phenyl	4-MeO-Ph	36
7f	**1n**	1	4-MeO-Ph	4-MeO-Ph	32

[a]See the Supporting Information for detailed experimental procedures.
[b]SM stands for starting materials for olefin metathesis and Diels-Alder reaction. SM was prepared from imines (**1j–1k)** from **1c** via the first synthetic step. [c]Isolated yields from **1l–1q**.

For the synthesis of scaffolds D and E, a vinyl group at the R^1 position of key substrate **1c** was necessary; therefore, the key intermediates **1l–1q** were prepared by the reaction of **1c** with allylic or homoallylic amines to afford *ortho*-alkynyl aldimines (**1j–1k**), which were diversified by nucleophilic addition with three different Grignard reagents. Using ring-closing metathesis (RCM) with second-generation Grubb's catalyst, intermediates **1l–1q** were converted to scaffold D, **5a–5c** and **6a–6c**, fused with 5- and 6-memeberd rings, respectively. Diels-Alder reaction of the diene moiety in intermediates **1l–1n**

with substituted maleimides afforded scaffold E with pyrimidine-containing tetracycles **7a**–**7f** (**Table 1-3**).

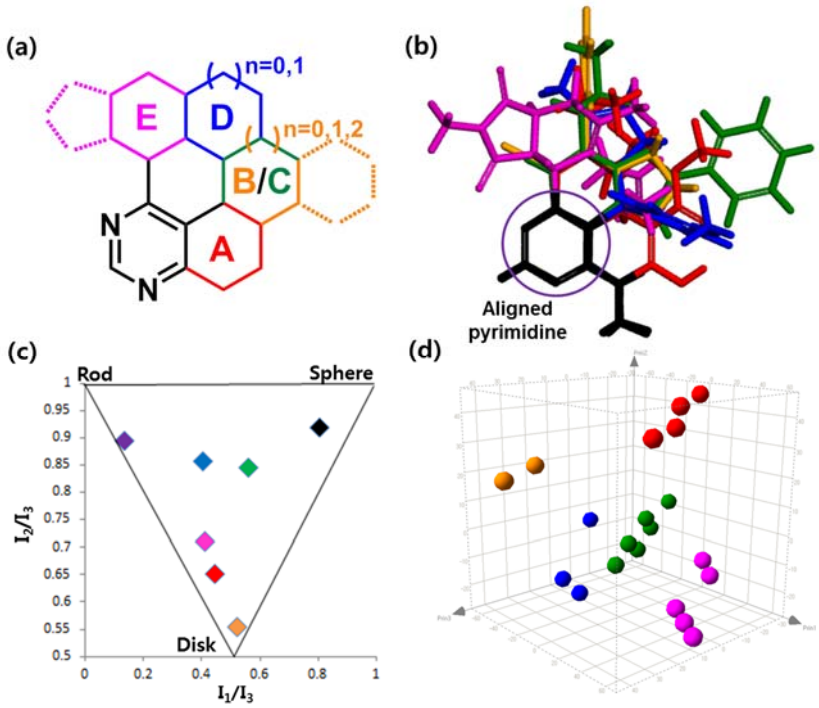

Figure 1-3. a) Schematic figure for spatial coverage around pyrimidine substructure with five unique core skeletons in different colors; b) overlay of energy-minimized conformers of five core skeletons with the alignment of pyrimidine substructure in their own color codes; c) PMI plot depicting five core skeletons in their own color codes along with intermediate 1a and 1l in violet and black colors, respectively; d) PCA of five different pyrimidine-containing polyheterocycles. Compounds from each skeleton were differently color-coded.

As stated earlier, we aimed to construct molecular diversity using pDOS strategy, particularly with diverse polyheterocycles around a pyrimidine substructure, which is schematically illustrated in Figure 3a. After fabricating five unique core skeletons, we clearly demonstrated the diverse orientation of each polyheterocycles with wide spatial coverage by *in silico* generation of the energy-minimized conformers and overlaying them in a three-dimensional (3D) space with the alignment of pyrimidine substructure (**Figure 1-3b**). We also performed the principal moment of inertia (PMI) analysis[20] to capture the shape-based distribution of small molecules as dots in an isosceles triangle defined by vertices (0,1), (0.5,0.5), and (1,1), which correspond to the rod, disc, and sphere

shapes, respectively. As shown in **Figure 1-3c**, five representative scaffolds and two key intermediates were dispersed in the PMI plot, indicating excellent diversity in the shape of each scaffold. Along with shape differences, we clearly visualized that the resulting five color-coded scaffolds were widely distributed in a 3D chemical space with maximum molecular diversity calculated by using unbiased molecular descriptors and analyzed by principal component analysis (PCA, **Figure 1-3d**). The molecular diversity of five different scaffolds was differentiated mainly by the topological polar surface area, van der Waals (VDW) surface area, and VDW volume.

1-3. Conclusion

We have developed a new pDOS strategy with pyrimidine as the privileged substructure. The resulting five scaffolds consist of unique pyrimidine-embedded polyheterocycles fused with different ring sizes and orientation. Scaffolds A–C were synthesized by Ag- or iodine-mediated 6-*endo* cyclization followed by tandem cyclization with different reactants. Scaffolds D and E were prepared from bicyclic intermediates **1l**–**1q** followed by RCM or Diels-Alder reaction. The molecular diversity of each scaffold was successfully confirmed by a series of computational studies, structural alignment of energy-minimized 3D conformers, shape diversity studies using PMI analysis, and *in silico* PCA analysis. This pDOS strategy allows the fabrication of unique polyheterocycles along with a wide spatial coverage around pyrimidine as the privileged substructure that ensures high potential for molecular interactions with biopolymers in a selective and specific manner.

1-4. Supporting information

I. General Experimental Information

All commercially available reagents and solvents were used without further purification unless noted otherwise. All the solvents were purchased from commercial venders. ^{1}H and ^{13}C NMR spectra were obtained using Agilent 400–MR DD2 (Agilent, USA) or Varian Inova–500 (Varian Assoc., Palo Alto, USA) instruments. Chemical shifts were reported in ppm from tetramethylsilane (TMS) as internal standard or the residual solvent peak ($CDCl_3$; ^{1}H: δ = 7.26 ppm; ^{13}C: δ = 77.23 ppm). Multiplicity was indicated as follows: s (singlet), d (doublet), t (triplet), q (quartet), m (multiplet), dd (doublet of doublet), dt (doublet of triplet), td (triplet of doublet), brs (broad singlet), and so on. Coupling constants are reported in hertz. Mass spectrometric analysis was performed using a Finnigan Surveyor MSQ Plus LC/MS (Thermo) with electrospray ionization (ESI). The high resolution mass spectrometric analyses were conducted at the Mass Spectrometry Laboratory of Seoul National University using mass spectrometer by direct injection for fast atomic bombardment (FAB). The conversion of starting materials was monitored by thin–layer chromatography (TLC) using pre–coated glass–backed plates (silica gel 60; F_{254} = 0.25 mm), and the reaction components were visualized by observation under UV light (254 and 365 nm) or by treatment of TLC plates with visualizing agents such as $KMnO_4$, phosphomolybdic acid, and ninhydrin followed by heating. Products were purified by flash column chromatography on silica gel (230–400 mesh) using a mixture of EtOAc/hexane or MeOH/CH_2Cl_2 as eluents. The energy–minimized structures of molecules were obtained by V_{conf} Interface v2.0 using default parameters and visualized by Discovery Studio 3.5.

II. General Experimental Procedures and Spectroscopic Data

1. General synthetic procedure for compounds 1a–1c

To the anhydrous *N*,*N*-dimethyformamide (DMF) solution (60.0 mL) of 4-chloro-6-(methylamino)pyrimidine-5-carbaldehyde (1.0 g), $Pd(PPh_3)_2Cl_2$ (5 mol%), and CuI (20 mol%), terminal alkynes (2.0 equiv.) and triethylamine (1.6 mL, 2.0 equiv.) were added under argon atmosphere. After being stirred at room temperature for 4 h, the reaction mixture was quenched with deionized water (200 mL). The resultant was extracted with EtOAc (100 mL × 3) and combined organic layer was washed with brine (100 mL). After drying with anhydrous Na_2SO_4(s), the solvent was removed under the reduced pressure. The residue was purified by silica-gel flash column chromatography to obtain **1a–1c**.

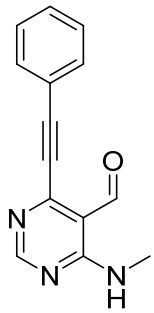

Compound 1a: Yield: 79.5%; ^{1}H NMR (400 MHz, $CDCl_3$) δ 10.55 (s, 1H), 8.91 (brs, 1H), 8.67 (s, 1H), 7.65–7.62 (m, 2H), 7.47–7.38 (m, 3H), 3.14 (d, J = 5.2 Hz, 3H); ^{13}C NMR (100 MHz, $CDCl_3$) δ 192.5, 161.5, 160.4, 155.0, 132.4, 130.3, 128.6, 120.6, 98.3, 83.8, 27.4; LRMS (ESI) *m/z* calcd for $C_{14}H_{11}N_3O$ $[M+H]^+$: 238.09; Found: 237.99.

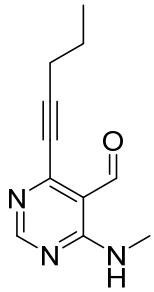

Compound 1b: Yield: 80.2%; ^{1}H NMR (400 MHz, $CDCl_3$) δ 10.42 (s, 1H), 8.86 (s 1H), 8.60 (s, 1H), 3.11 (d, J = 5.2 Hz, 3H), 2.50 (t, J = 6.8 Hz, 2H), 1.72–1.66 (m, 2H), 1.07 (t, J = 7.2 Hz, 3H); ^{13}C NMR (100 MHz, $CDCl_3$) δ 192.9, 161.4, 160.4, 155.5, 111.9, 101.3, 76.0, 27.3, 21.5, 21.4, 13.6; LRMS (ESI) *m/z* calcd for $C_{11}H_{13}N_3O$ $[M+H]^+$: 204.11; Found: 204.02.

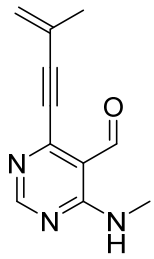

Compound 1c: Yield: 30.0%; ^{1}H NMR (400 MHz, $CDCl_3$) δ 10.42 (s, 1H), 8.88 (brs, 1H), 8.63 (s, 1H), 5.64–5.63 (m, 1H), 5.54–5.53 (m, 1H), 3.13 (d, *J* = 4.8 Hz, 3H), 2.03 (t, *J* = 5.6 Hz, 3H); ^{13}C NMR (100 MHz, $CDCl_3$) δ 192.6, 161.4, 160.4, 154.9, 126.6, 125.2, 111.8, 99.2, 82.6, 27.4, 22.6; LRMS (ESI) *m/z* calcd for $C_{11}H_{11}N_3O$ $[M+H]^+$: 202.09; Found: 201.84.

2. General synthetic procedure for compounds 1d–1k

To a dichloroethane (DCE) solution of **1a–1c** (3.0 mmol), amine (5.0 equiv.) or tosylhydrazine (5.0 equiv.), Na_2SO_4, and AcOH were added. After stirring at 80 °C until starting materials were consumed, the reaction mixture was quenched with deionized water. The resultant was extracted with dichloromethane (DCM) twice and dried with anhydrous Na_2SO_4(s). After the solvent was removed under the reduced pressure, the residue was purified by silica-gel flash column chromatography to obtain **1d**–**1k**.

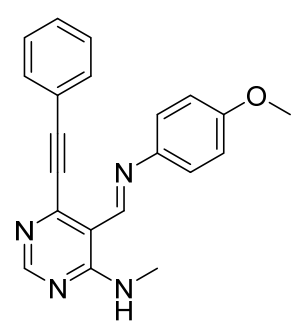

Compound 1d: Yield: 84%; ^{1}H NMR (400 MHz, $CDCl_3$) δ 10.12 (s, 1H), 9.18 (s, 1H), 8.58 (s, 1H), 7.60 (d, *J* = 6.8 Hz, 2H), 7.40 (t, *J* = 7.6 Hz, 3H), 7.26 (d, *J* = 8.0 Hz, 2H), 6.97 (d, *J* = 8.4 Hz, 2H), 3.85 (s, 3H), 3.18 (d, *J* = 4.8 Hz, 3H); ^{13}C NMR (100 MHz, $CDCl_3$) δ 160.2, 158.78, 158.61, 156.3, 150.5, 143.5, 132.1, 129.8, 128.5, 122.3, 121.3, 114.6, 112.1, 97.0, 85.1, 55.5, 27.5; LRMS (ESI) *m/z* calcd for $C_{21}H_{18}N_4O$ $[M+H]^+$: 343.15; Found: 343.00.

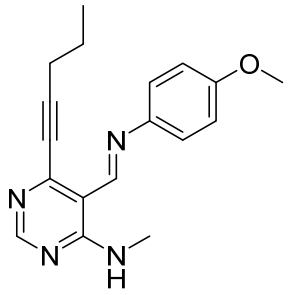

Compound 1e: Yield: 68%; ^{1}H NMR (400 MHz, $CDCl_3$) δ 10.06 (d, *J* = 4.4 Hz, 1H), 9.08 (s, 1H), 8.52 (s, 1H), 7.21 (d, *J* = 7.2 Hz, 2H), 6.95 (d, *J* = 6.8 Hz, 2H), 3.85 (s, 3H), 3.15 (d, *J* = 4.8 Hz, 3H), 2.49 (t, *J* = 6.8 Hz, 3H), 1.73–1.64 (m, 2H), 1.07 (t, *J* = 7.2 Hz, 3H); ^{13}C NMR (100 MHz, $CDCl_3$) δ 160.2, 158.6, 158.5, 156.8, 151.2, 143.6, 122.3, 114.5, 111.9, 99.6, 76.8, 55.5, 27.4, 21.6, 21.5, 13.6; LRMS (ESI) *m/z* calcd for $C_{18}H_{20}N_4O$ $[M+H]^+$: 309.16; Found: 309.06.

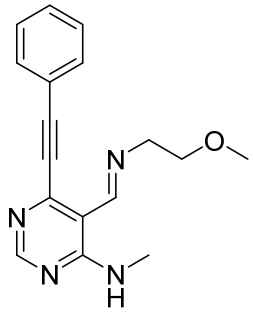

Compound 1f: Yield: 84.6%; ^{1}H NMR (500 MHz, $CDCl_3$) δ 9.98 (brs, 1H), 8.97 (s, 1H), 8.55 (s, 1H), 7.62–7.60 (m, 2H), 7.42–7.36 (m, 3H), 3.84 (t, *J* = 5.2 Hz, 2H), 3.71 (t, *J* = 5.2 Hz, 2H), 3.4 (s, 3H), 3.11 (d, *J* = 4.8 Hz, 3H); ^{13}C NMR (125 MHz, $CDCl_3$) δ 161.8, 160.5, 158.4, 150.4, 111.3, 99.0, 77.1, 72.2, 61.0, 58.9, 27.2, 21.6, 21.5, 13.6; LRMS (ESI) *m/z* calcd for $C_{17}H_{18}N_3O$ $[M+H]^+$: 295.15; Found: 295.00.

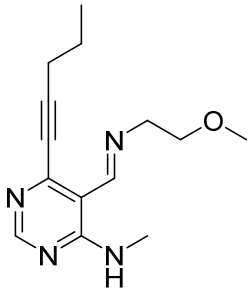

Compound 1g: Yield: 92.3%; ^{1}H NMR (500 MHz, $CDCl_3$) δ 9.91 (brs, 1H), 8.86 (s, 1H), 8.48 (s, 1H), 3.80 (t, *J* = 5.0 Hz, 2H), 3.69 (t, *J* = 5.0 Hz, 2H), 3.39 (s, 3H), 3.08 (d, *J* = 4.5 Hz, 3H), 2.47 (t, *J* = 7.0 Hz, 2H), 1.71–1.66 (m, 2H), 1.07 (t, *J* = 7.5 Hz, 3H); ^{13}C NMR (125 MHZ, $CDCl_3$) δ 161.8, 160.5, 158.4, 150.4, 111.3, 99.0, 77.1, 72.2, 61.0, 58.9, 27.2, 21.6, 21.5, 13.6; LRMS (ESI) *m/z* calcd for $C_{14}H_{20}N_4O$ $[M+H]^+$: 261.16; Found: 261.05.

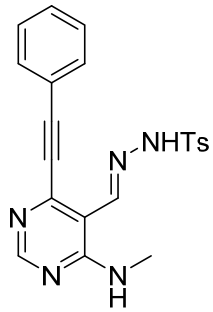

Compound 1h: Yield: 60.3%; ^{1}H NMR (400 MHz, $CDCl_3$) δ 8.45 (s, 1H), 8.38 (s, 2H), 7.83 (d, *J* = 6.8 Hz, 2H), 7.30 (d, *J* = 7.6 Hz, 2H), 7.20 (t, *J* = 6.8 Hz, 1H), 7.12–7.06 (m, 4H), 3.04 (d, *J* = 5.2 Hz, 3H), 2.38 (s, 3H); ^{13}C NMR (100 MHz, $CDCl_3$) δ 158.8, 157.5, 147.9, 145.5, 144.6, 135.1, 131.7, 129.8, 129.7, 128.1, 127.8, 120.5, 110.2, 97.7, 84.2, 27.7, 21.6; LRMS (ESI) *m/z* calcd for $C_{21}H_{19}N_5O_2S$ $[M+H]^+$: 406.13; Found: 405.93.

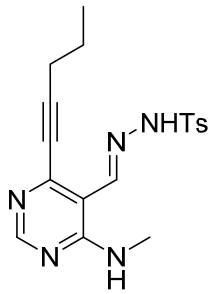

Compound 1i: Yield: 37.5%; ^{1}H NMR (400 MHz, $CDCl_3$) δ 9.67 (brs, 1H), 8.46–8.43 (s, 2H), 8.42 (s, 1H), 7.81 (d, *J* = 6.8 Hz, 2H), 7.33 (d, *J* = 7.8 Hz, 2H), 7.38 (t, *J* = 7.6 Hz, 1H), 3.08 (d, *J* = 5.2 Hz, 3H), 2.43 (s, 3H), 2.18 (t, *J* = 7.2 Hz, 2H), 1.46–1.37(m, 2H), 0.84 (t, *J* = 7.2 Hz, 3H); ^{13}C NMR (100 MHz, $CDCl_3$) δ 159.0, 157.7, 149.0, 145.9, 144.7, 135.0, 129.8, 127.7, 109.9, 100.2, 76.4, 27.7, 21.6, 21.4, 21.3, 13.5; LRMS (ESI) *m/z* calcd for $C_{18}H_{21}N_5O_2S$ $[M+H]^+$: 372.14; Found: 371.93.

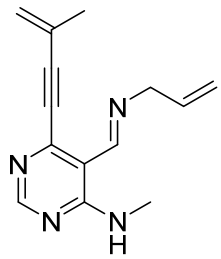

Compound 1j: Yield: 57%; ^{1}H NMR (400 MHz, $CDCl_3$) δ 9.97 (brs, 1H), 8.83 (s, 1H), 8.51 (s, 1H), 6.09-6.00 (m, 1H), 5.58-5.57 (m, 1H), 5.47-5.46 (m, 1H), 5.25-5.18 (m, 2H), 4.29-4.26 (m, 2H), 3.10 (d, *J* = 4.8 Hz, 3H), 2.02 (d, *J* = 0.8 Hz, 3H); ^{13}C NMR (100 MHz, $CDCl_3$) δ 160.7, 160.4, 158.4, 149.8, 135.3, 125.6, 125.2, 116.3, 111.4, 97.5, 83.8, 63.3, 27.3, 22.8; LRMS (ESI) *m/z* calcd for $C_{14}H_{16}N_4O$ $[M+H]^+$: 241.14; Found: 240.91.

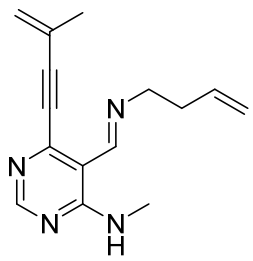

Compound 1k: Yield: 62%; ^{1}H NMR (400 MHz, $CDCl_3$) δ 9.99 (s, 1H), 8.79 (t, *J* = 2.0 Hz, 1H), 8.50 (s, 1H), 5.89-5.82 (m, 1H), 5.57 (d, *J* = 0.8 Hz, 1H), 5.47-5.45 (m, 1H), 5.14-5.08 (m, 2H), 3.71-3.68 (m, 2H), 3.08 (d, *J* = 4.4 Hz, 3H), 2.48-2.43 (m, 2H), 2.02 (d, *J* = 0.8 Hz, 3H); ^{13}C NMR (100 MHz, $CDCl_3$) δ 160.5, 159.9, 158.4, 149.6, 135.9, 125.7, 125.1, 116.4, 111.5, 97.5, 84.0, 60.8, 35.4, 27.2, 22.9; LRMS (ESI) *m/z* calcd for $C_{15}H_{18}N_4$ $[M+H]^+$: 255.15; Found: 255.06.

3. General synthetic procedure for compounds 1l–1q

To a DCE solution of 5-((allylimino)methyl)-*N*-methyl-6-(3-methylbut-3-en-1-yn-1-yl)pyrimidin-4-amine (0.4 mmol) or 5-((but-3-en-1-ylimino)methyl)-*N*-methyl-6-(3–methylbut-3-en-1-yn-1-yl)pyrimidin-4-amine (0.4 mmol), AgOTf (10 mol%) was added. After stirring at 80 ^{o}C for 2 h, the reaction mixture was filtered under Na_2SO_4 pad and washed with DCM. After the removal of solvent under the reduced pressure, anhydrous THF was added under argon atmosphere. Then, Grignard reagent was added and stirred at room temperature for 2 h. The reaction mixture was quenched with aqueous NH_4Cl solution and extracted twice with DCM. After drying with anhydrous Na_2SO_4(s), the solvent was removed under the reduced pressure. The residue was purified by silica-gel flash column chromatography to obtain **1l–1q**.

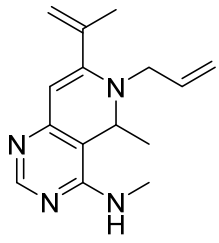

Compound 1l: Yield: 36%; ^{1}H NMR (400 MHz, $CDCl_3$) δ 8.37 (s, 1H), 5.72–5.65 (m, 1H), 5.64 (s, 1H), 5.30 (t, *J* = 2.0 Hz, 1H), 5.16 (t, *J* = 3.2 Hz, 1H), 5.12–5.10 (m, 1H), 5.08 (dd, *J* = 1.6 Hz, *J* = 1.2 Hz, 1H), 5.05 (dd, *J* = 1.2 Hz, *J* = 0.8 Hz, 1H), 4.53 (d, *J* = 4.8 Hz, 1H), 3.71–3.65 (m, 1H), 3.59–3.53 (m, 1H), 2.99 (d, *J* = 4.4 Hz, 3H), 1.90 (s, 3H), 1.11 (d, *J* = 6.8 Hz, 3H) ; ^{13}C NMR (100 MHz, $CDCl_3$) δ 157.7, 156.8, 154.8, 153.6, 140.8, 135.2, 117.8,

117.1, 104.6, 102.1, 54.1, 49.1, 28.1, 21.2, 17.1; LRMS (ESI) *m/z* calcd for $C_{15}H_{20}N_4$ $[M+H]^+$: 257.11; Found: 257.07.

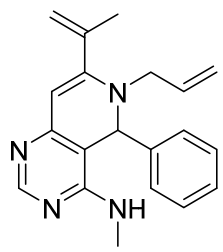

Compound 1m: Yield: 42%; ^{1}H NMR (300 MHz, $CDCl_3$) δ 8.48 (s, 1H), 7.31 (m, 5H), 5.86–5.73 (m, 1H), 5.31 (s, 1H), 5.25–5.21 (m, 2H), 5.13 (s, 1H), 4.21 (d, *J* = 3.9 Hz, 1H), 3.83 (dd, *J* = 5.1 Hz, *J* = 5.1 Hz, 1H), 3.60 (dd, *J* = 6.6 Hz, *J* = 6.6 Hz, 1H), 2.94 (d, *J* = 4.8 Hz, 3H), 1.84 (s, 3H); ^{13}C NMR (100 MHz, $CDCl_3$) δ 157.4, 156.9, 153.9, 152.7, 134.4, 128.8, 128.4, 126.7, 118.9, 118.2, 117.9, 66.6, 61.6, 56.9, 53.5, 47.1, 28.2, 21.1; LRMS (ESI) *m/z* calcd for $C_{20}H_{22}N_4$ $[M+H]^+$: 319.18; Found: 319.12.

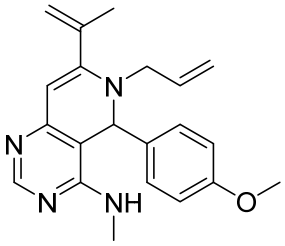

Compound 1n: Yield: 38%; ^{1}H NMR (400 MHz, $CDCl_3$) δ 8.43 (s, 1H), 7.21 (d, *J* = 4.8 Hz, 2H), 6.79 (d, *J* = 3.2 Hz, 2H), 5.81–5.71 (m, 1H), 5.56 (s, 1H), 5.27 (d, *J* = 6.4 Hz, 1H), 5.23–5.15 (m, 2H), 5.09 (d, *J* = 2.0 Hz, 1H), 4.19 (d, *J* = 4.4 Hz, 1H), 3.83–3.77 (m, 1H), 3.75 (s, 3H), 3.59–3.46 (m, 1H), 2.90 (d, *J* = 4.8 Hz, 3H), 1.81 (s, 3H); ^{13}C NMR (100 MHz, $CDCl_3$) δ 159.5, 158.4, 157.3, 155.5, 154.5, 140.7, 134.6, 132.9, 128.0, 118.0, 117.7, 114.0, 101.1, 85.5, 77.3, 56.3, 55.2, 53.3, 28.2, 21.2; LRMS (ESI) *m/z* calcd for $C_{21}H_{24}N_4O$ $[M+H]^+$: 349.20; Found: 349.01.

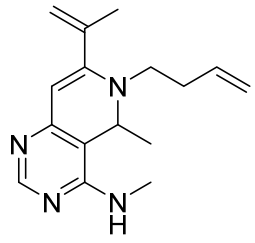

Compound 1o: Yield: 46%; ^{1}H NMR (500 MHz, $CDCl_3$) δ 8.40 (s, 1H), 5.70–5.62 (m, 1H), 5.61 (s, 1H), 5.32 (s, 1H), 5.17 (s, 1H), 4.98 (t, *J* = 4.5 Hz, 1H), 4.94 (s, 1H), 4.54 (d, *J* = 4.0 Hz, 1H), 4.28 (dd, *J* = 6.5 Hz, *J* = 7.0 Hz, 1H), 4.13 (dd, *J* = 7.0 Hz, *J* = 6.5 Hz, 1H), 3.34–3.29 (m, 1H), 3.11 (d, *J* = 5.0 Hz, 1H), 3.07 (d, *J* = 3.6, 3H), 2.23–2.18 (m, 2H), 2.05 (s, 1H), 1.95 (s, 3H), 1.27 (t, *J* = 14.5 Hz, 1H), 1.18 (d, *J* = 6.5 Hz, 3H); ^{13}C NMR

(100 MHz, $CDCl_3$) δ 157.5, 156.4, 154.0, 141.1, 134.8, 118.0, 116.9, 104.2, 101.1, 51.6, 50.4, 34.5, 28.1, 21.3, 17.3, 14.2; LRMS (ESI) *m/z* calcd for $C_{16}H_{22}N_4$ $[M+H]^+$: 271.18; Found: 271.07.

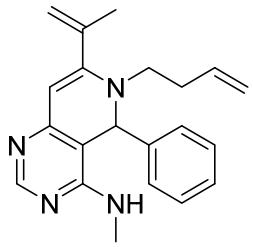

Compound 1p: Yield: 50%; ^1H NMR (400 MHz, $CDCl_3$) δ 8.44 (s, 1H), 7.28–7.24 (m, 5H), 5.73–5.63 (m, 1H), 5.57 (s, 1H), 5.28 (dd, *J* = 0.8 Hz, *J* = 0.8 Hz, 1H), 5.24 (s, 1H), 5.11–5.10 (m, 1H), 4.99 (dd, *J* = 1.6 Hz, *J* = 1.6 Hz, 1H), 4.98–4.97 (m, 1H), 4.95 (t, *J* = 4.8 Hz, 1H), 4.40 (d, *J* = 4.4 Hz, 1H), 3.41–3.33 (m, 1H), 3.15–3.08 (m, 1H), 2.95 (d, *J* = 4.8 Hz, 3H), 2.31–2.25 (m, 2H), 1.81 (s, 3H); ^{13}C NMR (100 MHz, $CDCl_3$) δ 158.5, 156.9, 155.3, 154.8, 140.9, 140.8, 134.7, 128.8, 128.4, 126.5, 118.1, 117.1, 103.0, 101.3, 58.2, 51.5, 50.8, 33.7, 29.2, 21.1; LRMS (ESI) *m/z* calcd for $C_{21}H_{24}N_4$ $[M+H]^+$: 333.20; Found: 333.04.

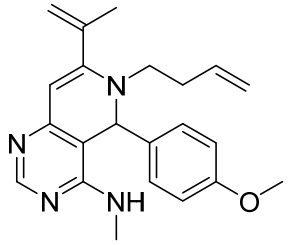

Compound 1q: Yield: 34%; ^1H NMR (400 MHz, $CDCl_3$) δ 8.44 (s, 1H), 7.18 (d, *J* = 3.2 Hz, 2H), 6.79 (d, *J* = 2.8 Hz, 2H), 5.71–5.63 (m, 1H), 5.55 (s, 1H), 5.26 (s, 1H), 5.16 (s, 1H), 5.09 (s, 1H), 4.99–4.98 (m, 2H), 4.95 (s, 1H), 4.21 (d, *J* = 4.8 Hz, 1H), 3.80 (t, *J* = 16.4 Hz, 1H), 3.76 (s, 3H), 3.37–3.30 (m, 1H), 3.13–3.05 (m, 1H), 2.94 (d, *J* = 4.8 Hz, 3H), 2.27 (dd, *J* = 7.6 Hz, *J* = 6.0 Hz, 2H), 1.80 (s, 3H); ^{13}C NMR (100 MHz, $CDCl_3$) δ 159.5, 158.3, 157.3, 155.6, 154.5, 140.9, 134.8, 133.1, 128.7, 127.8, 117.9, 117.0, 114.1, 113.7, 103.3, 101.5, 57.6, 55.2, 51.3, 33.6, 28.2, 21.2; LRMS (ESI) *m/z* calcd for $C_{22}H_{26}N_4O$ $[M+H]^+$: 363.21; Found: 362.98.

4. General procedure for the preparation of scaffold A (2a–2f)

To a DCE solution of **1d–1g** (0.3 mmol), AgOTf (10 mol%) and AcOH (2.0 equiv.) were added. After stirring at 80 °C for 2 h, the reaction mixture was

filtered under Na_2SO_4 pad and washed with DCM. After the removal of solvent under the reduced pressure, the reaction mixture was dissolved with dimethylformamide (DMF). 1,8-diazabicyclo[5.4.0]undec-7-ene (DBU) and dialkylmalonates were added to the solution and stirred at 80 ºC for 2 h. The resultant was quenched with deionized water and extracted twice with ethyl acetate (EtOAc). Combined organic layer was washed with brine and dried with anhydrous Na_2SO_4(s). After the solvent was removed under the reduced pressure, the residue was purified by silica-gel flash column chromatography to obtain **2a–2f**.

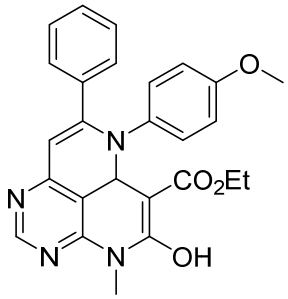

Compound 2a: Yield: 74%; ^{1}H NMR (400 MHz, $CDCl_3$) δ 12.57 (s, 1H), 8.78 (s, 1H), 8.68 7.42–7.34 (m, 5H), 6.76 (d, *J* = 6.8 Hz, 2H), 6.69 (d, *J* = 6.4 Hz, 2H), 5.85 (s, 1H), 5.43 (q, *J* = 7.2 Hz, 2H), 3.80 (s, 3H), 3.73 (s, 3H), 1.40 (t, *J* = 7.2 Hz, 3H); ^{13}C NMR (100 MHz, $CDCl_3$) δ 165.1, 162.6, 159.8, 157.6, 156.4, 155.2 ,137.9, 136.7, 132.8, 129.5, 128.54, 128.51, 124.7, 121.1, 114.0, 105.4, 92.2, 61.7, 55.4, 28.6, 14.3; HRMS (FAB+) *m/z* calcd for $C_{26}H_{24}N_4O_4$ $[M+H]^+$: 457.1876; Found: 457.1877.

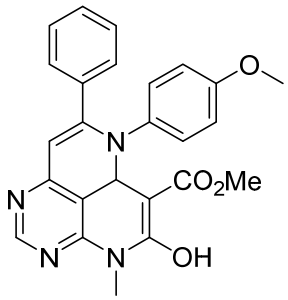

Compound 2b: Yield: 70%; ^{1}H NMR (500 MHz, $CDCl_3$) δ 12.58 (s, 1H), 8.79 (s, 1H), 8.73 (s, 1H), 7.42–7.36 (m, 5H), 6.77 (d, *J* = 8.5 Hz, 2H), 6.70 (d, *J* = 8.0 Hz, 2H), 5.86 (s, 1H), 3.96 (s, 3H), 3.80 (s, 3H), 3.74 (s, 3H); ^{13}C NMR (125 MHz, $CDCl_3$) δ 165.4, 162.6, 159.7, 158.9, 157.7, 156.4, 155.2, 138.4, 136.6, 132.8, 129.5, 128.52, 128.49, 124.7, 120.4, 114.0, 105.3, 92.1, 55.3, 52.6, 28.7; HRMS (FAB+) *m/z* calcd for $C_{25}H_{22}N_4O_4$ $[M+H]^+$:443.1719; Found: 443.1728.

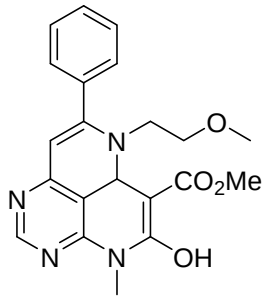

Compound 2c: Yield: 97%; ^{1}H NMR (500 MHz, $CDCl_3$) δ 11.10 (s, 1H), 8.71 (s, 1H), 8.62 (s, 1H), 7.49–7.47 (m, 3H), 7.44–7.42 (m, 2H), 5.55 (s, 1H), 3.91 (s, 3H), 3.77 (s, 3H), 3.49 (t, *J* = 5.5 Hz, 2H), 3.42 (t, *J* = 6.0 Hz, 2H), 3.40 (s, 3H); ^{13}C NMR (100 MHz, $CDCl_3$) δ 165.5, 163.6, 162.8, 159.9, 157.8, 155.1, 138.6, 136.4, 129.5, 128.6, 127.8, 119.6, 104.5, 89.3, 71.9, 59.0, 52.5, 44.9, 28.6; HRMS (FAB+) *m/z* calcd for $C_{21}H_{22}N_4O_4$ $[M+H]^+$: 395.1719; Found: 395.1728.

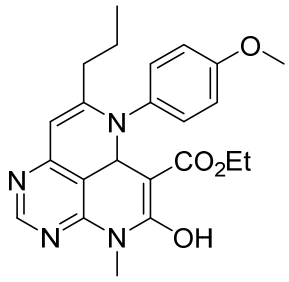

Compound 2d: Yield: 84%; ^{1}H NMR (500 MHz, $CDCl_3$) δ 12.50 (s, 1H), 8.69 (s, 1H), 8.63 (s, 1H), 7.13 (d, *J* = 8.0 Hz, 2H), 6.93 (d, *J* = 8.5 Hz, 2H), 5.66 (s, 1H), 4.44 (q, *J* = 7.0 Hz, 2H), 3.85 (s, 3H), 3.77 (s, 3H), 2.40 (t, *J* = 7.5 Hz, 2H), 1.58–1.54 (m, 2H), 1.43 (t, *J* = 7.0 Hz, 3H), 0.90 (t, *J* = 7.5 Hz, 3H); ^{13}C NMR (125 MHz, $CDCl_3$) δ 165.4, 164.1, 162.7, 159.9, 157.5, 155.1, 138.4, 127.8, 127.7, 120.2, 115.0, 113.7, 104.2, 87.3, 61.6, 55.9, 28.9, 22.1, 14.4, 14.2; HRMS (FAB+) *m/z* calcd for $C_{23}H_{26}N_4O_4$ $[M+H]^+$: 423.2032; Found: 423.2031.

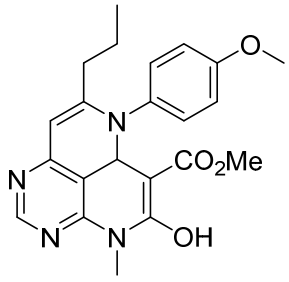

Compound 2e: Yield: 83%; ^{1}H NMR (500 MHz, $CDCl_3$) δ 12.51 (s, 1H), 8.73 (s, 1H), 8.63 (s, 1H), 7.13 (d, *J* = 8.5 Hz, 2H), 6.93 (d, *J* = 9.0 Hz, 2H), 5.66 (s, 1H), 3.98 (s, 3H), 3.85 (s, 3H), 3.77 (s, 3H), 2.40 (t, *J* = 7.5 Hz, 2H), 1.59–1.54 (m, 2H), 0.90 (t, *J* = 7.5 Hz, 3H); ^{13}C NMR (125 MHZ, $CDCl_3$) δ 165.8, 164.2, 162.7, 159.8, 157.7, 157.5, 155.1, 138.8, 138.6, 131.3, 127.3, 119.5, 114.4, 104.2, 87.6, 55.5, 52.6, 35.4, 28.6, 22.1, 13.8; HRMS (FAB+) *m/z* calcd for $C_{22}H_{24}N_4O_4$ $[M+H]^+$: 409.1876; Found: 409.1882.

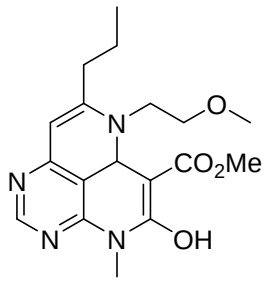

Compound 2f: Yield: 77%; ^{1}H NMR (500 MHz, $CDCl_3$) δ 11.17 (s, 1H), 8.67 (s, 1H), 8.57 (s, 1H), 5.48 (s, 1H), 3.96 (s, 3H), 3.75 (s, 3H), 3.62 (t, *J* = 5.0 Hz, 2H), 3.57 (t, *J* = 5.0 Hz, 2H), 3.45 (s, 3H), 2.40 (t, *J* = 8.0 Hz, 2H), 1.71–1.61 (m, 2H), 1.06 (t, *J* = 7.0 Hz, 3H); ^{13}C NMR (100 MHZ, $CDCl_3$) δ 165.9, 165.4, 162.7, 160.0, 157.8, 155.1, 138.9, 118.9, 103.8, 86.8, 71.6, 59.1, 52.5, 43.2, 35.8, 29.6, 28.5, 22.0, 14.0; HRMS (FAB+) *m/z* calcd for $C_{18}H_{24}N_4O_4$ $[M+H]^+$: 361.1876; Found: 361.1873.

5. General procedure for the preparation of scaffold B (3a–3i)

To the *t*–BuOH solution of **1a–1b** (0.4 mmol), diaminoalkane (5.0 equiv.) was added. After stirring at 80 ºC for 2 h, iodine (10.0 equiv.) was added to the reaction mixture and stirred at 80 ºC for additional 1 h. The reaction mixture was quenched with aqueous sodium thiosulfate solution and extracted twice with DCM. After drying with anhydrous Na_2SO_4(s), the solvent was removed under the reduced pressure. The residue was purified by silica-gel flash column chromatography to obtain **3a**–**3i**.

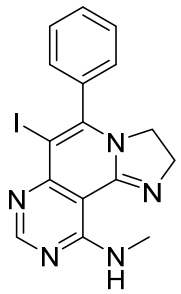

Compound 3a: Yield: 60%; ^{1}H NMR (400 MHz, $CDCl_3$) δ 9.52 (d, *J* = 4.0 Hz, 1H), 8.63 (s, 1H), 7.51 (t, *J* = 7.2 Hz, 3H), 7.30 (d, *J* = 7.2 Hz, 2H), 3.97 (t, *J* = 10.0 Hz, 2H), 3.66 (t, *J* = 10.0 Hz, 2H), 3.13 (d, *J* = 5.2 Hz, 3H); ^{13}C NMR (100 MHz, $CDCl_3$) δ 160.6, 160.4, 157.2, 155.8, 150.8, 138.0, 129.7, 129.0, 127.9, 99.3, 73.2, 52.8, 50.1, 27.6; HRMS (FAB+) *m/z* calcd for $C_{16}H_{14}IN_5$ $[M+H]^+$:404.0372; Found: 404.0370.

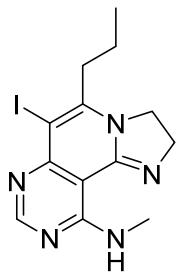

Compound 3b: Yield: 35%; ^{1}H NMR (400 MHz, $CDCl_3$) δ 9.48 (brs, 1H), 8.52 (s, 1H), 4.08 (t, *J* = 5.2 Hz, 4H), 3.09 (d, *J* = 5.2 Hz, 3H), 2.78 (t, *J* = 8.0 Hz, 2H), 1.72–1.62 (m, 2H), 1.10 (t, *J* = 7.2 Hz, 3H); ^{13}C NMR (100 MHz, $CDCl_3$) δ 160.5, 160.2, 157.0, 156.1, 151.1, 98.5, 72.9, 52.7, 48.3, 40.3, 29.7, 27.5, 20.8, 14.1; HRMS (FAB+) *m/z* calcd for $C_{13}H_{16}IN_5$ $[M+H]^+$: 370.0529; Found: 370.0526.

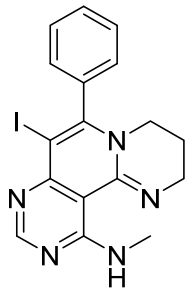

Compound 3c: Yield: 57%; ^{1}H NMR (400 MHz, $CDCl_3$) δ 8.57 (s, 1H), 7.53–7.48 (m, 3H), 7.25–7.23 (m, 2H), 3.58 (t, *J* = 5.6 Hz, 2H), 3.46 (t, *J* = 5.6 Hz, 2H), 3.12 (s, 3H), 1.79 (quintet, *J* = 5.6 Hz, 2H); ^{13}C NMR (100 MHz, $CDCl_3$) δ 161.1, 159.0, 155.0, 151.8, 149.4, 138.9, 129.4, 129.2, 128.5, 103.7, 77.7, 49.6, 43.6, 27.6, 20.9; HRMS (FAB+) *m/z* calcd for $C_{16}H_{14}IN_5$ $[M+H]^+$:418.0529; Found: 418.0526.

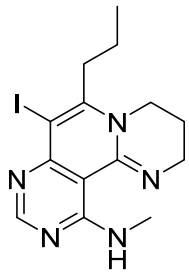

Compound 3d: Yield: 53%; ^{1}H NMR (400 MHz, $CDCl_3$) δ 11.52 (brs, 1H), 8.51 (s, 1H), 3.92 (t, *J* = 6.0 Hz, 2H), 3.60 (t, *J* = 6.0 Hz, 2H), 3.06 (s, 3H), 2.95 (t, *J* = 8.0 Hz, 2H), 1.95(quintet, *J* = 6.0 Hz, 2H), 1.68–1.58 (m, 2H), 1.09 (t, *J* = 8.4 Hz, 3H); ^{13}C NMR (100 MHz, $CDCl_3$) δ 160.9, 158.6, 154.8, 151.2, 149.6, 103.1, 78.3, 46.7, 43.4, 39.3, 27.5, 21.1, 21.0, 14.0; HRMS (FAB+) *m/z* calcd for $C_{14}H_{18}IN_5$ $[M+H]^+$: 384.0685; Found: 384.0688.

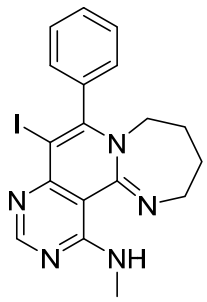

Compound 3e: Yield: 25%; ^{1}H NMR (400 MHz, $CDCl_3$) δ 8.59 (s, 1H), 7.51–7.49 (m, 3H), 7.36–7.39 (m, 2H), 3.91–3.89 (m, 2H), 3.60–3.57 (m, 2H), 3.11 (s, 3H), 1.98–1.92 (m, 2H), 1.67–1.60 (m, 2H); ^{13}C NMR (100 MHz, $CDCl_3$) δ 160.6, 158.7, 155.2, 153.0, 138.1, 129.6, 129.4, 128.6, 104.7, 78.2, 53.3, 48.6, 28.0, 27.7, 26.2, 25.2; HRMS (FAB+) *m/z* calcd for $C_{18}H_{18}IN_5$ $[M+H]^+$: 432.0685; Found: 432.0679.

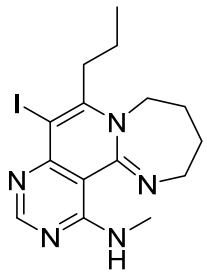

Compound 3f: Yield: 39%; ^{1}H NMR (400 MHz, $CDCl_3$) δ 11.08 (brs, 1H), 8.53 (s, 1H), 3.91 (t, *J* = 5.6 Hz, 4H), 3.06 (s, 3H), 2.81 (t, *J* = 8.0 Hz, 2H), 1.98 (t, *J* = 3.2 Hz, 4H), 1.75–1.69 (m, 2H), 1.09 (t, *J* = 7.2 Hz, 3H); ^{13}C NMR (100 MHz, $CDCl_3$) δ 160.4, 158.5, 154.9, 152.9, 152.5, 104.0, 78.3, 50.8, 48.3, 38.7, 29.7, 27.5, 26.2, 25.1, 22.2, 14.1; HRMS (FAB+) *m/z* calcd for $C_{15}H_{20}IN_5$ $[M+H]^+$: 398.0842; Found: 398.0844.

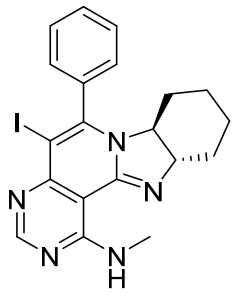

Compound 3g: Yield: 47%; ^{1}H NMR (500 MHz, $CDCl_3$) δ 9.78 (d, *J* = 4.5 Hz, 1H), 8.83 (s, 1H), 7.59–7.53 (m, 3H), 7.37 (d, *J* = 7.5 Hz, 2H), 3.33 (d, *J* = 5.0 Hz, 3H), 2.81 (t, *J* = 6.5 Hz, 2H), 1.80–1.73 (m, 4H), 1.60–1.58 (m, 4H); ^{13}C NMR (100 MHz, $CDCl_3$) δ 159.2, 157.3, 148.0, 143.9, 140.3, 137.6, 130.20, 130.05, 128.3, 122.2, 101.0, 90.4, 28.0, 25.2, 23.5, 23.3, 22.4; HRMS (FAB+) *m/z* calcd for $C_{20}H_{20}IN_5$ $[M+H]^+$: 458.0685; Found: 458.0678.

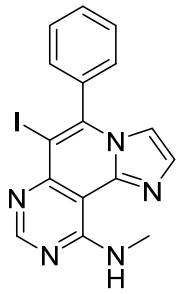

Compound 3h: Yield: 10%; ^{1}H NMR (400 MHz, $CDCl_3$) δ 9.50 (brs, 1H), 8.87 (s, 1H), 7.63 (t, *J* = 6.4 Hz, 3H), 7.49 (d, *J* = 1.6 Hz, 1H), 7.46 (d, *J* = 7.6 Hz, 2H), 7.08 (d, *J* = 1.2 Hz, 1H), 3.33 (d, *J* = 4.8 Hz, 3H); ^{13}C NMR (100 MHz, $CDCl_3$) δ 159.3, 157.8, 149.3, 143.5, 141.3, 136.5, 131.2, 130.1, 129.5, 129.0, 114.0, 101.2, 89.6, 28.0; HRMS (FAB+) *m/z* calcd for $C_{16}H_{12}IN_5$ $[M+H]^+$: 402.0216; Found: 402.0212.

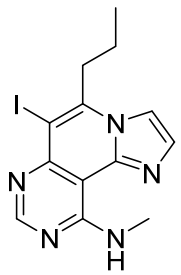

Compound 3i: Yield: 34%; ^{1}H NMR (400 MHz, $CDCl_3$) δ 9.48 (brs, 1H), 8.83 (s, 1H), 7.66 (d, *J* = 1.6 Hz, 1H), 7.63 (d, *J* = 1.6 Hz, 1H), 3.39 (t, *J* = 8.0 Hz, 2H), 3.30 (d, J= 5.2 Hz, 3H), 1.88–1.79 (m, 2H), 1.17 (t, *J* = 7.2 Hz, 3H); ^{13}C NMR (100 MHz, $CDCl_3$) δ 159.3, 157.7, 149.0, 143.9, 141.3, 131.7, 112.1, 100.6, 89.3, 39.6, 28.0, 19.6, 14.1; HRMS (FAB+) *m/z* calcd for $C_{13}H_{14}IN_5$ $[M+H]^+$: 368.0372; Found: 368.0375.

6. General procedure for the preparation of scaffold C (4a–4f)

To the DCE of **1h–1i** (0.25 mmol), AgOTf (20 mol%) was added. After stirring at 80 °C for 2 h, the reaction mixture was cooled to room temperature. After the addition of DBU (3.0 equiv.) and terminal alkyne (1.5 equiv.), the reaction mixture was stirred for 2 h. The resultant was quenched with water and extracted with DCM in two times. After drying with anhydrous Na_2SO_4(s), the solvent was removed under the reduced pressure. The residue was purified by silica-gel flash column chromatography to obtain **4a**–**4f**.

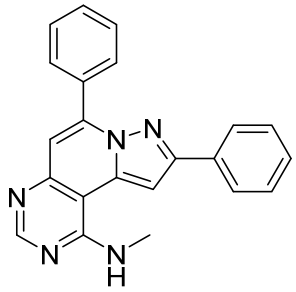

Compound 4a: Yield: 64%; ^{1}H NMR (400 MHz, $CDCl_3$) δ 8.76 (s, 1H), 8.00–7.97 (m, 2H), 7.92 (d, *J* = 8.0, 2H), 7.55–7.53 (m, 3H), 7.41 (t, *J* = 7.2 Hz, 2H), 7.35 (t, *J* = 7.6 Hz, 1H), 7.13 (s, 1H), 7.07 (s, 1H), 5.77 (d, *J* = 5.6 Hz, 1H), 3.29 (d, *J*= 4.4 Hz, 3H); ^{13}C NMR (100 MHz, $CDCl_3$) δ 158.3, 156.8, 153.6, 150.3, 144.8, 136.3, 132.7, 130.0, 129.7, 128.8, 128.7, 128.3, 126.4, 112.6, 103.7, 95.8, 28.7; HRMS (FAB+) *m/z* calcd for $C_{22}H_{17}N_5$ $[M+H]^+$: 352.1562; Found: 352.1556.

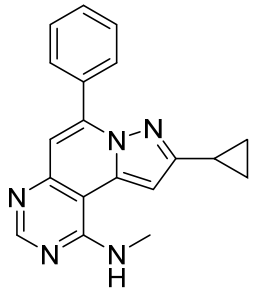

Compound 4b: Yield: 72%; ^{1}H NMR (400 MHz, $CDCl_3$) δ 8.73 (s, 1H), 7.93–7.91 (m, 2H), 7.53–7.49 (m, 3H), 7.05 (s, 1H), 6.47 (s, 1H), 5.69 (d, *J* = 4.8 Hz, 1H), 3.28 (d, *J* = 4.8 Hz, 3H), 2.19–2.13 (m, 1H), 1.07–1.02 (m, 2H), 0.91–0.87 (m, 2H); ^{13}C NMR (100 MHz, $CDCl_3$) δ 158.7, 158.3, 156.6, 150.2, 144.6, 135.7, 132.8, 129.9, 129.5, 128.2, 111.6, 103.4, 95.1, 28.7, 9.7, 9.1; HRMS (FAB+) *m/z* calcd for $C_{19}H_{17}N_5$ $[M+H]^+$: 316.1563; Found: 316.1565.

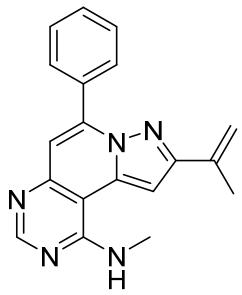

Compound 4c: Yield: 51%; ^{1}H NMR (400 MHz, $CDCl_3$) δ 8.75 (s, 1H), 8.00–7.97 (m, 2H), 7.54–7.52 (m, 3H), 7.12 (s, 1H), 6.92 (s, 1H), 5.77 (s, 1H), 5.74 (s, 1H), 5.26 (s, 1H), 3.31 (d, *J* = 5.2 Hz, 3H), 2.22 (s, 3H); ^{13}C NMR (100 MHZ, $CDCl_3$) δ 158.3, 156.8, 154.9, 150.3, 144.8, 136.7, 135.8, 132.6, 130.0, 129.7, 128.2, 114.7, 112.4, 103.6, 95.6, 28.7, 20.3; HRMS (FAB+) *m/z* calcd for $C_{19}H_{17}N_5$ $[M+H]^+$: 316.1562; Found: 316.1563.

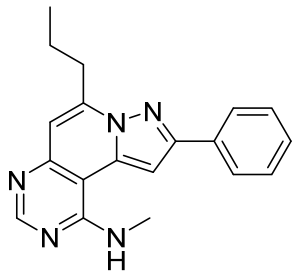

Compound 4d: Yield: 70%; ^{1}H NMR (400 MHz, $CDCl_3$) δ 8.73 (s, 1H), 8.00 (d, *J* = 7.6 Hz, 2H), 7.46 (t, *J* = 7.6 Hz, 2H), 7.38 (t, *J* = 7.6 Hz, 1H), 6.98 (s, 1H), 6.88 (s, 1H), 5.67 (d, *J* = 4.4 Hz, 1H), 3.27 (d, *J* = 4.8 Hz, 3H), 3.18 (t, *J* = 7.8 Hz, 2H), 1.97–1.87 (m, 2H), 1.09 (t, *J* = 7.2 Hz, 3H); ^{13}C NMR (100 MHz, $CDCl_3$) δ 158.3, 156.6, 153.3, 150.1, 146.7, 135.4, 132.6, 128.73, 128.71, 126.4, 109.9, 103.1, 95.6, 33.1, 28.6, 19.7, 13.9; HRMS (FAB+) *m/z* calcd for $C_{19}H_{19}N_5$ $[M+H]^+$: 318.1719; Found: 318.1717.

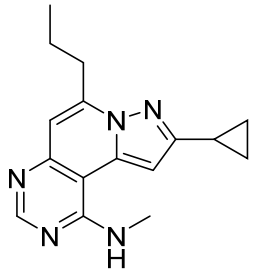

Compound 4e: Yield: 69%; ^{1}H NMR (400 MHz, $CDCl_3$) δ 8.71 (s, 1H), 6.84 (s, 1H), 6.43 (s, 1H), 5.62 (d, *J* = 4.0 Hz, 1H), 3.27 (d, *J* = 4.8 Hz, 3H), 3.15 (t, *J* = 7.6 Hz, 2H), 2.22–2.15(m, 1H), 1.96–1.86 (m, 2H), 1.1–1.07 (m, 5H), 0.96–0.92 (m, 2H); ^{13}C NMR (100 MHz, $CDCl_3$) δ 158.4, 158.2, 156.5, 146.5, 135.8, 108.9, 102.8, 95.1, 33.1, 28.6, 19.6, 13.9, 9.7, 9.0; HRMS (FAB+) *m/z* calcd for $C_{16}H_{19}N_5$ $[M+H]^+$: 282.1719; Found: 282.1718.

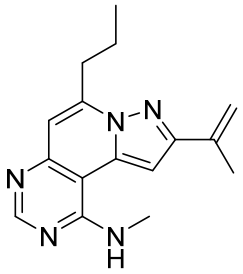

Compound 4f: Yield: 69%; ^{1}H NMR (400 MHz, $CDCl_3$) δ 8.72 (s, 1H), 6.87 (s, 1H), 6.84 (s, 1H), 5.80 (s, 1H), 5.67 (d, *J* = 4.4 Hz, 1H), 5.29–5.28 (m, 1H), 3.28 (d, *J* = 4.8 Hz, 3H), 3.17 (t, *J* = 7.6 Hz, 2H), 2.28 (s, 3H), 1.97–1.87 (m, 2H), 1.08 (t, *J* = 7.6 Hz, 3H); ^{13}C NMR (100 MHz, $CDCl_3$) δ 158.3, 156.6, 154.6, 150.2, 146.8, 136.8, 134.9, 114.4, 109.8, 103.1, 95.4, 33.1, 28.6, 20.3, 19.7, 13.9; HRMS (FAB+) *m/z* calcd for $C_{16}H_{19}N_5$ $[M+H]^+$: 282.1719; Found: 282.1718.

7. General procedure for the preparation of scaffold D (5a–5c, 6a–6c)

To an anhydrous DCM solution of **1l–1q** (0.1 mmol), second generation Grubb's catalyst (10 mol%) was added under argon atmosphere. After stirring at 40 ºC for 2 h, second generation Grubb's catalyst (10 mol%) was added to the reaction mixture and stirred for additional 3 h. After the removal of solvent under the reduced pressure, the residue was purified by silica-gel flash column chromatography to obtain **5a**–**5c** and **6a–6c**.

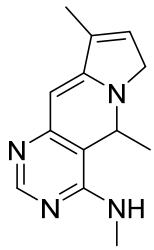

Compound 5a: Yield: 50%; ^{1}H NMR (400 MHz, $CDCl_3$) δ 8.54 (s, 1H), 6.63 (d, *J* = 2.8 Hz, 1H), 6.07 (d, *J* = 2.8 Hz, 1H), 5.06 (dd, *J* = 6.8 Hz, *J* = 7.6 Hz, 1H), 4.6 (s, 1H), 3.97 (d, *J* = 20.8 Hz, 1H), 3.83 (d, *J* = 21.2 Hz, 1H), 3.10 (d, *J* = 4.8 Hz, 3H), 2.07 (s, 3H), 1.52 (d, *J* = 6.4 Hz, 3H); ^{13}C NMR (100 MHz, $CDCl_3$) δ 158.6, 157.9, 156.8, 151.5, 116.3, 113.4, 110.4, 62.2, 48.6, 29.1, 28.3, 23.1, 10.7; HRMS (FAB+) *m/z* calcd for $C_{13}H_{16}N_4$ $[M+H]^+$: 229.1453; Found: 229.1458.

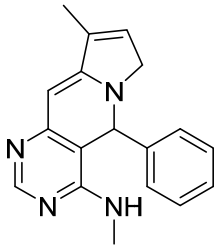

Compound 5b: Yield: 48%; ^{1}H NMR (400 MHz, $CDCl_3$) δ 8.59 (s, 1H), 7.56–7.21 (m, 5H), 6.58 (d, *J* = 2.8 Hz, 1H), 6.02 (d, *J* = 2.8 Hz, 1H), 5.88 (s, 1H), 4.48 (s, 1H), 4.06 (s, 2H), 2.90 (d, *J* = 4.8 Hz, 3H), 2.06 (s, 3H); ^{13}C NMR (100 MHz, $CDCl_3$) δ 159.2, 157.6, 157.1, 140.0, 129.7, 129.0, 126.9, 121.2, 116.9, 113.5, 110.97, 110.91, 77.6, 76.7, 57.3, 29.2, 28.4, 10.7; HRMS (FAB+) *m/z* calcd for $C_{18}H_{18}N_4$ $[M+H]^+$: 291.1610; Found: 291.1606.

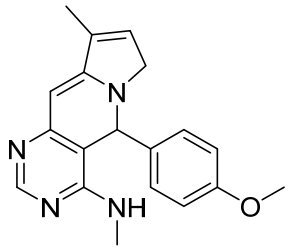

Compound 5c: Yield: 48%; ^{1}H NMR (500 MHz, $CDCl_3$) δ 8.60 (s, 1H), 7.17 (d, *J* = 9.5 Hz, 2H), 6.86 (d, *J* = 8.5 Hz, 2H), 6.60 (d, *J* = 2.5 Hz, 1H), 6.02 (d, *J* = 3.0 Hz, 1H), 5.86 (s, 1H), 4.47 (s, 1H), 4.06 (s, 2H), 3.77 (s, 3H), 2.93 (d, *J* = 4.5 Hz, 3H), 2.07 (s, 3H); ^{13}C

NMR (100 MHz, $CDCl_3$) δ 159.9, 159.2, 157.5, 142.5, 132.0, 129.1, 115.7, 113.4, 111.0, 107.7, 100.7, 61.8, 51.0, 39.5, 37.2, 29.2, 26.2; HRMS (FAB+) *m/z* calcd for $C_{19}H_{20}N_4$ $[M+H]^+$: 321.1715; Found: 321.1709.

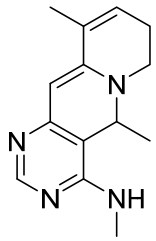

Compound 6a: Yield: 48%; ^{1}H NMR (400 MHz, $CDCl_3$) δ 8.36 (s, 1H), 5.89 (s, 1H), 5.48 (s, 1H), 4.36 (dd, *J* = 11.6 Hz, *J* = 6.4 Hz 1H), 4.30 (s, 1H), 3.34–3.27 (m, 1H), 3.08–3.06 (m, 1H), 3.03 (d, *J* = 3.6 Hz, 3H), 2.33 (d, *J* = 4.0 Hz, 2H), 1.91 (s, 1H), 1.19 (d, *J* = 6.4 Hz, 3H); ^{13}C NMR (100 MHz, $CDCl_3$) δ 157.0, 152.7, 132.3, 130.1, 127.3, 109.9, 94.4, 53.9, 45.1, 29.7, 28.1, 25.0, 18.7, 13.6; HRMS (FAB+) *m/z* calcd for $C_{14}H_{18}N_4$ $[M+H]^+$: 243.1610; Found: 243.1614.

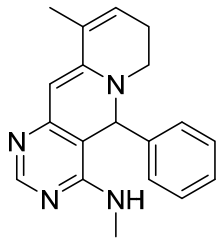

Compound 6b: Yield: 60%; ^{1}H NMR (400 MHz, $CDCl_3$) δ 8.39 (s, 1H), 7.42–7.40 (m, 2H), 7.32–7.29 (m, 2H), 5.81 (s, 1H), 5.47 (s, 1H), 5.16 (s, 1H), 4.01 (s, 1H), 2.87–2.85 (d, *J* = 4.8 Hz, 3H), 2.82–2.75 (m, 1H), 1.91 (s, 3H); ^{13}C NMR (100 MHz, $CDCl_3$) δ 157.60, 157.56, 155.7, 147.6, 139.7, 129.8, 129.0, 128.9, 127.2, 104.4, 94.3, 76.7, 63.4, 44.7, 35.6, 35.0, 28.2, 26.97, 26.85, 26.32, 26.29, 26.12, 26.10, 24.7, 18.9; HRMS (FAB+) *m/z* calcd for $C_{19}H_{20}N_4$ $[M+H]^+$: 305.1766; Found: 305.1761.

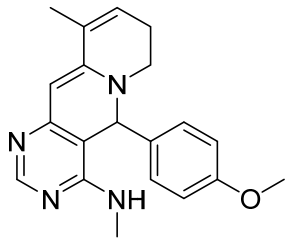

Compound 6c: Yield: 52%; ^{1}H NMR (400 MHz, $CDCl_3$) δ 8.38 (s, 1H), 7.32 (d. *J* = 2.4 Hz, 2H), 6.83 (d, *J* = 2.0 Hz, 2H), 5.81 (s, 1H), 5.46 (s, 1H), 5.14 (s, 1H), 4.53 (s, 1H), 3.96 (s, 3H), 2.86 (d, *J* = 4.8 Hz, 3H), 2.36 (s, 2H), 2.30 (s, 2H), 1.90 (s, 3H); ^{13}C NMR (100 MHz, $CDCl_3$) δ 158.6, 158.0, 138.7, 128.5, 127.4, 123.7, 119.0, 114.2, 98.4, 95.7, 76.7, 60.1, 55.1, 48.3, 37.5, 29.7, 28.2, 24.7, 22.9, 21.5; HRMS (FAB+) *m/z* calcd for $C_{20}H_{22}N_4O$ $[M+H]^+$: 335.1872; Found: 335.1875.

8. General procedure for the preparation of scaffold E (7a–7f)

To a toluene solution of **1l–1n** (0.1 mmol), maleimide (2.0 equiv.) was added. After stirring at 85 ºC for 3 days, organic solvent was removed under the reduced pressure. The residue was purified by silica-gel flash column chromatography to obtain **7a–7f**.

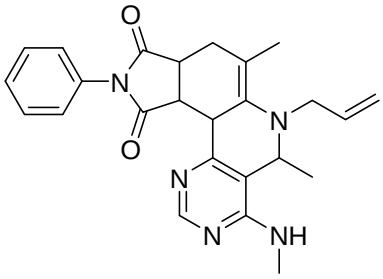

Compound 7a: Yield: 36%; ^{1}H NMR (400 MHz, $CDCl_3$) δ 8.30 (s, 1H), 7.41–7.29 (m, 5H), 5.72–5.69 (m, 1H), 5.36 (d, *J* = 6.8 Hz, 1H), 5.21–5.13 (m, 2H), 5.06 (s, 1H), 4.27–4.20 (m, 2H), 3.96–3.87 (m, 2H), 3.79–3.75 (m, 1H), 3.70–3.63 (m, 1H), 2.99 (d, *J* = 4.4 Hz, 3H), 2.96–2.89 (m, 1H), 1.96 (s, 3H), 1.18 (d, *J* = 6.4 Hz, 3H); ^{13}C NMR (100 MHz, $CDCl_3$) δ 179.7, 179.5, 177.0, 157.32, 157.27, 156.2, 156.1, 153.9, 152.3, 139.9, 134.7, 133.1, 129.0, 128.2, 126.78, 126.76, 119.7, 117.4, 117.2, 104.3, 76.7, 53.5, 53.3, 48.9, 48.7, 41.3, 40.3, 37.9, 35.8, 29.7, 28.2, 22.3, 16.4, 16.3; HRMS (FAB+) *m/z* calcd for $C_{25}H_{27}N_5O_2$ $[M+H]^+$: 430.2243; Found: 430.2236.

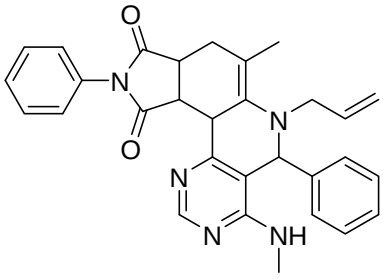

Compound 7b: Yield: 32%; ^{1}H NMR (400 MHz, $CDCl_3$) δ 8.35 (s, 1H), 7.75–7.26 (m, 10H), 5.77–5.71 (m, 1H), 5.34 (s, 1H), 5.30–5.26 (m, 2H), 5.23 (s, 1H), 4.09–4.08 (m, 2H), 4.02–3.95 (m, 2H), 3.61–3.55 (m, 1H), 2.94 (m, 1H), 2.91 (d, *J* = 4.8 Hz, 3H), 2.30 (d, *J* = 4.8 Hz, 1H), 1.75 (s, 3H); ^{13}C NMR (100 MHz, $CDCl_3$) δ 179.6, 176.7, 158.2, 156.8, 156.7, 153.9, 140.4, 133.9, 133.4, 129.3, 129.0, 128.9, 128.7, 128.2, 128.1, 127.2, 126.9, 126.77, 126.70, 119.2, 118.2, 118.1, 103.4, 56.9, 52.9, 40.4, 37.4, 35.6, 29.7, 28.2, 22.5; HRMS (FAB+) *m/z* calcd for $C_{30}H_{29}N_5O_2$ $[M+H]^+$: 492.2400; Found: 492.2394.

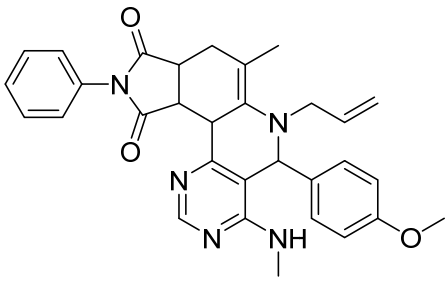

Compound 7c: Yield: 42%; ^{1}H NMR (400 MHz, $CDCl_3$) δ 8.35 (s, 1H), 7.50–7.20 (m, 7H), 6.89–6.86 (m, 2H), 5.78–5.74 (m, 1H), 5.35 (s, 1H), 5.33–5.26 (m, 2H), 5.21 (s, 1H), 4.06–4.03 (m, 2H), 3.98–3.96 (m, 2H), 3.81 (s, 3H), 3.63–3.57 (m, 1H), 3.01–2.96 (m, 1H), 2.95 (d, *J* = 12.0 Hz, 3H), 2.85 (d, *J* = 4.8 Hz, 1H), 1.77 (s, 3H); ^{13}C NMR (100 MHz, $CDCl_3$) δ 178.4, 177.3, 170.7, 159.7, 159.2, 158.2, 158.0, 156.6, 150.1, 133.9, 132.6, 127.99, 127.86, 118.2, 114.5, 114.36, 114.32, 86.0, 76.7, 64.6, 55.5, 55.3, 40.4, 35.5, 29.7, 28.3, 26.7, 25.0, 17.1; HRMS (FAB+) *m/z* calcd for $C_{31}H_{31}N_5O_3$ $[M+H]^+$: 522.2505; Found: 522.2488.

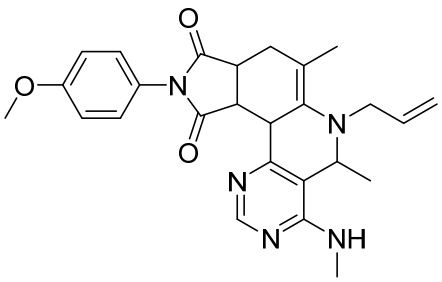

Compound 7d: Yield: 34%; ^{1}H NMR (400 MHz, $CDCl_3$) δ 8.30 (s, 1H), 7.28–7.20 (m, 3H), 6.97–6.93 (m, 1H), 5.74–5.63 (m, 1H), 5.36 (d, *J* = 7.6 Hz, 1H), 5.22–5.13 (m, 2H), 5.05 (s, 1H), 4.27–4.17 (m, 2H), 3.90–3.83 (m, 2H), 3.80 (s, 3H), 3.75–3.63 (m, 2H), 2.93 (d, *J* = 9.6 Hz, 3H), 2.94–2.85 (m, 1H), 1.96 (s, 3H), 1.18 (d, *J* = 6.8 Hz, 3H); ^{13}C NMR (100 MHz, $CDCl_3$) δ 177.2, 159.3, 157.37, 157.33, 156.2, 156.1, 153.9, 152.3, 139.9, 134.8, 127.94, 127.92, 119.7, 117.4, 117.2, 116.4, 114.40, 114.38, 55.48, 55.46, 53.3, 48.9, 48.7, 41.3, 40.3, 37.8, 29.7, 28.20, 28.17, 22.3, 16.4, 16.3; HRMS (FAB+) *m/z* calcd for $C_{26}H_{29}N_5O_3$ $[M+H]^+$: 460.2349; Found: 460.2359.

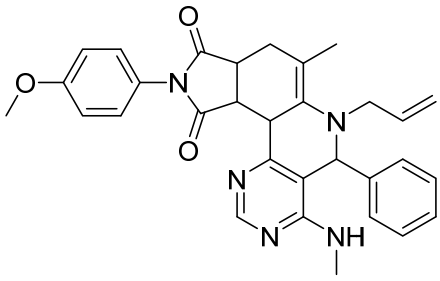

Compound 7e: Yield: 32%; ^{1}H NMR (400 MHz, $CDCl_3$) δ 8.34 (s, 1H), 7.35–7.22 (m, 7H), 6.99–6.97 (m, 2H), 5.75 (m, 1H), 5.35 (s, 1H), 5.35–5.28 (m, 2H), 5.24 (s, 1H), 4.13–4.10 (m, 2H), 4.00 (m, 2H), 3.82 (d, *J* = 5.2 Hz, 3H), 3.62–3.60 (m, 1H), 2.94–2.91 (m, 1H), 2.89 (d, *J* = 4.8 Hz, 3H), 2.84 (d, *J* = 4.8 Hz, 1H), 1.85 (s, 3H); ^{13}C NMR (100 MHz, $CDCl_3$) δ 179.9, 177.3, 159.3, 158.1, 156.7, 140.4, 134.0, 133.9, 129.3, 129.1, 128.9, 128.7, 127.9, 127.6, 127.2, 126.7, 118.3, 116.4, 114.8, 114.5, 114.4, 114.1, 103.3, 76.7, 55.5, 40.4, 35.5, 29.7, 28.29, 28.26; HRMS (FAB+) *m/z* calcd for $C_{31}H_{31}N_5O_3$ $[M+H]^+$: 522.2505; Found: 522.2502.

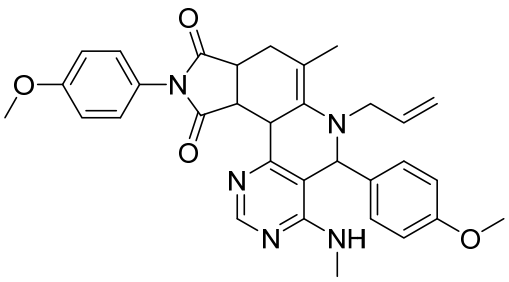

Compound 7f: Yield: 32%; ^{1}H NMR (400 MHz, $CDCl_3$) δ 8.32 (s, 1H), 7.40–7.16 (m, 4H), 6.98–6.95 (m, 2H), 6.86–6.84 (m, 2H), 5.74–5.73 (m, 1H), 5.32 (d, *J* = 6.0 Hz, 1H), 5.28–5.26 (m, 2H), 5.23 (s, 1H), 4.05–4.00 (m, 2H), 3.96–3.92 (m, 2H), 3.79 (s, 3H), 3.77 (s, 3H), 3.61–3.55 (m, 1H), 2.95–2.89 (m, 1H), 2.87 (d, *J* = 4.8 Hz, 3H), 2.83 (d, *J* = 4.8 Hz, 1H), 1.83 (s, 3H); ^{13}C NMR (100 MHz, $CDCl_3$) δ 177.7, 177.2, 168.2, 159.8, 159.3, 156.6, 151.1, 134.0, 132.6, 128.5, 128.0, 127.9, 118.1, 114.46, 114.40, 60.8, 55.5, 55. 2, 52.6, 40.4, 35.5, 31.9, 31.4, 30.2, 29.7, 28.2, 22.6; HRMS (FAB+) *m/z* calcd for $C_{32}H_{33}N_5O_4$ $[M+H]^+$: 552.2611; Found: 552.2605.

III. Principal Component Analysis (PCA) Data

1. Eigenvalues of the covariance matrix

Eigenvalues of the covariance matrix				
	Eigenvalue	Difference	Proportion	Cumulative
Prin 1	1599.23729	1030.25068	0.6138	0.6138
Prin 2	568.98661	265.65905	0.2184	0.8321
Prin 3	303.32756	199.55242	0.1164	0.9485

2. Eigenvectors in principal component analysis

Eigenvectors			
	Prin 1	**Prin 2**	**Prin 3**
Ring Energy	0.304456	0.182719	0.262972
Molecular weight	0.370201	–0.062337	0.347968
Topological PSA	0.454293	0.212850	–0.024271
2D VDW surface	0.405094	–0.093542	0.144375
2D VDW volume	0.394177	–0.145550	0.166564
Fraction of 2D VSA hydrophobic	–0.056418	–0.092711	0.084747
Fraction of 2D VSA polar	0.162504	0.308346	–0.347758
Fraction of 2D VSA H-bond donor	–0.245592	0.817384	0.216717
Fraction of 2D VSA H-bond acceptor	0.389214	0.254489	–0.599958
Charge polarization	0.054814	0.225686	0.474925

1-5. Reference

[1] Hajduk, P. J.; Galloway W. R. J. D.; Spring, D. R. *Nature* **2011**, *470,* 42.

[2] O' Connor, C. J.; Laraia, L.; Spring, D. R. *Chem. Soc. Rev.* **2011**, *40,* 4332.

[3] Swinney, D. C.; Anthony, J. *Nat. Rev. Drug Disc.* **2011**, *10,* 517.

[4] Schreiber, S. L. *Science* **2000**, *187,* 1964.

[5] O' Connor, C. J.; Beckmann, S. G.; Spring, D. R. *Chem. Soc. Rev.* **2012**, *41,* 4444.

[6] Oh, S.-M; Park, S. B. *Chem. Commun.* **2011**, *47,* 12754.

[7] Oh, S.; Nam, H. J.; Park, J.; Baek, S. H.; Park, S. B. *ChemMedChem* **2010**, *5,* 529.

[8] Oh, S.; Cho, S. W.; Yang, J.-Y.; Sun, H. J.; Chung, Y. S.; Shin, C. S.; Park, S. B. *Med. Chem. Commun.* **2011**, *2,* 76.

[9] Zhu, M.; Kim, M. H.; Lee, S; Bae, S. J.; Kim, S. H.; Park, S. B. *J. Med. Chem.* **2010**, *53,* 8760.

[10] Oh, S.; Kim, J.; Hwang, J. H.; Lee, H. Y.; Ryu, M. J.; Park, J.; Jo, Y. S.; Kim, Y. K.; Lee. C.-H.; Kweon, K. R.; Shong, M.; Park, S. B. *J. Med. Chem.* **2010**, *53,* 7405.

[11] Ribble, W., Hill, W. E., Ochsner, U. A., Jarvis, T. C., Guiles, J. W., Janjic, N., Bullard, J. M. *Antimicrob. Agents. Chemother.* **2010**, *54,* 4648.

[12] Giblin, M. P.; O'Shaughenessy, C. T.; Naylor, A.; Mitchell, W. L.; Eatherton, A. J.; Slingsby, B. P.; Rawlings, A.; Goldsmith, P.; Brown, A. J.; Haslam, C. P.; Clayton, N. M.; Wilson, A. W.; Chessell, I. P.; Wittington, A. R.; Green, R. *J. Med. Chem.* **2007**, *50,* 2597.

[13] Yaziji, V.; Rodriquez, D.; Gutierrez-de-Teran, H.; Coelho, A.; Caamano, O.; Garcia-Mera, X.; Brea, J.; Loza, M. I.; Cadavid, M. I.; Sotelo, E. *J. Med. Chem.* **2011**, *54,* 457.

[14] Meng, W.; Brigance, R. P.; Chao, H. J.; Fura, A.; Harrity, T.; Marcinkeviciene, J.; O'Connor, S. P.; Tamura, J. K.; Xie, D.; Zhang, Y.; Klei,

H. E.; Kish, K.; Weigelt, C. A.; Turdi, H.; Wang, A.; Zahler, R.; Kirby, M. S.; Hamann, L. G. *J. Med. Chem.* **2010**, *53,* 5620.

[15] Cikotiene, I., Buksnaitene, R., Sazinas, R. *Tetaheron* **2011**, *67,* 706.

[16] Asao, N.; Yunda, S. S.; Nogami, T.; Yamamoto, Y. *Angew. Chem. Int. Ed.* **2005**, *44,* 5526.

[17] Patil, N. T.; Mutyala, A. K.; Lakshmi, P. G. V. V.; Raju, V. K.; Sridlhar, B. *Eur. J. Org. Chem.* **2010**, 1999.

[18] Ouyang, H.-C.; Tang, R.,-Y.; Zhang, X.-G.; Li, J.-H. *J. Org. Chem.* **2011**, *76,* 223.

[19] Chen, Z.; Yang, X.; Wu, J. *Chem. Commun.* **2009**, 3469.

[20] Sauer, W. H. B., Schwarz, M. K. *J. Chem. Inf. Comp. Sci.* **2003**, *43,* 987.

Part 2. Diverse Display of Non-Covalent Interacting Elements using Pyrimidine-Embedded Polyheterocycles

Chem. Commun. **2015**, *51*, 13040–13043.

2-1. Introduction

Phenotype-based screening is an inevitable choice for the discovery of novel bioactive chemical entities with new modes of action in the field of drug discovery and chemical biology, which can lead to the development of first-in-class therapeutics.[1–3] The collection of drug-like small molecules with high skeletal diversity plays a pivotal role in the discovery of promising small-molecule ligands using both a conventional target-based approach[4] and a phenotype-based approach.[5] For maximizing the molecular diversity in such a collection, the biomedical research community has applied diversity-oriented synthesis (DOS) as the major strategy.[6–8] Along with this endeavor, a privileged substructure-based DOS (pDOS) strategy has emerged for the generation of the novel collection of drug-like small molecules exhibiting high efficiency and improved biological relevance.[9] In addition, this pDOS strategy focuses on the reconstruction of diverse and unprecedented drug-like polyheterocycles, which are embedded with privileged substructures frequently observed in bioactive natural products and therapeutic agents.[10] The unique value of a pDOS library has been demonstrated by the identification of novel small-molecule modulators exhibiting various therapeutic effects toward neuroinflammation,[11] type II diabetes,[12] stem-cell differentiation,[13] and cancer.[14]

For maximizing the coverage of chemical space employing pDOS strategy, we focused on the diversification of conformationally restricted polyheterocycles in a three-dimensional (3-D) space.[15,16] Meanwhile, we also envisioned that the small-molecule-based perturbation of specific biopolymers can be achieved by

a unique display of diverse non-covalent interacting elements, especially electrostatic and hydrogen-bonding interactions, within a well-defined single molecular framework containing privileged substructures.

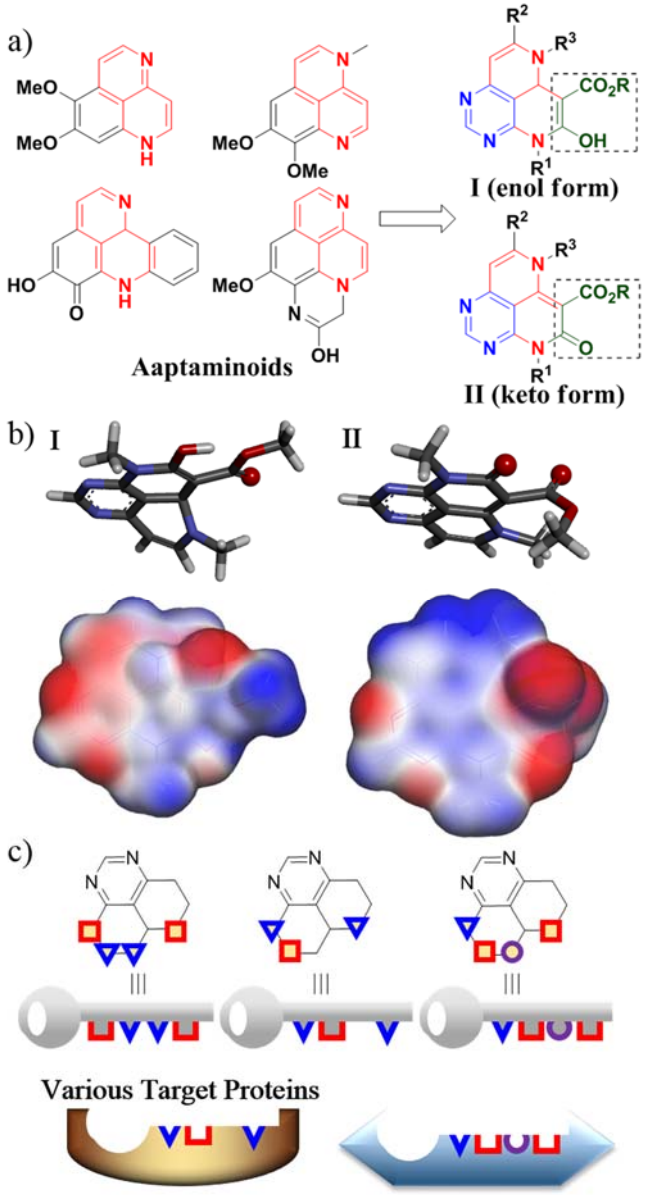

Figure 2-1. (a) Chemical structures of marine alkaloid–aaptaminoids and pyrimidine-containing polyheterocyclic skeletons I and II; (b) energyminimized conformers of the two skeletons and their polar surface areas illustrated by isosurface diagrams; (c) unique display of non-covalent interacting elements within pyrimidine-containing polyheterocycles. ioactive small molecules containing carbohybrid, pyrimidine, pyrazole,

For this purpose, we explored various skeletons that can uniquely display diverse non-covalent interacting elements using single polyheterocycles with high biological relevance. Among those attempts, we designed pyrimidine-embedded aza-tricyclic skeletons containing a structural framework similar to that of aaptaminoids,[17] which are natural marine alkaloids exhibiting various bioactivities such as anticancer,[18] antiviral,[19] and antifungal activities (**Figure 2-1a**).[20] These skeletons **I** and **II** not only employed unique skeletal features of aaptaminoids, but also exhibited distinguishable polar surface area and hydrogen-bonding capability, caused by the differentiation of the enol and keto forms, respectively (**Figure 2-1b**). In addition, the existence of one sp^3 carbon in skeleton **I** allowed for the 3-D discrete conformation different from that of skeleton **II**. Moreover, skeletons **I** and **II** were designed to accommodate diverse non-covalent interacting elements, such as electrostatic interactions, hydrogen bonding, and even hydrogen atom, within a single polyheterocyclic skeleton (**Figure 2-1c**).

Result and Discussion

Scheme 2-1. Retrosynthetic analysis of skeletons **I** and **II**.

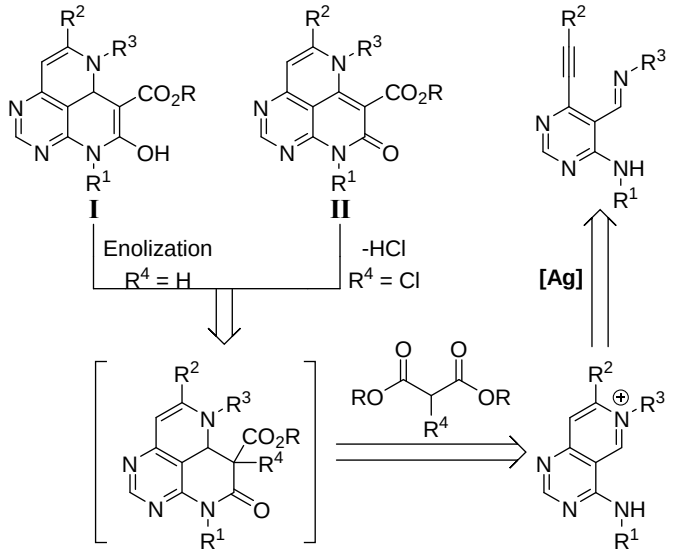

For preparing the skeletons **I** and **II**, a cascade cyclization strategy was adopted starting from tri-substituted *ortho*-alkynylpyrimidine aldimine. As shown in **Scheme 2-1**, the key substrate aldimines were first transformed into bicyclic pyridinium intermediates by Ag-catalyzed 6-*endo* cyclization.[21] Next, the resulting pyridinium compounds were subjected to nucleophilic addition with dialkyl malonates,[22] followed by cyclization via simultaneous lactamization with the amino group at the 4-position of the pyrimidine ring. After the formation of the tricyclic core structures, skeletons **I** and **II** were differentiated by enolization (in the case of R^4 = H) and dehydrodechlorination (in the case of R^4 = Cl), respectively. This unique three-step transformation allows for the efficient one-pot preparation of skeletons **I** and **II**.

Table 2-1. Synthesis of imines as well as the collection of polyheterocycles containing skeleton **I**.

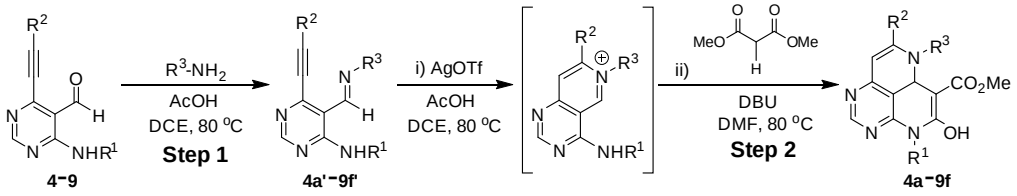

R^1	R^2 \ R^3		a	b	c	d	e	f
CH_3		4	86 / 95	84 / 70	89 / 76	91 / 69	91 / 62	86 / 78
		5	66 / 77	68 / 83	74 / 79	80 / 58	84 / 69	95 / 49
		6	83 / 74	66 / 87	99 / 76	93 / 53	93 / 87	95 / 47
		7	67 / 61	62 / 70	84 / 91	88 / 70	85 / 67	86 / 56
		8	66 / 62	69 / 85	94 / 74	83 / 48	84 / 64	92 / 48
		9	87 / 67	61 / 92	95 / 72	92 / 65	71 / 64	92 / 55

[a] See the Supporting Information for detailed experimental procedures. [b,c] Isolated yields of step 1 and step 2.

To construct the molecular collection of skeletons **I** and **II**, the facile condensation[22] between aldehydes (**4**–**9**) and various amines afforded stable imines **4a`–9f`** (**Step 1**). The molecular diversity of skeletons **I** and **II** was readily achieved by the combination of various R^1, R^2, and R^3 groups, such as

aliphatic, aromatic, heterocyclic, and/or carbocyclic motifs, affording products in high yields (average 83%, **Table 2-1**). In Step 2, the tandem cyclization of the imines prepared in Step 1 with dimethyl malonate provided pyrimidine-containing tricyclic cores, which were spontaneously tautomerized to the enol form (skeleton **I**), caused by the conjugation effect and the intramolecular hydrogen bonding with the malonate-derived ester group. This tandem cyclization protocol afforded a series of polyheterocycles containing skeleton **I** in an average yield of 70%, irrespective of the R^1, R^2, and R^3 substituents.

Table 2-2. Synthesis of the collection of polyheterocycles containing skeleton **II**[a]

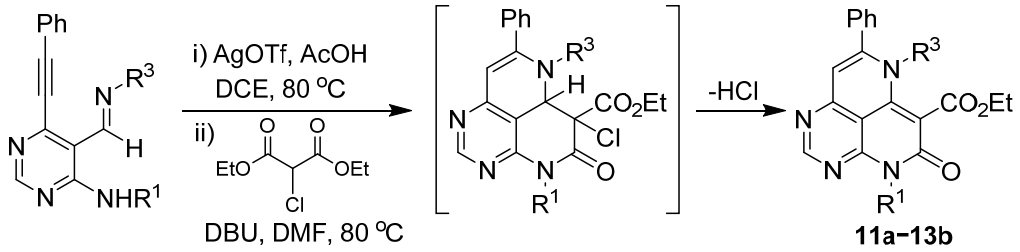

Product	R^1	R^3	Yield(%)[b]
11a	methyl	2-methoxyethyl	53
11b		4-methoxyphenyl	76
11c		benzyl	69
11d		3,4-dimethxoyphenethyl	57
11f		1-Boc-4-(aminomethyl)piperidyl	53
11g		4-methoxybenzyl	60
12a	benzyl	2-methoxyethyl	52[c]
12b		4-methoxyphenyl	53
12c		benzyl	53[c]
12d		3,4-dimethoxyphenethyl	52
13a	4-methoxybenzyl	2-methoxyethyl	48[c]
13b		4-methoxyphenyl	57

[a]See ESI for detailed experimental procedures. [b]Isolated yields.
[c]*t*-BuOH was used as solvent instead of DMF.

For skeleton **II**, the nucleophilic addition of diethyl chloromalonate, instead of dimethyl malonate, to the iminium intermediates afforded the keto form

(skeleton **II**) by lactamization and the subsequent removal of hydrochloride (**Table 2-2**). This tandem three-step cyclization provided a series of polyheterocycles containing skeleton **II** in moderate-to-good yields. Hence, such a divergent strategy at the later stage of synthesis efficiently afforded two unique skeletons containing different non-covalent interacting elements.

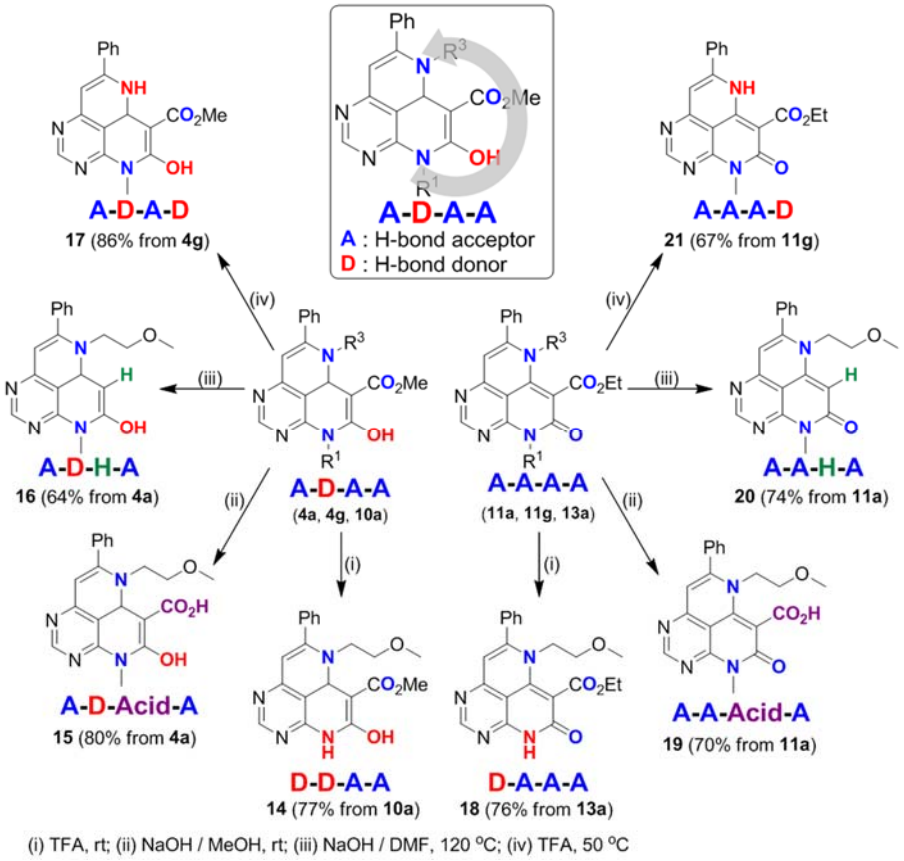

Figure 2-2. Distinct display of diverse non-covalent interacting elements on pyrimidine-embedded polyheterocycles.

For the discrete display of various non-covalent interacting elements in a single polyheterocyclic framework, we further diversified the representative compounds from skeleton **I** and **II**. As shown in **Figure 2-2**, we analyzed each substituent using different color codes to reveal the different capability of non-covalent interactions, such as H-bonding donor, H-bonding acceptor, as well as

electrostatic interactions and hydrogen atom. For example, a code of **A-D-A-A** for compound **4a** suggests that it consists of a H-bonding acceptor, a H-bonding donor, a H-bonding acceptor, and a H-bonding acceptor at the color-coded sites by the sequence of the curved arrow (**Figure 2-2**). This code differentiates the resulting collection of each polyheterocycle containing unique arrays of non-covalent interacting elements. Accordingly, ten differently coded structures were generated from the single molecular framework, which can induce specific interactions with various biopolymers.

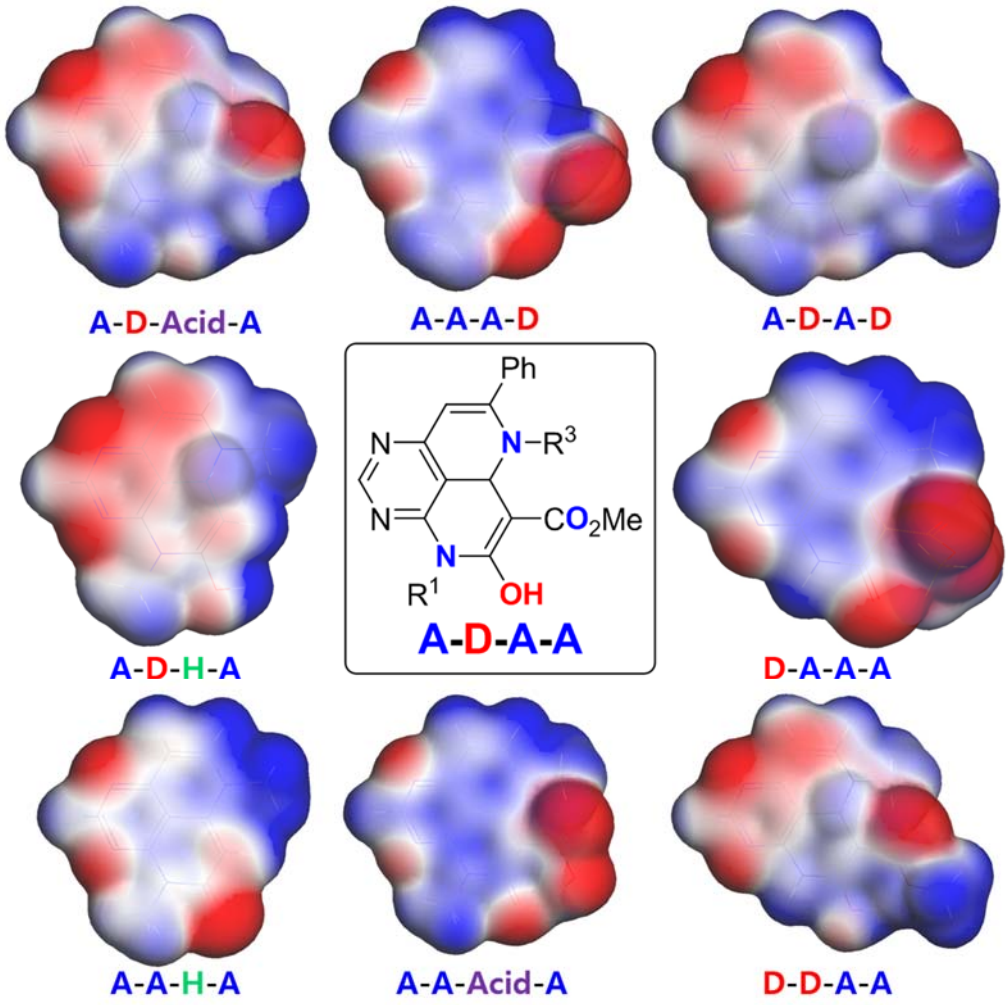

Figure 2-3. Polar surface areas of eight differently coded structures are illustrated by isosurface diagrams (isovalue is set as 0.017 C).

For visualizing the molecular diversity of differently coded structures, especially their electrostatic polar surface area, energy minimized conformers as well as the isosurface diagram of each representative compound with different codes were obtained by the calculation of electrostatic potentials and electron density. As shown in **Figure 2-3**, a molecular set having different codes exhibited discrete distributions for the polar surface area in a single molecular framework. This result indicates that by using a well-defined aza-tricyclic molecular framework, which demonstrates potential for inducing discrete biological events, the pyrimidine-containing polyheterocyclic skeletons **I** and **II** can display diverse non-covalent interacting elements.

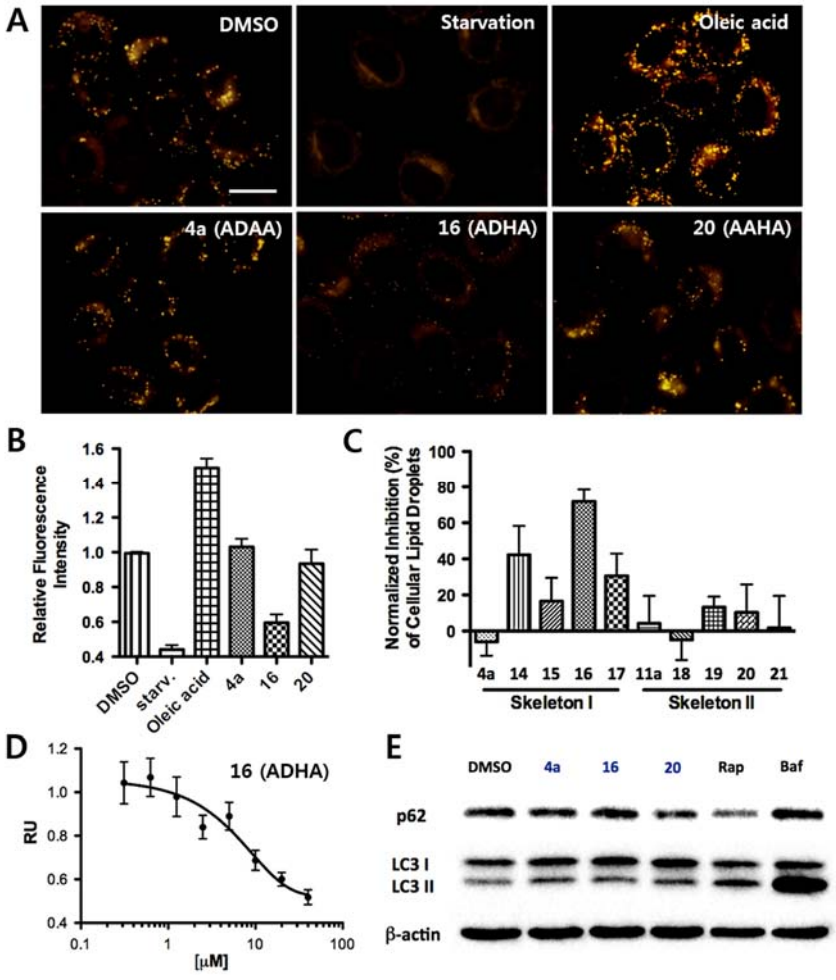

Figure 2-4. Cell-based phenotypic analysis for the evaluation of the different bioactivities exhibited by the representative coded compounds. (A) Fluorescence micrographs showing cellular LDs in HeLa cells stained with SF44. Cells were incubated with DMSO, serum-freemedia,oleic acid (5 mM), 4a, 16, and 20 (10 mM). Scale bar: 20 mm; (B) quantified fluorescence intensities of cellular LDs represented in A; (C) normalized cellular LD inhibition (%) exhibited by 10 coded compounds shown in Fig. 3; (D) A dose‑response curve of cellular LDs in relative units (RU) upon treatment with 16; (E) western blot data monitoring the conversion of microtubule-associated protein 1 light chain 3 (LC3) I to LC3 II and the degradation of p62 upon treatment with DMSO, 4a, 16, 20 (10 mM each), rapamycin (Rap, 200 nM), and bafilomycin (Baf, 10 nM).

After constructing a series of aza-tricycles containing skeletons **I** and **II**, we hypothesized that this pDOS strategy probably results in different biological activities on the basis of their display patterns of non-covalent interacting elements. Hence, to test this hypothesis, we made a collection of pyrimidine-embedded polyheterocycles with 10 different codes (**Figure 2-2**) and subjected them to cell viability assays and several image-based phenotypic screenings. Among these screening experiments, the results from the high-content screening for autophagy or cellular lipid biogenesis[23] by monitoring a lipid droplet (LD) with the use of a fluorogenic bioprobe SF44[24] exhibited an interesting pattern. As shown in Figs. 5a and 5b, the changes of cellular LDs in human cervical cancer HeLa cells can be easily quantified by the fluorescence intensity of SF44. Surprisingly, the cellular LDs in HeLa cells were decreased upon treatment with compounds containing skeleton **I**, whereas those in HeLa cells were not decreased by compounds containing skeleton **II** (**Figure 2-4c**). Among the derivatives containing skeleton **I**, **16** exhibited the best potency for LD decrease in a dose-dependent manner without cellular cytotoxicity; however, its keto counterpart **20** did not affect the cellular LDs (**Figure 2-4a**, **4d**, and **S4**, ESI†). Previously, we have reported that the changes in the LDs can be induced by the perturbation on lipid biogenesis or an autophagy-related recycling pathway.[23] To test whether **16** affects cellular LD levels by autophagy, we performed western blot analysis for monitoring the changes in the autophagy biomarkers

microtubule-associated protein 1 light chain 3 (LC3) and p62; the conversion of LC3 I to LC3 II was related to the maturation of autophagosome, and the degradation of p62 reflects the entire flux of the autophagic process. As shown in Fig 5e, the treatment with **16** did not affect the change of the p62 level as well as the conversion ratio of LC3 I to II, indicating that **16** does not reduce cellular LDs by the activation of autophagy. Even though the mechanistic study on the inhibition of lipid biogenesis is currently underway, this drastic difference in the phenotypic changes is quite interesting, especially in the lipid biogenesis, by simple changes between the enol and keto forms in pyrimidine-embedded polyheterocycles.

2-3. Conclusion

We successfully constructed pyrimidine-based polyheterocycles containing the aza-tricyclic core skeletons, which share the structural features of bioactive marine alkaloids—aaptaminoids. For diverse display of non-covalent interacting elements using this unique polyheterocyclic framework, we designed and synthesized two distinct skeletons; skeletons **I** and **II** were differentiated by the enol and keto forms, which exhibit different H-bonding abilities and polar surface areas. The further diversification of substituents afforded 10 differently coded structures with discrete non-covalent interacting elements as well as the different distribution of polar surface areas. The utility of this pyrimidine-based pDOS pathway was confirmed by the differential bioactivities of skeletons **I** and **II** using image-based high-content screening for lipid biogenesis and autophagy.

2-4. Supporting information

I. General Experimental Information

All commercially available reagents and solvents were used without further purification unless noted otherwise. All the solvents were purchased from commercial venders. ^{1}H and ^{13}C NMR spectra were obtained using Agilent 400–MR DD2 (Agilent, USA) or Varian Inova–500 (Varian Assoc., Palo Alto, USA) instruments. Chemical shifts were reported in ppm from tetramethylsilane (TMS) as internal standard or the residual solvent peak ($CDCl_3$; ^{1}H: δ = 7.26 ppm; ^{13}C: δ = 77.23 ppm). Multiplicity was indicated as follows: s (singlet), d (doublet), t (triplet), q (quartet), m (multiplet), dd (doublet of doublet), dt (doublet of triplet), td (triplet of doublet), brs (broad singlet), and so on. Coupling constants are reported in hertz. Mass spectrometric analysis was performed using a Finnigan Surveyor MSQ Plus LC/MS (Thermo) with electrospray ionization (ESI). The conversion of starting materials was monitored by thin–layer chromatography (TLC) using pre–coated glass–backed plates (silica gel 60; F_{254} = 0.25 mm), and the reaction components were visualized by observation under UV light (254 and 365 nm) or by treatment of TLC plates with visualizing agents such as $KMnO_4$, phosphomolybdic acid, and ninhydrin followed by heating. Products were purified by flash column chromatography on silica gel (230–400 mesh) using a mixture of EtOAc/hexane or MeOH/CH_2Cl_2 as eluents. The energy–minimized structures of molecules were obtained by V_{conf} Interface v2.0 using default parameters and visualized by Discovery Studio 3.5. The polar surface area is illustrated by an isosurface diagram (isovalule is set as 0.017 C) after calculations were performed using the Materials Studio 4.2 program. A generalized gradient of approximation (GAA) for the exchange correlation function of Perdew, Burke, and Ernzerhof (PBE) was used with the double-numerical basis set with polarization (DNP) as implemented in DMol3.

II. Synthetic Procedures and Characterization of All Compounds

1. General synthetic procedure for compounds 1–3

To a solution of 4,6-dichloropyrimidine-5-carbaldehyde (5.0 g) in chloroform (280 mL), amine (1.2 equiv.) and trimethylamine (5.9 mL, 1.5 equiv.) were added at room temperature. After 1 h (the reaction completion was checked by TLC), the reaction mixture was diluted with dichloromethane (DCM) and washed with deionized water and brine. The combined organic layer was dried with anhydrous Na_2SO_4(s). After the removal of solvent under the reduced pressure, the residue was purified by silica-gel flash column chromatography to obtain the desired compounds (**1**–**3**).

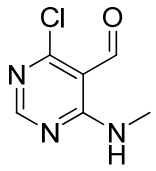

Compound 1: Yield: 92%; white solid; ^{1}H NMR (400 MHz, $CDCl_3$) δ 10.37 (s, 1H), 9.17 (brs, 1H), 8.45 (s, 1H), 3.12 (d, *J* = 4.8 Hz, 3H); ^{13}C NMR (100 MHz, $CDCl_3$) δ 191.3, 165.2, 161.7, 160.8, 108.1, 27.8; IR (neat)*ν*max: 3438, 2942, 2833, 2509, 2042, 1661, 1450, 1414, 1028, 729; LRMS (ESI) *m/z* calcd for $C_6H_6ClN_3O$ $[M+H]^+$: 172.02; Found: 172.0; Registration No.:14160-94-2.

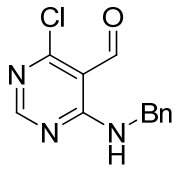

Compound 2: Yield: 97%; pale brown solid; ^{1}H NMR (400 MHz, $CDCl_3$) δ 10.37 (s, 1H), 9.52 (brs, 1H), 8.45 (s, 1H), 7.37-7.27 (m, 5H), 4.81 (d, *J* = 5.6 Hz, 2H); ^{13}C NMR (100 MHz, $CDCl_3$) δ 191.4, 165.4, 161.1, 160.9, 137.0, 128.8, 128.60, 128.55, 127.7, 127.6, 127.5, 108.0, 44.8; IR (neat)*ν*max: 3476, 2829, 2404, 2038, 1663, 1582, 1418, 1386, 1120, 1068, 1026; LRMS (ESI) *m/z* calcd for $C_{12}H_{10}ClN_3O$ $[M+H]^+$: 248.05; Found: 248.00; Registration No.: 59311-82-9.

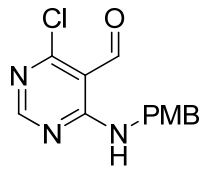

Compound 3: Yield: 63%; yellow solid; ^{1}H NMR (400 MHz, $CDCl_3$) δ 10.36 (s, 1H), 9.46 (brs, 1H), 8.46 (s, 1H), 7.25 (d, *J* = 8.4 Hz, 2H), 6.88 (d, *J* = 8.4 Hz, 2H), 4.74 (d, *J* = 4.8 Hz, 2H), 3.80 (s, 3H); ^{13}C NMR (100 MHz, $CDCl_3$) δ 191.3, 165.3, 160.9, 160.8, 159.2, 129.06, 129.03, 114.2, 108.0, 55.3, 44.4; IR (neat)*v*max: 3531, 2947, 2830, 2471, 2040, 1652, 1119, 1022; LRMS (ESI) *m/z* calcd for $C_{13}H_{12}ClN_3O_2$ $[M+H]^+$: 278.06; Found: 278.10; Registration No.: 1532748-79-0.

2. General synthetic procedure for compounds 4–10

To a solution of **1–3** (1.0 g), $Pd(PPh_3)_2Cl_2$ (5 mol%), and CuI (20 mol%) in anhydrous DMF (60 mL), terminal alkynes (2.0 equiv.) and triethylamine (2.0 equiv.) were added under the argon atmosphere. After being stirred at room temperature for 4 h, the reaction mixture was quenched with deionized water (200 mL). The resultant was extracted with EtOAc (100 mL × 3) and the combined organic layer was washed with brine (100 mL). After drying with anhydrous Na_2SO_4(s), the filtered solution was concentrated under the reduced pressure. The residue was purified by silica-gel flash column chromatography to obtain the desired compound (**4–10**).

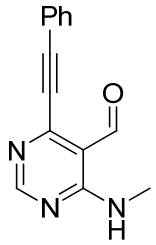

Compound 4: Yield: 98%; Pale yellow solid; ^{1}H NMR (400 MHz, $CDCl_3$) δ 10.55 (s, 1H), 8.91 (brs, 1H), 8.67 (s, 1H), 7.65–7.62 (m, 2H), 7.47–7.38 (m, 3H), 3.14 (d, *J* = 5.2 Hz, 3H); ^{13}C NMR (100 MHz, $CDCl_3$) δ 192.5, 161.5, 160.4, 155.0, 132.4, 130.3, 128.6, 120.6, 98.3, 83.8, 27.4; IR (neat)*v*max: 3969, 3856, 2832, 2534, 2223, 2041, 1517, 1110, 1022; LRMS (ESI) *m/z* calcd for $C_{14}H_{11}N_3O$ $[M+H]^+$: 238.09; Found: 237.99; Registration No.: 1477472-98-2.

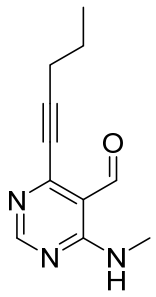

Compound 5: Yield: 96%; Brown solid; ^{1}H NMR (400 MHz, $CDCl_3$) δ 10.42 (s, 1H), 8.86 (s 1H), 8.60 (s, 1H), 3.11 (d, *J* = 5.2 Hz, 3H), 2.50 (t, *J* = 6.8 Hz, 2H), 1.72–1.66 (m, 2H), 1.07 (t, *J* = 7.2 Hz, 3H); ^{13}C NMR (100 MHz, $CDCl_3$) δ 192.9, 161.4, 160.4, 155.5, 111.9, 101.3, 76.0, 27.3, 21.5, 21.4, 13.6; IR (neat)*ν*max: 3859, 3715, 3387, 2830, 2505, 2228, 2038, 1446, 1115, 1020; LRMS (ESI) *m/z* calcd for $C_{11}H_{13}N_3O$ $[M+H]^+$: 204.11; Found: 204.02; Registration No.: 1477472-99-3.

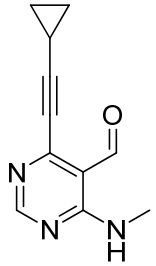

Compound 6: Yield: 97%; Brown solid; ^{1}H NMR (400 MHz, $CDCl_3$) δ 10.36 (s, 1H), 8.84 (brs, 1H), 8.57 (s, 1H), 3.10 (d, *J* = 4.8 Hz, 3H), 1.58–1.52 (m, 1H), 1.04-0.95 (m, 4H); ^{13}C NMR (100 MHz, $CDCl_3$) δ 192.8, 161.3, 160.4, 155.5, 111.8, 104.9, 71.3, 27.3, 9.4; IR (neat)*ν*max: 3973, 3856, 3394, 3252, 2828, 2521, 2216, 2034, 1696, 1631, 1471, 1016; LRMS (ESI) *m/z* calcd for $C_{11}H_{11}N_3O$ $[M+H]^+$: 202.09; Found: 201.90.

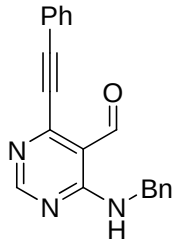

Compound 7: Yield: 55%; Brown solid; ^{1}H NMR (400 MHz, $CDCl_3$) δ 10.57 (s, 1H), 9.26 (brs, 1H), 8.67 (s, 1H), 7.62 (d, *J* = 4.0 Hz, 2H), 7.45–7.25 (m, 8H), 4.81 (d, *J* = 5.6 Hz, 2H); ^{13}C NMR (100 MHz, $CDCl_3$) δ 192.6, 161.6, 159.9, 155.3, 137.4, 132.5, 130.4, 128.8, 128.7, 127.66, 127.61, 120.7, 111.7, 98.5, 83.8, 44.4; IR (neat)*ν*max: 3365, 2830, 2515, 2201, 2038, 1693, 1626, 1471, 1120, 1017; LRMS (ESI) *m/z* calcd for $C_{20}H_{15}N_3O$ $[M+H]^+$: 314.12; Found: 314.01; Registration No.: 1103638-86-9.

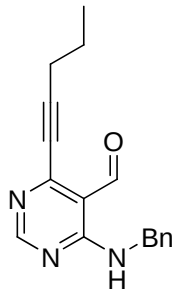

Compound 8: Yield: 78%; Brown solid; ^{1}H NMR (400 MHz, $CDCl_3$) δ 10.43 (s, 1H), 9.23 (brs, 1H), 8.61 (s, 1H), 7.36–7.27 (m, 5H), 4.79 (d, *J* = 5.6 Hz, 2H), 2.50 (t, *J* = 7.2 Hz, 2H), 1.74–1.65 (m, 2H), 1.06 (t, *J* = 7.2 Hz, 3H); ^{13}C NMR (100 MHz, $CDCl_3$) δ 193.0, 161.5, 159.9, 155.8, 137.5, 128.7, 127.59, 127.56, 111.8, 101.5, 76.1, 44.3, 21.55, 21.47, 13.6; IR (neat)*ν*max: 3858, 3703, 3451, 2946, 2832, 2437, 2230, 2041, 1539, 1481, 1112, 1022; LRMS (ESI) *m/z* calcd for $C_{17}H_{17}N_3O$ $[M+H]^+$: 280.14; Found: 280.06.

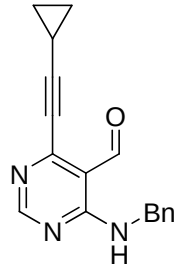

Compound 9: Yield: 97%; Orange solid; ^{1}H NMR (400 MHz, $CDCl_3$) δ 10.37 (s, 1H), 9.21 (brs, 1H), 8.58 (s, 1H), 7.36–7.27 (m, 5H), 4.78 (d, *J* = 5.5 Hz, 2H), 1.58–1.51 (m, 1H), 1.04–0.94 (m, 4H); ^{13}C NMR (100 MHz, $CDCl_3$) δ 192.9, 161.5, 159.8, 155.7, 137.5, 128.7, 127.58, 127.56, 111.7, 105.1, 71.3, 44.3, 9.5; IR (neat)*ν*max: 3856, 3421, 2943, 2832, 2445, 2221, 2041, 1517, 1122, 1023; LRMS (ESI) *m/z* calcd for $C_{17}H_{15}N_3O$ $[M+H]^+$: 278.12; Found: 278.06.

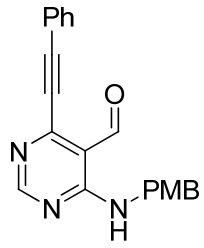

Compound 10: Yield: 82%; Pale brown solid; ^{1}H NMR (400 MHz, $CDCl_3$) δ 10.55 (s, 1H), 9.20 (brs, 1H), 8.68 (s, 1H), 7.63 (d, *J* = 8.4 Hz, 2H), 7.45–7.38 (m, 3H), 7.28 (d, *J* = 9.2 Hz, 2H), 6.89 (d, *J* = 8.4 Hz, 2H), 4.74 (d, *J* = 5.6 Hz, 2H), 3.80 (s, 3H); ^{13}C NMR (100 MHz, $CDCl_3$) δ 192.6, 161.6, 159.7, 159.1, 155.2, 132.4, 130.4, 129.4, 129.1, 128.6, 120.7, 114.2, 111.6, 98.4, 83.9, 55.3, 43.9; IR (neat)*ν*max: 3496, 2946, 2833, 2437, 2040, 1453, 1117, 1017; LRMS (ESI) *m/z* calcd for $C_{21}H_{17}N_3O_2$ $[M+H]^+$: 344.13; Found: 344.02.

3. General synthetic procedure for compounds 4a`–10b`

To a solution of **4–10** (3.0 mmol) in dichloroethane (DCE), amine (5.0 equiv.), Na_2SO_4, and AcOH were added. After stirring at 80 °C until starting materials were consumed, the reaction mixture was quenched with deionized water. The resultant was extracted with dichloromethane (DCM) twice and dried with anhydrous Na_2SO_4(s). After the solvent was removed under the reduced pressure, the residue was purified by silica-gel flash column chromatography to obtain **4a`–10b`**.

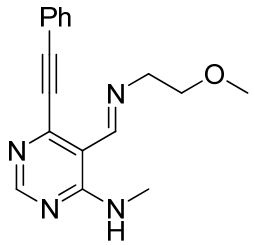

Compound 4á: Yield: 86%; Pale yellow solid; ^{1}H NMR (500 MHz, $CDCl_3$) δ 9.98 (brs, 1H), 8.97 (s, 1H), 8.55 (s, 1H), 7.62–7.60 (m, 2H), 7.42–7.36 (m, 3H), 3.84 (t, *J* = 5.2 Hz, 2H), 3.71 (t, *J* = 5.2 Hz, 2H), 3.4 (s, 3H), 3.11 (d, *J* = 4.8 Hz, 3H); ^{13}C NMR (125 MHz, $CDCl_3$) δ 161.8, 160.5, 158.4, 150.4, 111.3, 99.0, 77.1, 72.2, 61.0, 58.9, 27.2, 21.6, 21.5, 13.6; IR (neat)*ν*max: 3422, 2811, 2521, 2216, 2041, 1694, 1453, 1122, 1021 cm^{-1}; LRMS (ESI) *m/z* calcd for $C_{17}H_{18}N_3O$ $[M+H]^+$: 295.15; Found: 295.00; Registration No.: 1477473-09-8.

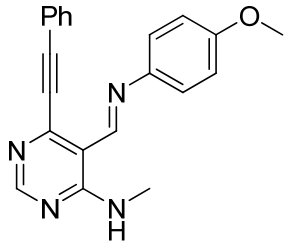

Compound 4b́: Yield: 84%; Yellow solid; ^{1}H NMR (400 MHz, $CDCl_3$) δ 10.12 (s, 1H), 9.18 (s, 1H), 8.58 (s, 1H), 7.60 (d, *J* = 6.8 Hz, 2H), 7.40 (t, *J* = 7.6 Hz, 3H), 7.26 (d, *J* = 8.0 Hz, 2H), 6.97 (d, *J* = 8.4 Hz, 2H), 3.85 (s, 3H), 3.18 (d, *J* = 4.8 Hz, 3H); ^{13}C NMR (100 MHz, $CDCl_3$) δ 160.2, 158.78, 158.61, 156.3, 150.5, 143.5, 132.1, 129.8, 128.5, 122.3, 121.3, 114.6, 112.1, 97.0, 85.1, 55.5, 27.5; IR (neat)*ν*max: 3983, 3857, 3672, 3361, 2935, 2828, 2525, 2214, 2036, 1668, 1450, 1117, 1018 cm^{-1}; LRMS (ESI) *m/z* calcd for $C_{21}H_{18}N_4O$ $[M+H]^+$: 343.15; Found: 343.00; Registration No.: 1477473-04-3.

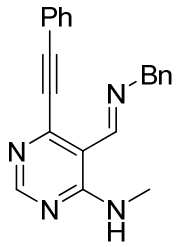

Compound 4ć: Yield: 89%; Brown solid; ^{1}H NMR (400 MHz, $CDCl_3$) δ 10.02 (d, *J* = 5.4 Hz, 1H), 9.03 (s, 1H), 8.56 (s, 1H), 7.56 (dd, *J* = 8.0 Hz, *J* = 1.8 Hz, 2H), 7.43-7.36 (m, 5H), 7.31 (t, *J* = 7.0 Hz, 3H), 4.88 (s, 2H), 3.09 (d, *J* = 4.7 Hz, 3H); ^{13}C NMR (100 MHz, $CDCl_3$) δ 160.8, 160.5, 158.6, 150.0, 138.5, 132.1, 129.7, 128.7, 128.5, 127.9, 127.3, 121.3, 111.5, 96.5, 85.0, 65.0, 27.4; IR (neat)*ν*max: 3981, 3859, 33672, 3613, 3586, 3411, 3358, 2939, 2824, 2510, 2215, 2043, 1633, 1454, 1120, 1021, 808 cm^{-1}; LRMS (ESI) *m/z* calcd for $C_{21}H_{18}N_4$ $[M+H]^+$: 327.15; Found: 327.03.

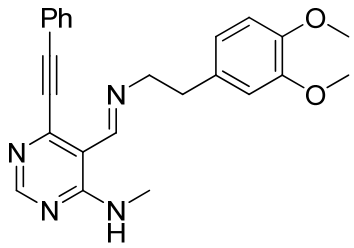

Compound 4d́: Yield: 91%; Brown oil; ^{1}H NMR (400 MHz, $CDCl_3$) δ 9.97 (brs, 1H), 8.85 (s, 1H), 8.54 (s, 1H), 7.57 (d, *J* = 7.6 Hz, 2H), 7.42–7.36 (m, 3H), 6.83–6.76 (m, 2H), 6.75 (s, 1H), 3.90 (t, *J* = 7.2 Hz, 2H), 3.85 (s, 3H), 3.84 (s, 3H), 3.05 (d, *J* = 4.8 Hz, 3H), 2.95 (t, *J* = 7.2 Hz, 2H); ^{13}C NMR (100 MHz, $CDCl_3$) δ 160.6, 160.1, 158.6, 149.8, 149.0, 147.7, 132.3, 132.2, 129.8, 128.6, 121.6, 121.0, 112.4, 111.6, 111.4, 96.5, 85.2, 63.2, 56.0, 55.9, 37.4, 27.4; IR (neat)*ν*max: 3984, 3857, 3686, 3359, 2944, 2818, 2508, 2216, 2040, 1632, 1444, 1022 cm^{-1}; LRMS (ESI) *m/z* calcd for $C_{24}H_{24}N_4O_2$ $[M+H]^+$: 401.19; Found: 401.13.

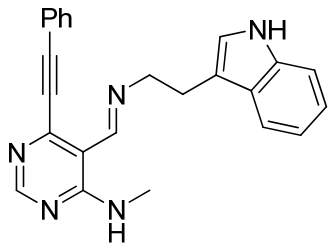

Compound 4é: Yield: 91%; Brown solid; ^{1}H NMR (400 MHz, $CDCl_3$) δ 10.02 (d, *J* = 5.1 Hz, 1H), 8.79 (s, 1H), 8.53 (s, 1H), 8.29 (brs, 1H), 7.64 (d, *J* = 7.8 Hz, 7.43–7.31 (m, 6H), 7.18 (t, *J* = 7.2 Hz, 1H), 7.12 (t, *J* = 7.2 Hz, 1H), 7.00 (s, 1H), 3.99 (t, *J* = 7.2 Hz, 2H), 3.17 (t, *J* = 7.2 Hz, 2H), 3.00 (d, *J* = 4.8 Hz, 3H); ^{13}C NMR (100 MHz, $CDCl_3$) δ 160.4, 159.9, 158.3, 149.5, 136.3, 132.1, 129.6, 128.4, 127.4, 122.03,

121.99, 121.3, 119.3, 118.7, 113.7, 111.5, 111.2, 96.4, 84.9, 62.0, 27.2, 27.0; IR (neat)*v*max: 3856, 3308, 2823, 2509, 2213, 2038, 1673, 1556, 1483, 1199, 1115, 1017 cm^{-1}; LRMS (ESI) *m/z* calcd for $C_{24}H_{21}N_5$ $[M+H]^+$: 380.18; Found: 380.12.

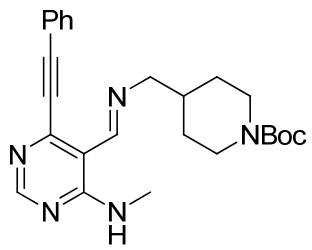

Compound 4f́: Yield: 86%; Yellow oil; ^{1}H NMR (400 MHz, $CDCl_3$) δ 9.96 (brs, 1H), 8.90 (s, 1H), 8.55 (s, 1H), 7.61 (dd, *J* = 7.6 Hz, *J* = 1.8 Hz, 2H), 7.43–7.26 (m, 3H), 4.16 (brs, 2H), 3.55 (d, *J* = 6.4 Hz, 2H), 3.11 (d, *J* = 4.8 Hz, 3H), 2.73 (t, *J* = 12.2 Hz, 2H), 1.85–1.81 (m, 1H), 1.74 (d, *J* = 12.0 Hz, 2H), 1.46 (s, 9H), 1.30–1.23 (m, 2H); ^{13}C NMR (100 MHz, $CDCl_3$) δ 160.7, 160.4, 158.7, 155.0, 149.9, 132.3, 129.9, 128.7, 121.6, 111.6, 96.6, 85.2, 79.5, 77.4, 67.9, 37.8, 30.5, 28.6, 27.5, 21.2, 14.3; IR (neat)*v*max: 3974, 3857, 3686, 3442, 3345, 3312, 3279, 2943, 2833, 2537, 2214, 2044, 1667, 1573, 1521, 1022 cm^{-1}; LRMS (ESI) *m/z* calcd for $C_{25}H_{31}N_5O_2$ $[M+H]^+$: 434.25; Found: 434.12.

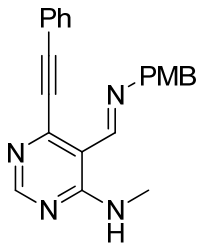

Compound 4ǵ: Yield: 86%; Brown oil; ^{1}H NMR (400 MHz, $CDCl_3$) δ 10.03 (brs, 1H), 8.97 (s, 1H), 8.55 (s, 1H), 7.54 (d, *J* = 7.6 Hz, 2H), 7.42–7.36 (m, 3H), 7.23 (d, *J* = 8.8 Hz, 2H), 6.92 (d, *J* = 8.4 Hz, 2H), 4.82 (s, 2H), 3.80 (s, 3H), 3.08 (d, *J* = 4.8 Hz, 3H); ^{13}C NMR (100 MHz, $CDCl_3$) δ 160.5, 160.3, 158.9, 158.5, 149.9, 132.1, 130.3, 129.7, 129.4, 128.5, 121.4, 114.1, 111.5, 96.5, 85.0, 64.2, 55.2, 27.3; IR (neat)*v*max: 3861, 3687, 3369, 2943, 2827, 2501, 2214, 2041, 1672, 1112, 1023 cm^{-1}; LRMS (ESI) *m/z* calcd for $C_{22}H_{20}N_4O$ $[M+H]^+$: 357.16; Found: 357.05.

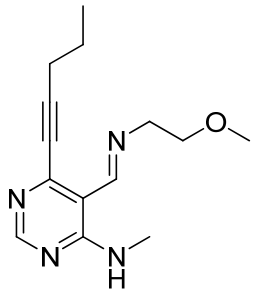

Compound 5á: Yield: 66%; Pale yellow solid; ^{1}H NMR (500 MHz, $CDCl_3$) δ 9.91 (brs, 1H), 8.86 (s, 1H), 8.48 (s, 1H), 3.80 (t, *J* = 5.0 Hz, 2H), 3.69 (t, *J* = 5.0 Hz, 2H), 3.39 (s, 3H), 3.08 (d, *J* = 4.5 Hz, 3H), 2.47 (t, *J* = 7.0 Hz, 2H), 1.71–1.66 (m, 2H), 1.07 (t, *J* = 7.5 Hz, 3H); ^{13}C NMR (125 MHZ, $CDCl_3$) δ 161.8, 160.5, 158.4, 150.4, 111.3, 99.0, 77.1, 72.2, 61.0, 58.9, 27.2, 21.6, 21.5, 13.6; IR (neat)*ν*max: 3822, 3670, 3318, 2946, 2791, 2520, 2229, 2037, 1679, 1553, 1415, 1233, 1125, 1016 cm^{-1}; LRMS (ESI) *m/z* calcd for $C_{14}H_{20}N_4O$ $[M+H]^+$: 261.16; Found: 261.05; Registration No.: 1477473-13-4.

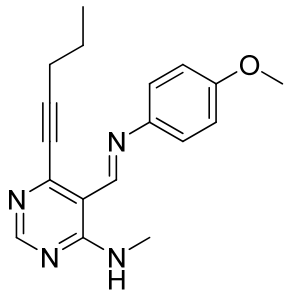

Compound 5b́: Yield: 68%; Yellow solid; ^{1}H NMR (400 MHz, $CDCl_3$) δ 10.06 (d, *J* = 4.4 Hz, 1H), 9.08 (s, 1H), 8.52 (s, 1H), 7.21 (d, *J* = 7.2 Hz, 2H), 6.95 (d, *J* = 6.8 Hz, 2H), 3.85 (s, 3H), 3.15 (d, *J* = 4.8 Hz, 3H), 2.49 (t, *J* = 6.8 Hz, 3H), 1.73–1.64 (m, 2H), 1.07 (t, *J* = 7.2 Hz, 3H); ^{13}C NMR (100 MHz, $CDCl_3$) δ 160.2, 158.6, 158.5, 156.8, 151.2, 143.6, 122.3, 114.5, 111.9, 99.6, 76.8, 55.5, 27.4, 21.6, 21.5, 13.6; IR (neat)*ν*max: 3970, 3858, 3321, 2945, 2831, 2526, 2228, 2041, 1668, 1249, 1115, 1019 cm^{-1}; LRMS (ESI) *m/z* calcd for $C_{18}H_{20}N_4O$ $[M+H]^+$: 309.16; Found: 309.06; Registration No.: 1477473-07-6.

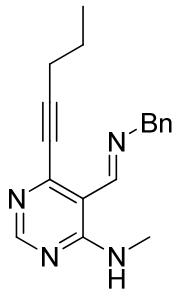

Compound 5ć: Yield: 74%; Brown oil; ^{1}H NMR (400 MHz, $CDCl_3$) δ 9.95 (brs, 1H), 8.94 (s, 1H), 8.49 (s, 1H), 7.40–7.29 (m, 5H), 4.83 (s, 2H), 3.28 (d, *J* = 4.4 Hz, 3H), 2.46 (t, *J* = 7.0 Hz, 2H), 1.72–1.63 (m, 2H), 1.06 (t, *J* = 7.4 Hz, 3H); ^{13}C NMR (100 MHz, $CDCl_3$) δ 160.4, 160.3, 158.3, 150.2, 148.8, 147.5, 132.3, 120.8, 112.1, 111.3, 111.1, 98.9, 63.0, 55.9, 55.8, 37.3, 27.1, 21.6, 21.5, 13.6; IR (neat)*ν*max: 3858, 3672, 3398, 2826, 2522, 2227, 2042,

1633, 1118, 1021 cm^{-1}; LRMS (ESI) *m/z* calcd for $C_{18}H_{20}N_4$ $[M+H]^+$: 293.17; Found: 293.07.

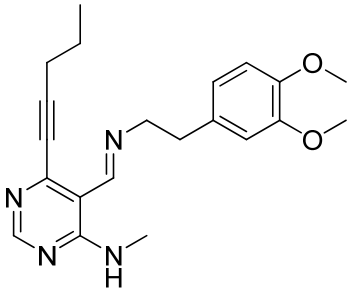

Compound 5d́: Yield: 80%; Brown oil; ^1H NMR (400 MHz, $CDCl_3$) δ 9.91 (brs, 1H), 8.75 (s, 1H), 8.47 (s, 1H), 6.82 (d, *J* = 7.6 Hz, 1H), 6.76 (d, *J* = 9.2 Hz, 2H), 3.87 (s, 3H), 3.86 (s, 3H), 3.84 (t, *J* = 6.8 Hz, 2H), 3.02 (d, *J* = 4.8 Hz, 3H), 2.93 (t, *J* = 6.8 Hz, 2H), 2.45 (t, *J* = 7.0 Hz, 2H), 1.69–1.64 (m, 2H), 1.05 (t, *J* = 7.2 Hz, 3H); ^{13}C NMR (100 MHZ, $CDCl_3$) δ 160.4, 160.3, 158.3, 150.2, 148.8, 147.5, 132.3, 120.8, 112.2, 111.3, 111.2, 98.9, 63.0, 55.9, 55.8, 37.3, 27.1, 21.6, 21.5, 13.6; IR (neat)*v*max: 3981, 3857, 3689, 3350, 2819, 2515, 2228, 2037, 1694, 1613, 1566, 1535, 1402, 1109, 1021 cm^{-1}; LRMS (ESI) *m/z* calcd for $C_{21}H_{26}N_4O_2$ $[M+H]^+$: 367.21; Found: 367.11.

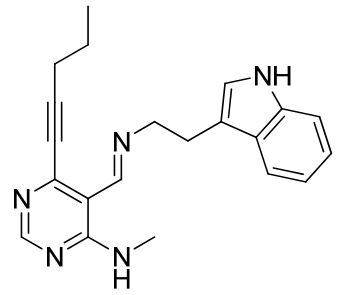

Compound 5é: Redish brown solid; Yield: 84%; ^1H NMR (400 MHz, $CDCl_3$) δ 9.97 (brs, 1H), 8.72 (s, 1H), 8.47 (s, 1H), 8.31 (brs, 1H), 7.63 (d, *J* = 8.0 Hz, 1H), 7.38 (d, *J* = 8.4 Hz, 1H), 7.20 (t, *J* = 7.6 Hz, 1H), 7.12 (t, *J* = 7.6 Hz, 1H), 7.00 (s, 1H), 3.94 (t, *J* = 6.8 Hz, 2H), 3.14 (t, *J* = 6.8 Hz, 2H), 2.96 (d, *J* = 4.8 Hz, 3H), 2.37 (t, *J* = 6.8 Hz, 2H), 1.63–1.54 (m, 2H), 1.00 (t, *J* = 7.2 Hz, 3H); ^{13}C NMR (100 MHZ, $CDCl_3$) δ 160.4, 160.2, 158.2, 150.1, 136.3, 127.4, 122.0, 121.9, 119.2, 118.7, 113.8, 111.4, 111.2, 99.0, 76.9, 61.9, 27.13, 27.11, 21.6, 21.4, 13.6; IR (neat)*v*max: 3574, 2829, 2472, 2200, 2039, 1681, 1615, 1565, 1478, 1401, 1262, 1021, 843, 771, 726; LRMS (ESI) *m/z* calcd for $C_{21}H_{23}N_5$ $[M+H]^+$: 346.20; Found: 346.15.

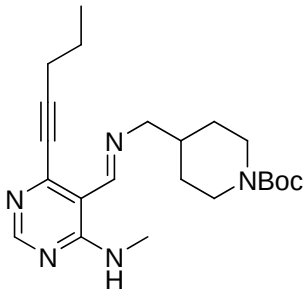

Compound 5f́: Pale yellow solid; Yield: 95%; ^{1}H NMR (400 MHz, $CDCl_3$) δ 9.90 (brs, 1H), 8.79 (s, 1H), 8.49 (s, 1H), 4.15 (brs, 2H), 3.51 (d, *J* = 6.0 Hz, 2H), 3.08 (d, *J* = 5.2 Hz, 3H), 2.73 (t, *J* = 11.2 Hz, 2H), 2.48 (t, *J* = 7.2 Hz, 2H), 1.86–1.79 (m, 1H), 1.74–1.65 (m, 4H), 1.46 (s, 9H), 1.30–1.17 (m, 2H), 1.07 (t, *J* = 7.2 Hz, 3H); ^{13}C NMR (100 MHz, $CDCl_3$) δ 160.6, 160.5, 158.4, 154.8, 150.3, 111.2, 99.0, 79.3, 77.1, 67.6, 37.6, 30.3, 28.4, 27.3, 21.6, 21.5, 13.6; IR (neat)*v*max: 3857, 3745, 3457, 2790, 2228, 2040, 1715, 1669, 1471, 1403, 1114, 1018; LRMS (ESI) *m/z* calcd for $C_{22}H_{33}N_5O_2$ $[M+H]^+$: 400.26; Found: 400.20.

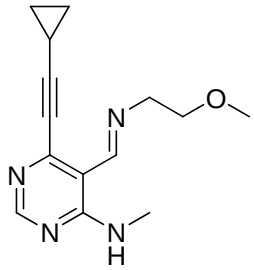

Compound 6á: Redish brown solid; Yield: 83%; ^{1}H NMR (400 MHz, $CDCl_3$) δ 9.91 (brs, 1H), 8.81 (s, 1H), 8.45 (s, 1H), 3.80 (t, *J* = 5.2 Hz, 2H), 3.69 (t, *J* = 5.2 Hz, 2H), 3.40 (s, 3H), 3.07 (d, *J* = 5.2 Hz, 3H), 1.52–1.50 (m, 1H), 0.98–0.94 (m, 4H); ^{13}C NMR (100 MHZ, $CDCl_3$) δ 161.7, 160.4, 158.3, 150.3, 111.3, 102.4, 72.25, 72.22, 61.0, 58.9, 27.2, 9.1, 0.3; IR (neat)*v*max: 3562, 2951, 2833, 2473, 2222, 1666, 1451, 1423, 1112, 1023; LRMS (ESI) *m/z* calcd for $C_{14}H_{18}N_4O$ $[M+H]^+$: 259.15; Found: 259.03.

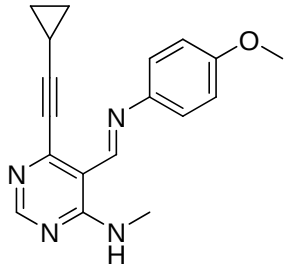

Compound 6b́: Yellow solid; Yield: 66%; ^{1}H NMR (400 MHz, $CDCl_3$) δ 10.04 (brs, 1H), 9.02 (s, 1H), 8.50 (s, 1H), 7.22 (d, *J* = 7.6 Hz, 2H), 6.97 (d, *J* = 7.6 Hz, 2H), 3.86 (s, 3H), 3.15 (d, *J* = 4.8 Hz, 3H), 1.56–1.52 (m, 1H), 1.00–0.92 (m, 4H); ^{13}C NMR (100 MHZ, $CDCl_3$) δ 160.2, 158.6, 158.5, 156.8, 151.1, 143.7, 122.3, 114.5, 103.0, 55.5, 27.4, 9.3, 0.4; IR (neat)*v*max: 3439, 3415, 3337, 3317, 2834, 2222, 1620, 1575, 1543, 1504, 1444, 1418, 1372, 1296, 1248, 1168, 1109,

1031, 932, 865, 832, 798, 636, 623; LRMS (ESI) *m/z* calcd for $C_{18}H_{18}N_4O$ $[M+H]^+$: 307.15; Found: 306.97.

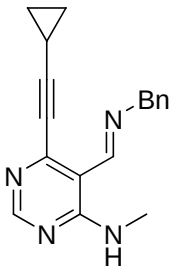

Compound 6ć: Brown solid; Yield: 99%; ^{1}H NMR (400 MHz, $CDCl_3$) δ 9.95 (brs, 1H), 8.88 (s, 1H), 8.46 (s, 1H), 7.37 (d, *J* = 7.2 Hz, 2H), 7.32 (t, *J* = 7.2 Hz, 3H), 4.84 (s, 2H), 3.05 (d, *J* = 4.8 Hz, 3H), 1.53–1.49 (m, 1H), 0.99-0.89 (m, 4H); ^{13}C NMR (100 MHz, $CDCl_3$) δ 161.2, 160.4, 158.4, 150.5, 138.7, 128.6, 127.8, 127.2, 111.2, 102.5, 72.2, 64.9, 27.3, 9.2, 0.3; IR (neat)*ν*max: 3974, 3857, 3356, 2941, 2828, 2520, 2223, 2040, 1667, 1119, 1022; LRMS (ESI) *m/z* calcd for $C_{18}H_{18}N_4$ $[M+H]^+$: 291.15; Found: 291.00.

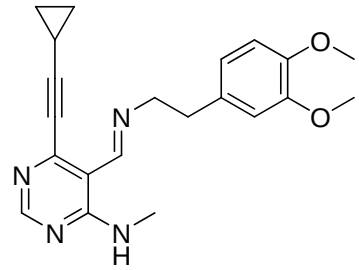

Compound 6d́: Brown solid; Yield: 93%; ^{1}H NMR (400 MHz, $CDCl_3$) δ 9.91 (brs, 1H), 8.70 (s, 1H), 8.44 (s, 1H), 6.83 (d, *J* = 7.8 Hz, 1H), 6.77 (d, *J* = 7.8 Hz, 2H), 3.87 (s, 3H), 3.863 (s, 3H), 3.862 (t, *J* = 6.9 Hz, 2H), 3.01 (d, *J* = 4.7 Hz, 3H), 2.93 (t, *J* = 6.9 Hz, 2H), 1.53–1.47 (m, 1H), 0.98–0.89 (m, 4H); ^{13}C NMR (100 MHz, $CDCl_3$) δ 160.4, 160.2, 158.2, 150.1, 148.8, 147.5, 132.2, 120.8, 112.1, 111.2, 111.1, 102.3, 72.1, 62.9, 55.9, 55.8, 37.2, 27.1, 9.1, 0.2; IR (neat)*ν*max: 3859, 3685, 3298, 2771, 2515, 2222, 2037, 1681, 1486, 1400, 1121, 1020; LRMS (ESI) *m/z* calcd for $C_{21}H_{24}N_4O_2$ $[M+H]^+$: 365.19; Found: 365.09.

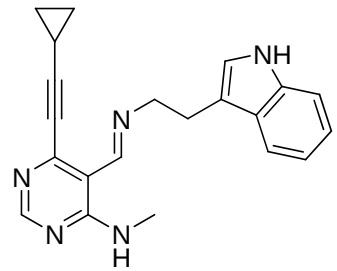

Compound 6é: Brown solid; Yield: 93%; ^{1}H NMR (400 MHz, $CDCl_3$) δ 9.98 (brs, 1H), 8.67 (s, 1H), 8.45 (s, 1H), 7.63 (d, *J* = 8.4 Hz, 1H), 7.37 (d, *J* = 8.4 Hz, 1H), 7.19 (t, *J* = 8.0 Hz, 1H), 7.12 (t, *J* = 8.0 Hz, 1H), 7.00 (s, 1H), 3.94 (t, *J* = 7.2 Hz, 2H), 3.14

(t, *J* = 7.2 Hz, 2H), 2.95 (d, *J* = 4.8 Hz, 3H), 1.45–1.38 (m, 1H), 0.90–0.87 (m, 2H), 0.84–0.81 (m, 2H); ^{13}C NMR (100 MHz, $CDCl_3$) δ 160.4, 160.1, 158.1, 149.9, 136.3, 127.4, 122.0, 121.9, 119.2, 118.7, 113.7, 111.3, 111.2, 102.4, 72.1, 61.9, 27.1, 9.1, 0.2; IR (neat)*ν*max: 3972, 3604, 2948, 2833, 2508, 2223, 2042, 1634, 1512, 1115, 1026, 801; LRMS (ESI) *m/z* calcd for $C_{21}H_{21}N_5$ $[M+H]^+$: 344.18; Found: 344.05.

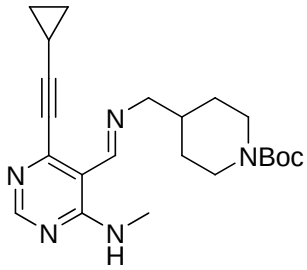

Compound 6f́: Brown solid; Yield: 95% ^{1}H NMR (400 MHz, $CDCl_3$) δ 9.90 (brs, 1H), 8.74 (s, 1H), 8.46 (s, 1H), 4.13 (brs, 2H), 3.52 (d, *J* = 6.0 Hz, 2H), 3.07 (d, *J* = 4.8 Hz, 3H), 2.73 (t, *J* = 11.4 Hz, 2H), 1.82 (brs, 1H), 1.72 (d, *J* = 12.8 Hz, 2H), 1.56–1.50 (m, 1H), 1.47 (s, 9H), 1.26–1.21 (m, 2H), 0.99–0.94 (m, 4H); ^{13}C NMR (100 MHz, $CDCl_3$) δ 160.44, 160.37, 158.2, 154.7, 150.1, 111.1, 102.3, 79.2, 72.1, 67.5, 30.2, 28.3, 27.2, 9.1, 0.2; IR (neat)*ν*max: 3858, 3326, 2942, 2821, 2522, 2222, 2039, 1926, 1633, 1447, 1167, 1021; LRMS (ESI) *m/z* calcd for $C_{22}H_{31}N_5O_2$ $[M+H]^+$: 398.25; Found: 398.19.

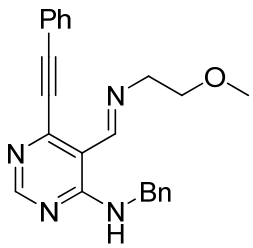

Compound 7á: Pale yellow solid; Yield: 67%; ^{1}H NMR (400 MHz, $CDCl_3$) δ 10.54 (brs, 1H), 8.99 (s, 1H), 8.55 (s, 1H), 7.62 (d, *J* = 7.6 Hz, 2H), 7.42–7.35 (m, 7H), 7.30–7.27 (m, 1H), 4.81 (d, *J* = 5.6 Hz, 2H), 3.81 (t, *J* = 5.6 Hz, 2H), 3.64 (t, *J* = 5.6 Hz, 2H), 3.33 (s, 3H); ^{13}C NMR (100 MHz, $CDCl_3$) δ 161.2, 159.9, 158.5, 150.1, 138.3, 132.1, 129.7, 128.6, 128.5, 127.3, 127.2, 121.4, 111.3, 96.6, 85.0, 72.1, 60.9, 58.9, 44.4; IR (neat)*ν*max: 3858, 3823, 3687, 3360, 3259, 2830, 2510, 2215, 2039, 1714, 1661, 1450, 1400, 1110, 1022; LRMS (ESI) *m/z* calcd for $C_{23}H_{22}N_4O$ $[M+H]^+$: 371.18; Found: 370.99.

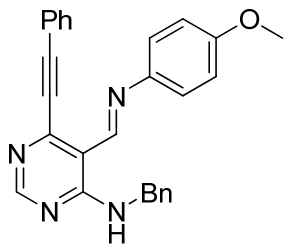

Compound 7b́: Yellow solid; Yield: 62%; ^{1}H NMR (400 MHz, $CDCl_3$) δ 10.70 (brs, 1H), 9.23 (s, 1H), 8.59 (s, 1H), 7.62 (d, *J* = 6.4 Hz, 2H), 7.41–7.30 (m, 8H), 7.20 (d, *J* = 8.4 Hz, 2H), 6.94 (d, *J* = 9.2 Hz, 2H), 4.88 (d, *J* = 5.6 Hz, 2H), 3.83 (s, 3H); ^{13}C NMR (100 MHZ, $CDCl_3$) δ 159.6, 158.9, 158.7, 155.9, 150.8, 143.2, 138.2, 132.2, 129.8, 128.7, 128.6, 127.3, 122.3, 121.3, 114.6, 111.9, 97.1, 85.2, 55.5, 44.6; IR (neat)*ν*max: 3356, 2797, 2523, 2144, 2042, 1680, 1614, 1557, 1472, 1412, 1107, 1017; LRMS (ESI) *m/z* calcd for $C_{27}H_{22}N_4O$ $[M+H]^+$: 419.18; Found: 419.24.

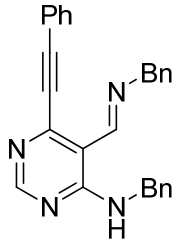

Compound 7ć: Pale yellow solid; Yield: 84%; ^{1}H NMR (400 MHz, $CDCl_3$) δ 10.57 (brs, 1H), 9.05 (s, 1H), 8.56 (s, 1H), 7.58 (d, *J* = 7.6 Hz, 2H), 7.42–7.36 (m, 3H), 7.30-7.24 (m, 7H), 7.22 (d, *J* = 7.6 Hz, 2H), 4.84 (s, 2H), 4.78 (d, *J* = 5.6 Hz, 2H); ^{13}C NMR (100 MHz, $CDCl_3$) δ 160.4, 159.8, 158.6, 150.2, 138.5, 138.1, 132.1, 129.7, 128.60, 128.58, 128.5, 127.8, 127.5, 127.2, 127.2, 121.3, 111.3, 96.6, 85.0, 65.0, 44.5; IR (neat)*ν*max: 3672, 3441, 2828, 2506, 2215, 2037, 1630, 1104, 1027, 796; LRMS (ESI) *m/z* calcd for $C_{27}H_{22}N_4$ $[M+H]^+$: 403.18; Found: 403.06.

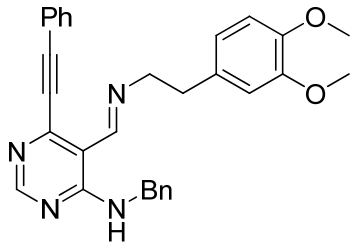

Compound 7d́: Yellow oil; Yield: 88%; ^{1}H NMR (500 MHz, $CDCl_3$) δ 10.53 (brs, 1H), 8.86 (s, 1H), 8.53 (s, 1H), 7.58 (d, *J* = 8.0 Hz, 2H), 7.42–7.28 (m, 8H), 6.69 (s, 3H), 4.78 (d, *J* = 5.5 Hz, 2H), 3.89 (t, *J* = 7.5 Hz, 2H), 3.792 (s, 3H), 3.787 (s, 3H), 2.91 (t, *J* = 7.0 Hz, 2H); ^{13}C NMR (100 MHz, $CDCl_3$) δ 160.02, 159.97, 158.5, 150.0, 148.8, 147.5, 138.5, 132.1, 132.0, 129.7, 128.6, 128.5, 127.2, 121.4, 120.8, 112.0, 111.3, 111.2, 96.5, 85.0, 63.0, 55.8, 55.7, 44.2, 37.1, 14.2; IR (neat)*ν*max: 3976, 3856, 3401, 2806, 2512, 2216, 2042, 1671, 1611, 1555,

1464, 1413, 1021; LRMS (ESI) *m/z* calcd for $C_{30}H_{28}N_4O_2$ $[M+H]^+$: 477.22; Found: 477.17.

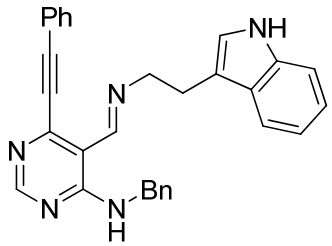

Compound 7é: Pale yellow solid; Yield: 85%; ^{1}H NMR (400 MHz, $CDCl_3$) δ 10.58 (brs, 1H), 8.82 (s, 1H), 8.53 (s, 1H), 7.89 (brs, 1H), 7.60 (d, *J* = 8.0 Hz, 1H), 7.48–7.45 (m, 2H), 7.41–7.29 (m, 8H), 7.17 (t, *J* = 7.2 Hz, 1H), 7.10 (t, *J* = 7.2 Hz, 1H), 6.8s1 (d, *J* = 2.4 Hz, 1H), 4.75 (d, *J* = 6.0 Hz, 2H), 3.96 (t, *J* = 6.8 Hz, 2H), 3.10 (t, *J* = 6.8 Hz, 2H); ^{13}C NMR (100 MHZ, $CDCl_3$) δ 159.94, 159.90, 158.4, 149.8, 138.6, 136.2, 132.1, 131.8, 129.7, 128.9, 128.8, 128.6, 128.5, 128.3, 127.4, 127.3, 127.2, 126.3, 122.1, 122.0, 121.3, 119.2, 118.6, 113.5, 111.3, 111.2, 96.6, 84.9, 61.6, 44.2, 27.0; IR (neat)*v*max: 3980, 3856, 3383, 2945, 2830, 2501, 2233, 2037, 1681, 1612, 1557, 1530, 1473, 1407, 1209, 1116, 1021; LRMS (ESI) *m/z* calcd for $C_{30}H_{25}N_5$ $[M+H]^+$: 456.21; Found: 456.15.

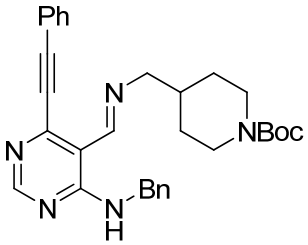

Compound 7f́: Yellow oil; Yield: 86%; ^{1}H NMR (400 MHz, $CDCl_3$) δ ^{1}H NMR (400 MHz, $CDCl_3$) δ 10.43 (brs, 1H), 8.91 (s, 1H), 8.57 (s, 1H), 7.61 (dd, *J* = 7.8 Hz, *J* = 1.6 Hz, 2H), 7.43–7.31 (m, 8H), 4.77 (d, *J* = 5.5 Hz, 2H), 4.06 (brs, 2H), 3.49 (d, *J* = 6.6 Hz, 2H), 2.62 (t, *J* = 11.4 Hz, 2H), 1.69–1.63 (m, 1H), 1.57 (d, *J* = 15.2 Hz, 2H), 1.46 (s, 9H), 1.16-1.05 (m, 2H); ^{13}C NMR (100 MHz, $CDCl_3$) δ 162.5, 160.0, 159.7, 158.5, 154.8, 149.9, 138.0, 132.1, 129.8, 128.6, 128.5, 127.8, 127.5, 121.3, 111.2, 96.6, 84.9, 79.3, 67.3, 44.8, 37.7, 36.4, 31.4, 30.2, 28.4, 28.3; IR (neat)*v*max: 3855, 3673, 3321, 2829, 2506, 2215, 2043, 1423, 1026; LRMS (ESI) *m/z* calcd for $C_{31}H_{35}N_5O_2$ $[M+H]^+$: 510.28; Found: 510.24.

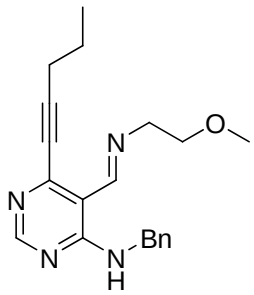

Compound 8á: Brown oil; Yield: 66%; ^{1}H NMR (400 MHz, $CDCl_3$) δ 10.49 (brs, 1H), 8.88 (s, 1H), 8.48 (s, 1H), 7.34 (d, *J* = 4.4 Hz, 4H), 7.30–7.25 (m, 1H), 4.79 (d, *J* = 5.6 Hz, 2H), 3.77 (t, *J* = 6.0 Hz, 2H), 3.62 (t, *J* = 6.0 Hz, 2H), 3.32 (s, 3H), 2.48 (t, *J* = 7.2 Hz, 2H), 1.73–1.64 (m, 2H), 1.07 (t, *J* = 7.2 Hz, 3H); ^{13}C NMR (100 MHz, $CDCl_3$) δ 161.6, 159.9, 158.4, 150.7, 138.4, 128.5, 127.3, 127.1, 111.1, 99.1, 72.2, 60.8, 58.9, 44.3, 21.6, 21.5, 13.6; IR (neat)*ν*max: 3453, 2936, 2833, 2229, 1643, 1604, 1554, 1522, 1450, 1113, 1030, 798, 742, 670, 645; LRMS (ESI) *m/z* calcd for $C_{20}H_{24}N_4O$ $[M+H]^+$: 337.20; Found: 337.06.

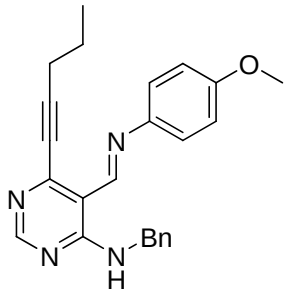

Compound 8b́: Yellow solid; Yield: 69%; ^{1}H NMR (400 MHz, $CDCl_3$) δ 10.65 (t, *J* = 4.9 Hz, 1H), 9.13 (s, 1H), 8.52 (s, 1H), 7.40-7.29 (m, 5H), 7.17 (d, *J* = 8.4 Hz, 2H), 6.93 (d, *J* = 8.4 Hz, 2H), 4.85 (d, *J* = 5.5 Hz, 2H), 3.83 (s, 3H), 2.50 (t, *J* = 7.0 Hz, 2H), 1.75–1.65 (m, 2H), 1.08 (t, *J* = 7.4 Hz, 3H); ^{13}C NMR (100 MHz, $CDCl_3$) δ 159.6, 158.8, 158.6, 156.4, 151.4, 143.3, 138.3, 128.6, 127.3, 127.3, 122.3, 114.5, 111.7, 99.7, 77.2, 55.5, 44.5, 21.7, 21.6, 13.7; IR (neat)*ν*max: 3857, 3686, 3332, 2941, 2830, 2941, 2228, 2040, 1412, 1022; LRMS (ESI) *m/z* calcd for $C_{24}H_{24}N_4O$ $[M+H]^+$: 385.20; Found: 385.14.

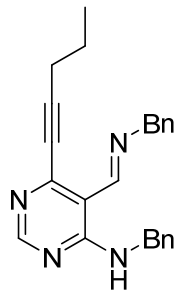

Compound 8ć: Brown solid; Yield: 94%; ^{1}H NMR (400 MHz, $CDCl_3$) δ 10.51 (brs, 1H), 8.95 (s, 1H), 8.49 (s, 1H), 7.33–7.26 (m, 8H), 7.21 (d, *J* = 7.2 Hz, 2H), 4.80 (s, 2H), 4.76 (d, *J* = 5.2 Hz, 2H), 2.47 (t, *J* = 7.2 Hz, 2H), 1.73–1.64 (m, 2H), 1.07 (t, *J* = 7.2 Hz, 3H); ^{13}C NMR (100 MHZ, $CDCl_3$) δ 160.9, 159.8, 158.6, 150.8, 138.7, 138.2, 128.6, 128.5, 127.7, 127.4, 127.2, 127.1, 111.2, 99.2, 65.0, 44.4, 21.6, 21.5, 13.7; IR (neat)*ν*max: 3981, 3857, 3351,

2830, 2498, 2217, 2043, 1695, 1406, 1022; LRMS (ESI) *m/z* calcd for $C_{24}H_{24}N_4$ $[M+H]^+$: 369.20; Found: 369.12.

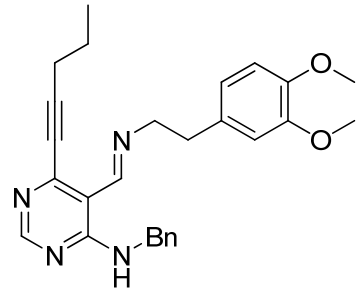

Compound 8d́: Brown oil; Yield: 83%; ^{1}H NMR (500 MHz, $CDCl_3$) δ 10.48 (brs, 1H), 8.76 (s, 1H), 8.46 (s, 1H), 7.34–7.26 (m, 5H), 6.71-6.66 (m, 3H), 4.76 (d, *J* = 5.5 Hz, 2H), 3.85 (t, *J* = 7.0 Hz, 2H), 3.82 (s, 3H), 3.81 (s, 3H), 2.89 (t, *J* = 7.0 Hz, 2H), 2.45 (t, *J* = 7.5 Hz, 2H), 1.70–1.63 (m, 2H), 1.05 (t, *J* = 7.5 Hz, 3H); ^{13}C NMR (100 MHZ, $CDCl_3$) δ 160.3, 159.9, 158.4, 150.5, 148.8, 147.4, 138.5, 132.0, 128.6, 128.5, 127.7, 127.3, 127.1, 120.8, 111.9, 111.1, 99.1, 62.9, 55.8, 55.7, 44.1, 37.1, 21.6, 21.5, 13.6; IR (neat)*ν*max: 3974, 3857, 3746, 3405, 2943, 2828, 2506, 2230, 2043, 1695, 1404, 1112, 1024; LRMS (ESI) *m/z* calcd for $C_{27}H_{30}N_4O_2$ $[M+H]^+$: 443.24; Found: 443.15.

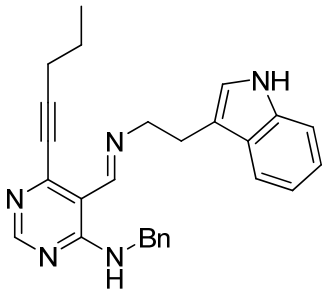

Compound 8é: Pale orange solid; Yield: 84%; ^{1}H NMR (400 MHz, $CDCl_3$) δ 10.54 (brs, 1H), 8.75 (s, 1H), 8.46 (s, 1H), 7.92 (brs, 1H), 7.59 (d, *J* = 7.8 Hz, 1H), 7.33–7.25 (m, 6H), 7.18 (t, *J* = 7.4 Hz, 1H), 7.10 (t, *J* = 7.4 Hz, 1H), 6.79 (s, 1H), 4.72 (d, *J* = 5.5 Hz, 2H), 3.93 (t, *J* = 6.8 Hz, 2H), 3.08 (t, *J* = 6.8 Hz, 2H), 2.39 (t, *J* = 7.0 Hz, 2H), 1.65-1.56 (m, 2H), 1.01 (t, *J* = 7.4 Hz, 3H); ^{13}C NMR (100 MHz, $CDCl_3$) δ 160.2, 159.9, 158.3, 150.4, 138.7, 136.2, 128.5, 127.4, 127.3, 127.1, 122.0, 121.9, 119.2, 118.6, 113.5, 111.19, 111.16, 99.1, 76.7, 61.5, 44.1, 27.1, 21.6, 21.4, 13.6; IR (neat)*ν*max: 3858, 3597, 2948, 2831, 2530, 2229, 2039, 1568, 1118, 1023, 744; LRMS (ESI) *m/z* calcd for $C_{27}H_{27}N_5$ $[M+H]^+$: 422.23; Found: 422.17.

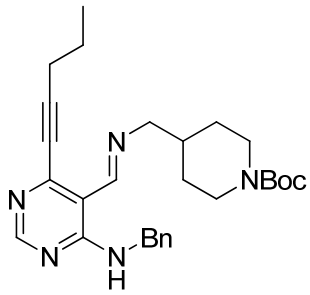

Compound 8f́: Yellow oil; Yield: 92%; ^{1}H NMR (400 MHz, $CDCl_3$) δ 10.38 (brs, 1H), 8.81 (s, 1H), 8.49 (s, 1H), 7.37–7.30 (m, 5H), 4.74 (d, *J* = 5.2 Hz, 2H), 4.05 (brs, 2H), 3.45 (d, *J* = 6.4 Hz, 2H), 2.61 (t, *J* = 12.0 Hz, 2H), 2.48 (t, *J* = 7.2 Hz, 2H), 1.72–1.63 (m, 3H), 1.55 (d, *J* = 12.4 Hz, 2H), 1.47 (s, 9H), 1.11 (td, *J* = 12.4 Hz, *J* = 4.0 Hz, 2H), 1.07 (t, *J* = 7.2 Hz, 3H); ^{13}C NMR (100 MHz, $CDCl_3$) δ 160.4, 159.7, 158.4, 154.8, 150.5, 138.1, 128.6, 127.7, 127.4, 111.0, 99.2, 79.3, 77.0, 67.2, 44.7, 37.7, 30.2, 28.4, 21.6, 21.5, 13.6; IR (neat)*ν*max: 3862, 3432, 2827, 2522, 2229, 2039, 1695, 1450, 1024; LRMS (ESI) *m/z* calcd for $C_{28}H_{37}N_5O_2$ $[M+H]^+$: 476.29; Found: 476.31.

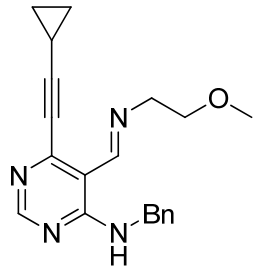

Compound 9á: Brown oil; Yield: 87%; ^{1}H NMR (400 MHz, $CDCl_3$) δ 10.49 (brs, 1H), 8.83 (s, 1H), 8.45 (s, 1H), 7.34 (d, *J* = 4.3 Hz, 4H), 7.30-7.24 (m, 1H), 4.78 (d, *J* = 5.8 Hz, 2H), 3.77 (t, *J* = 5.3 Hz, 2H), 3.62 (t, *J* = 5.3 Hz, 2H), 3.33 (s, 3H), 1.56–1.49 (m, 1H), 0.97-0.94 (m, 4H); ^{13}C NMR (100 MHZ, $CDCl_3$) δ 161.5, 159.9, 158.4, 150.6, 138.4, 128.5, 127.3, 127.1, 111.1, 102.5, 72.2, 60.8, 58.9, 44.3, 9.2, 0.3; IR (neat)*ν*max: 3972, 3858, 3347, 2516, 2223, 2040, 1494, 1192, 1115, 1023; LRMS (ESI) *m/z* calcd for $C_{20}H_{22}N_4O$ $[M+H]^+$: 335.18; Found: 335.04.

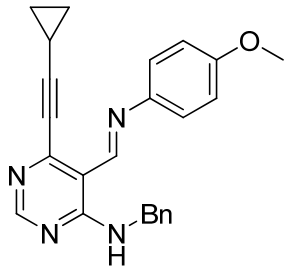

Compound 9b́: Brown solid; Yield: 61%; ^{1}H NMR (400 MHz, $CDCl_3$) δ 10.63 (brs, 1H), 9.06 (s, 1H), 8.50 (s, 1H), 7.40–7.34 (m, 4H), 7.29 (d, *J* = 6.7 Hz, 1H), 7.17 (d, *J* = 8.8 Hz, 2H), 6.94 (d, *J* = 8.8 Hz, 2H), 4.84 (d, *J* = 5.9 Hz, 2H), 3.83 (s, 3H), 1.58–1.52 (m, 1H), 1.00-0.94 (m, 4H); ^{13}C NMR (100 MHZ, $CDCl_3$) δ 159.6, 158.7, 158.6, 156.4, 151.3, 143.3, 138.3, 128.6, 127.3, 127.3, 122.3, 116.4, 114.8, 114.6, 111.7,

103.2, 72.3, 55.5, 44.5, 9.3, 0.4; IR (neat)*v*max: 3859, 3690, 3357, 2826, 2506, 2221, 2040, 1696, 1615, 1567, 1414, 1020; LRMS (ESI) *m/z* calcd for $C_{24}H_{22}N_4O$ $[M+H]^+$: 383.18; Found: 383.10.

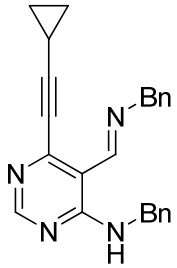

Compound 9ć: Orange solid; Yield: 95%; ^{1}H NMR (400 MHz, $CDCl_3$) δ 10.55 (brs, 1H), 8.88 (s, 1H), 8.46 (s, 1H), 7.32–7.24 (m, 8H), 7.19 (d, *J* = 8.0 Hz, 2H), 4.79 (s, 2H), 4.74 (d, *J* = 5.6 Hz, 2H), 1.53-1.50 (m, 1H), 0.97–0.93 (m, 4H); ^{13}C NMR (100 MHZ, $CDCl_3$) δ 160.7, 159.8, 158.2, 150.3, 138.6, 138.1, 128.6, 128.5, 127.7, 127.4, 127.2, 127.1, 111.0, 98.9, 71.9, 64.9, 44.5, 9.3, 0.3; IR (neat)*v*max: 3857, 3698, 3389, 2825, 2500, 2223, 2042, 1447, 1023; LRMS (ESI) *m/z* calcd for $C_{24}H_{22}N_4$ $[M+H]^+$: 367.18; Found: 367.09.

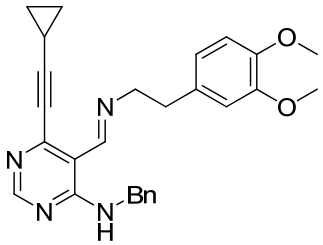

Compound 9d́: Brown oil; Yield: 92%; ^{1}H NMR (400 MHz, $CDCl_3$) δ 10.49 (brs, 1H), 8.71 (s, 1H), 8.44 (s, 1H), 7.35–7.26 (m, 5H), 6.69 (t, *J* = 6.5 Hz, 3H), 4.75 (d, 5.9 Hz, 2H), 3.85 (t, *J* = 7.0 Hz, 2H), 3.82 (s, 3H), 3.81 (s, 3H), 2.89 (t, *J* = 7.0 Hz, 2H), 1.54–1.47 (m, 1H), 0.98-0.89 (m, 4H); ^{13}C NMR (100 MHz, $CDCl_3$) δ 160.3, 160.1, 158.0, 148.9, 147.6, 138.5, 132.2, 128.7, 127.32, 127.31, 120.9, 112.1, 111.2, 111.1, 63.0, 56.0, 55.9, 44.3, 37.3, 9.4, 0.3; IR (neat)*v*max: 3857, 3360, 2823, 2514, 2222, 2040, 1680, 1612, 1558, 1478, 1024; LRMS (ESI) *m/z* calcd for $C_{27}H_{28}N_4O_2$ $[M+H]^+$: 441.22; Found: 441.16.

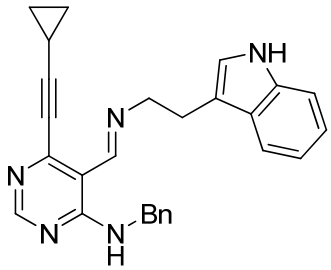

Compound 9é: Yellow solid; Yield: 71%; ^{1}H NMR (400 MHz, $CDCl_3$) δ 10.53 (brs, 1H), 8.70 (s, 1H), 8.44 (s, 1H), 7.79 (brs, 1H), 7.60 (d, *J* = 8.0 Hz, 1H), 7.35–7.21 (m, 5H), 7.19 (t, *J* = 7.4 Hz, 1H), 7.11 (t, *J* = 7.4 Hz, 1H), 6.79 (s, 1H), 4.72 (d, *J* = 5.6 Hz,

2H), 3.93 (t, *J* = 6.8 Hz, 2H), 3.08 (t, *J* = 6.8 Hz, 2H), 1.47–1.43 (m, 1H), 0.95-0.84 (m, 4H); ^{13}C NMR (100 MHz, $CDCl_3$) δ 160.1, 159.9, 158.2, 150.3, 138.6, 136.2, 128.5, 127.35, 127.27, 127.1, 122.0, 121.9, 119.2, 118.6, 113.5, 111.2, 111.1, 102.6, 72.1, 61.5, 44.1, 27.1, 9.1, 0.3; IR (neat)*ν*max: 3977, 3857, 3682, 3374, 2806, 2502, 2224, 2038, 1402, 1113, 1025; LRMS (ESI) *m/z* calcd for $C_{27}H_{25}N_5$ $[M+H]^+$: 420.21; Found: 420.13.

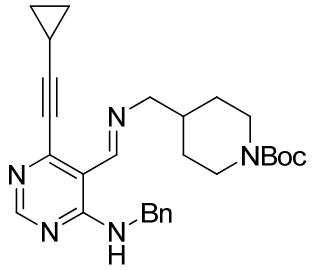

Compound 9f́: Yellow oil; Yield: 92%; ^{1}H NMR (400 MHz, $CDCl_3$) δ 10.38 (brs, 1H), 8.76 (s, 1H), 8.47 (s, 1H), 7.35–7.30 (m, 5H), 4.73 (d, *J* = 5.2 Hz, 2H), 4.05 (brs, 1H), 3.45 (d, *J* = 6.8 Hz, 2H), 2.61 (t, *J* = 10.8 Hz, 2H), 1.65–1.62 (m, 1H), 1.57-1.51 (m, 3H), 1.47 (s, 9H), 1.11-1.07 (m, 2H), 0.98-0.95 (m, 4H); ^{13}C NMR (100 MHz, $CDCl_3$) δ 160.3, 159.6, 158.3, 154.7, 150.4, 138.1, 128.6, 127.7, 127.4, 111.0, 102.5, 79.3, 72.1, 67.2, 44.7, 37.7, 30.2, 28.4, 9.2, 0.3; IR (neat)*ν*max: 3973, 3857, 3571, 2941, 2831, 2517, 2224, 2042, 1571, 1023; LRMS (ESI) *m/z* calcd for $C_{28}H_{35}N_5O_2$ $[M+H]^+$: 474.28; Found: 474.14.

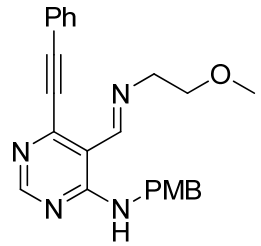

Compound 10á: Yellow solid; Yield: 95%; ^{1}H NMR (400 MHz, $CDCl_3$) δ 10.46 (t, *J* = 5.5 Hz, 1H), 8.98 (s, 1H), 8.55 (s, 1H), 7.61 (dd, *J* = 7.6 Hz, *J* = 1.8 Hz, 2H), 7.44–7.36 (m, 3H), 7.29 (d, *J* = 8.6 Hz, 2H), 6.89 (d, *J* = 8.6 Hz, 2H), 4.73 (d, *J* = 5.5 Hz, 2H), 3.80 (s, 3H), 3.77 (t, *J* = 5.5 Hz, 2H), 3.63 (t, *J* = 5.5 Hz, 2H), 3.33 (s, 3H); ^{13}C NMR (100 MHz, $CDCl_3$) δ 161.2, 159.8, 158.8, 158.5, 150.1, 132.1, 130.4, 129.7, 128.7, 128.5, 121.4, 114.0, 111.3, 96.5, 85.0, 72.2, 60.9, 58.9, 55.2, 43.9; IR (neat)*ν*max: 3591, 2947, 2836, 2504, 2039, 1649, 1116, 1020; LRMS (ESI) *m/z* calcd for $C_{24}H_{24}N_4O_2$ $[M+H]^+$: 401.19; Found: 401.15.

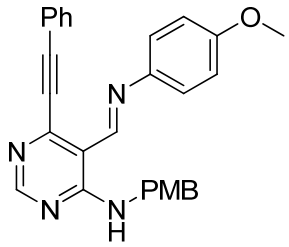

Compound 10b́: Yellow solid; Yield: 92%; ^{1}H NMR (400 MHz, $CDCl_3$) δ 10.63 (brs, 1H), 9.22 (s, 1H), 8.59 (s,1H), 7.62 (d, *J* = 7.2 Hz, 2H), 7.44–7.38 (m, 3H), 7.34 (d, *J* = 8.4 Hz, 2H), 7.20 (d, *J* = 8.8 Hz, 2H), 6.94 (d, *J* = 8.8 Hz, 2H), 6.91 (d, *J* = 8.4 Hz, 2H), 4.80 (d, *J* = 5.6 Hz, 2H), 3.84 (s, 3H), 3.82 (s, 3H); ^{13}C NMR (100 MHz, $CDCl_3$) δ 159.5, 158.89, 159.87, 158.7, 155.9, 150.7, 143.2, 132.2, 130.2, 129.8, 128.7, 128.6, 122.3, 121.4, 114.6, 114.1, 111.9, 97.1, 85.1, 55.5, 55.3, 44.1; IR (neat)*v*max: 3974, 3856, 3660, 3372, 2831, 2516, 2225, 2040, 1473, 1118, 1021; LRMS (ESI) *m/z* calcd for $C_{28}H_{24}N_4O_2$ $[M+H]^+$: 449.19; Found: 449.15.

4. General synthetic procedure for compounds 4a–10a

To a DCE solution of **4á**–**10á** (0.3 mmol), AgOTf (10 mol%) and AcOH (2.0 equiv.) were added. After stirring at 80 °C for 2 h (the reaction completion was monitored by TLC), the reaction mixture was filtered under Na_2SO_4 pad and washed thrice with DCM. After the removal of solvent under the reduced pressure, the reaction mixture was dissolved with dimethylformamide (DMF) and added with 1,8-diazabicyclo[5.4.0]undec-7-ene (DBU) (3.0 equiv.) and dimethylmalonates (3.0 equiv.). The resulting mixture was stirred at 80 °C for 2 h. The resultant was quenched by addition of deionized water and extracted twice with ethyl acetate (EtOAc). The combined organic layer was washed with brine and dried with anhydrous Na_2SO_4(s). After the solvent was removed under the reduced pressure, the residue was purified by silica-gel flash column chromatography to obtain **4a**–**10a**.

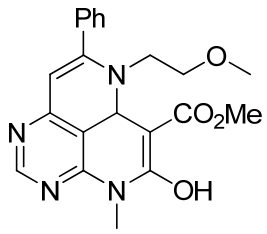

Compound 4a: Yield: 97%; Yellow solid; mp: 124–128 ^{o}C; ^{1}H NMR (500 MHz, $CDCl_3$) δ 11.10 (s, 1H), 8.71 (s, 1H), 8.62 (s, 1H), 7.49–7.47 (m, 3H), 7.44–7.42 (m, 2H), 5.55 (s, 1H), 3.91 (s, 3H), 3.77 (s, 3H), 3.49 (t, *J* = 5.5 Hz, 2H), 3.42 (t, *J* = 6.0 Hz, 2H), 3.40 (s, 3H); ^{13}C NMR (100 MHz, $CDCl_3$) δ 165.5, 163.6, 162.8, 159.9, 157.8, 155.1, 138.6, 136.4, 129.5, 128.6, 127.8, 119.6, 104.5, 89.3, 71.9, 59.0, 52.5, 44.9, 28.6; IR (neat)*ν*max: 3859, 3526, 2948, 2834, 2413, 2041, 1661, 1568, 1119, 1021 cm^{-1}; HRMS (FAB+) *m/z* calcd for $C_{21}H_{22}N_4O_4$ $[M+H]^+$: 395.1719; Found: 395.1728; Registration No.: 1477473-56-5.

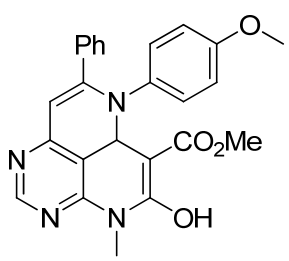

Compound 4b: Yield: 70%; Scarlet solid; mp: 141–145 ^{o}C; ^{1}H NMR (500 MHz, $CDCl_3$) δ 12.58 (s, 1H), 8.79 (s, 1H), 8.73 (s, 1H), 7.42–7.36 (m, 5H), 6.77 (d, *J* = 8.5 Hz, 2H), 6.70 (d, *J* = 8.0 Hz, 2H), 5.86 (s, 1H), 3.96 (s, 3H), 3.80 (s, 3H), 3.74 (s, 3H); ^{13}C NMR (125 MHz, $CDCl_3$) δ 165.4, 162.6, 159.7, 158.9, 157.7, 156.4, 155.2, 138.4, 136.6, 132.8, 129.5, 128.52, 128.49, 124.7, 120.4, 114.0, 105.3, 92.1, 55.3, 52.6, 28.7; IR (neat)*ν*max: 3858, 3607, 2944, 2832, 2437, 2041, 1661, 1110, 1022 cm^{-1}; HRMS (FAB+) *m/z* calcd for $C_{25}H_{22}N_4O_4$ $[M+H]^+$:443.1719; Found: 443.1728; Registration No.: 1477473-54-3.

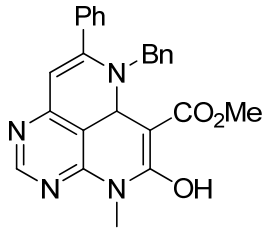

Compound 4c: Yield: 76%; Yellow solid; mp: 126–130 ^{o}C; ^{1}H NMR (400 MHz, $CDCl_3$) δ 11.31 (brs, 1H), 8.66 (s, 1H), 8.64 (s, 1H), 7.47–7.40 (m, 5H), 7.34 (t, *J* = 7.2 Hz, 2H), 7.28 (d, *J* = 7.2 Hz, 1H), 7.23 (d, *J* = 7.2 Hz, 2H), 5.62 (s, 1H), 4.48(d, *J* = 6.2 Hz, 2H), 3.92 (s, 3H), 3.77 (s, 1H); ^{13}C NMR (100 MHz, $CDCl_3$) δ 165.5, 163.8, 163.0, 159.9, 157.9, 155.2, 138.8, 138.6, 136.2, 129.6, 128.7, 128.6, 127.8, 127.4, 126.7, 120.0,

112.5, 104.7, 89.8, 63.9, 52.6, 48.9, 28.6; IR (neat)*v*max: 3985, 3857, 3623, 2506, 2229, 2041, 1661, 1450, 1106, 1023 cm^{-1}; HRMS (ESI) *m/z* calcd for $C_{25}H_{22}N_4O_3$ $[M+Na]^+$: 449.1590; Found: 449.1584.

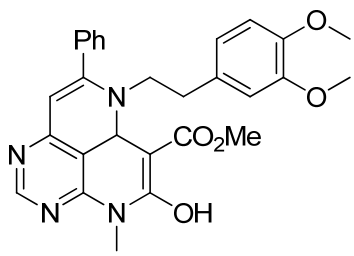

Compound 4d: Yield: 69%; Yellow solid; mp: 145–149 °C; ^1H NMR (400 MHz, $CDCl_3$) δ 10.96 (brs, 1H), 8.59 (s, 1H), 8.55 (s, 1H), 7.46–7.44 (m, 3H), 7.31-7.29 (m, 2H), 6.80 (d, *J* = 8.0 Hz, 1H), 6.70 (d, *J* = 8.0 Hz, 1H), 6.60 (s, 1H), 5.48 (s, 1H), 3.95 (s, 3H), 3.91 (s, 3H), 3.77 (s, 3H), 3.76 (s, 3H), 3.49 (q, *J* = 6.4 Hz, 2H), 2.79 (t, *J* = 6.4 Hz, 2H); ^{13}C NMR (100 MHz, $CDCl_3$) δ 165.5 163.7, 162.7, 159.9, 157.7, 155.1, 149.0, 147.9, 138.6, 136.5, 130.8, 129.4, 128.5, 127.7, 121.0, 119.6, 112.0, 111.2, 104.4, 89.2, 77.2, 56.0, 55.7, 52.5, 46.9, 37.0, 28.6; IR (neat)*v*max: 3858, 3466, 2831, 2226, 2039, 1681, 1414, 1112, 1024 cm^{-1}; HRMS (ESI) *m/z* calcd for $C_{28}H_{28}N_4O_5$ $[M+Na]^+$: 523.1957; Found: 523.1954.

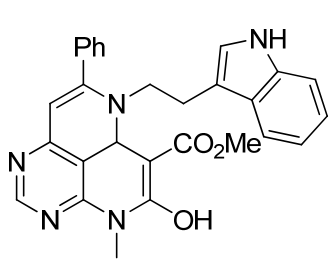

Compound 4e: Yield: 62%; Scarlet solid; mp: 155–159 °C; ^1H NMR (500 MHz, $CDCl_3$) δ 11.00 (brs, 1H), 8.58 (s, 1H), 8.37 (s, 1H), 8.07 (brs, 1H), 7.46-7.38 (m, 5H), 7.33 (dd, *J* = 7.8 Hz, *J* = 1.0 Hz, 2H), 7.20 (t, *J* = 7.4 Hz, 1H), 7.07-7.04 (m, 2H), 5.48 (s, 1H), 3.90 (s, 3H), 3.75 (s, 3H), 3.59 (q, *J* = 6.9 Hz, 2H), 3.01 (t, *J* = 6.9 Hz, 2H); ^{13}C NMR (100 MHz, $CDCl_3$) δ 165.5, 163.8, 162.6, 159.9, 157.7, 155.1, 138.7, 136.5, 136.3, 129.4, 128.6, 127.7, 127.2, 122.6, 122.2, 119.4, 118.5, 112.3, 111.3, 104.4, 89.1, 52.5, 45.8, 28.6, 26.9; IR (neat)*v*max: 3760, 3452, 2920, 2834, 2524, 2231, 2043, 1734, 1649, 1553, 1454, 1284, 1230 ,1120, 1027, 800, 733 cm^{-1}; HRMS (ESI) *m/z* calcd for $C_{28}H_{25}N_5O_3$ $[M+Na]^+$: 502.1855; Found: 502.1847.

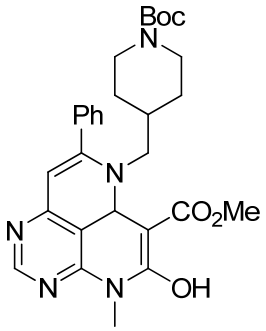

Compound 4f: Yield: 78%; Yellow solid; mp: 136–140 °C; ^{1}H NMR (500 MHz, $CDCl_3$) δ 11.03 (brs, 1H), 8.68 (s, 1H), 8.61 (s, 1H), 7.49 (t, *J* = 3.0 Hz, 3H), 7.42–7.40 (m, 2H), 5.54 (s, 1H), 4.11 (brs, 2H), 3.92 (s, 3H), 3.77 (s, 3H), 3.16 (t, *J* = 6.4 Hz, 2H), 2.67 (brs, 2H), 1.69–1.61 (m, 3H), 1.44 (s, 9H), 1.15–1.07 (m, 2H)s; ^{13}C NMR (100 MHz, $CDCl_3$) δ 165.5, 164.0, 162.7, 159.8, 157.8, 155.2, 154.7, 138.6, 136.4, 129.6, 128.7, 127.8, 119.8, 104.6, 89.3, 79.5, 52.5, 50.8, 37.8, 29.7, 28.6, 28.4; IR (neat)*ν*max: 3979, 3856, 3647, 2947, 2833, 2451, 2226, 2040, 1668, 1023 cm^{-1}; HRMS (ESI) *m/z* calcd for $C_{29}H_{35}N_5O_5$ $[M+Na]^+$: 556.2536; Found: 556.2533.

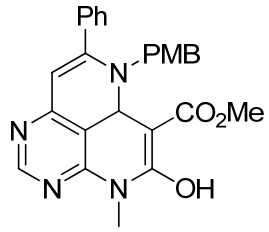

Compound 4g: Yield: 78%; Yellow solid; mp: 142–146 °C; ^{1}H NMR (400 MHz, $CDCl_3$) δ 11.25 (brs, 1H), 8.65 (s, 1H), 8.63 (s, 1H), 7.48–7.40 (m, 5H), 7.14 (d, *J* = 8.8 Hz, 2H), 6.87 (d, *J* = 8.8 Hz, 2H), 5.60 (s, 1H), 4.40 (d, *J* = 6.0 Hz, 2H), 3.92 (s, 3H), 3.80 (s, 3H), 3.77 (s, 3H); ^{13}C NMR (100 MHz, $CDCl_3$) δ 165.6, 163.7, 162.9, 159.9, 158.9, 157.9, 155.2, 138.6, 136.3, 130.7, 129.6, 128.6, 128.0, 127.8, 119.9, 114.1, 104.7, 89.6, 55.3, 53.7, 52.6, 48.5, 29.7, 28.6; IR (neat)*ν*max: 3857, 3526, 2942, 2830, 2410, 2222, 2043, 1648, 1118, 1026 cm^{-1}; HRMS (ESI) *m/z* calcd for $C_{26}H_{24}N_4O_4$ $[M+Na]^+$: 479.1695; Found: 479.1690.

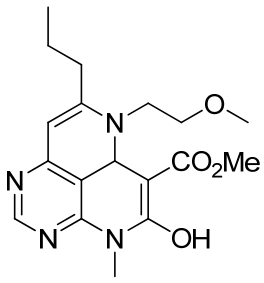

Compound 5a: Yield: 77%; Yellow solid; mp: 131–135 °C; ^{1}H NMR (500 MHz, $CDCl_3$) δ 11.17 (s, 1H), 8.67 (s, 1H), 8.57 (s, 1H), 5.48 (s, 1H), 3.96 (s, 3H), 3.75 (s, 3H), 3.62 (t, *J* = 5.0 Hz, 2H), 3.57 (t, *J* = 5.0 Hz, 2H), 3.45 (s, 3H), 2.40 (t, *J* = 8.0 Hz, 2H), 1.71–1.61 (m, 2H), 1.06 (t, *J* = 7.0 Hz, 3H); ^{13}C NMR (100 MHZ, $CDCl_3$) δ 165.9,

165.4, 162.7, 160.0, 157.8, 155.1, 138.9, 118.9, 103.8, 86.8, 71.6, 59.1, 52.5, 43.2, 35.8, 29.6, 28.5, 22.0, 14.0; IR (neat)*ν*max: 3858, 3600, 2947, 2830, 2446, 2042, 1536, 1117, 1021 cm^{-1}; HRMS (FAB+) *m/z* calcd for $C_{18}H_{24}N_4O_4$ $[M+H]^+$: 361.1876; Found: 361.1873; Registration No.:1477473-62-3.

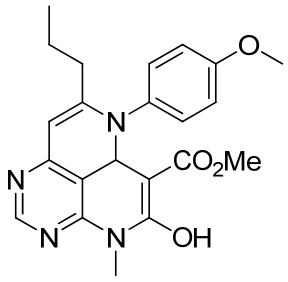

Compound 5b: Yield: 83%; Scarlet solid; mp: 124–128 °C; ^{1}H NMR (500 MHz, $CDCl_3$) δ 12.51 (s, 1H), 8.73 (s, 1H), 8.63 (s, 1H), 7.13 (d, *J* = 8.5 Hz, 2H), 6.93 (d, *J* = 9.0 Hz, 2H), 5.66 (s, 1H), 3.98 (s, 3H), 3.85 (s, 3H), 3.77 (s, 3H), 2.40 (t, *J* = 7.5 Hz, 2H), 1.59–1.54 (m, 2H), 0.90 (t, *J* = 7.5 Hz, 3H); ^{13}C NMR (125 MHZ, $CDCl_3$) δ 165.8, 164.2, 162.7, 159.8, 157.7, 157.5, 155.1, 138.8, 138.6, 131.3, 127.3, 119.5, 114.4, 104.2, 87.6, 55.5, 52.6, 35.4, 28.6, 22.1, 13.8; IR (neat)*ν*max: 3987, 3856, 3611, 3516, 2514, 2227, 2041, 1680, 1446, 1117, 1026 cm^{-1}; HRMS (FAB+) *m/z* calcd for $C_{22}H_{24}N_4O_4$ $[M+H]^+$: 409.1876; Found: 409.1882; Registration No.: 1477473-60-1.

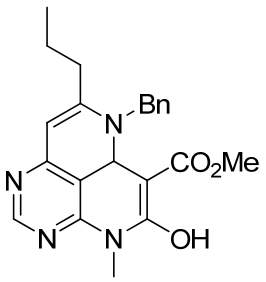

Compound 5c: Yield: 79%; Brown oil; ^{1}H NMR (400 MHz, $CDCl_3$) δ 11.40 (brs, 1H), 8.70 (s, 1H), 8.54 (s, 1H), 7.41–7.30 (m, 5H), 5.55 (s, 1H), 4.64 (d, *J* = 6.4 Hz, 2H), 3.97 (s, 3H), 3.75 (s, 3H), 2.40 (t, *J* = 7.6 Hz, 2H), 1.71–1.63 (m, 3H), 1.04 (t, *J* = 7.6 Hz, 3H); ^{13}C NMR (100 MHz, $CDCl_3$) δ 165.8, 165.6, 162.9, 157.8, 155.1, 138.9, 138.2, 128.9, 128.3, 127.8, 127.6, 126.6, 119.1, 104.0, 87.2, 52.6, 47.1, 35.7, 28.6, 14.1; IR (neat)*ν*max: 3981, 3857, 3444, 2231, 2041, 1683, 1453, 1024 cm^{-1}; HRMS (ESI) *m/z* calcd for $C_{22}H_{24}N_4O_3$ $[M+Na]^+$: 415.1746; Found: 415.1742.

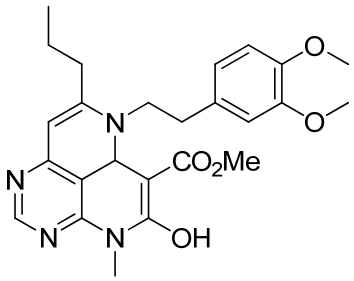

Compound 5d: Yield: 58%; Brown oil; ^{1}H NMR (500 MHz, $CDCl_3$) δ 11.03 (brs, 1H), 8.65 (s, 1H), 8.41 (s, 1H), 6.86–6.83 (m, 2H), 6.76 (s, 1H), 5.43 (s, 1H), 3.96 (s, 3H), 3.88 (s, 3H), 3.83 (s, 3H), 3.74 (s, 3H), 3.64 (q, *J* = 6.9 Hz, 2H), 2.92 (t, *J* = 6.9 Hz, 2H), 2.32 (t, *J* = 7.9 Hz, 2H), 1.66–1.61 (m, 2H), 1.04 (t, *J* = 7.4 Hz, 3H); ^{13}C NMR (100 MHz, $CDCl_3$) δ 165.9, 165.3, 162.6, 159.9, 157.6, 155.1, 149.0, 148.0, 138.8, 130.7, 120.9, 118.9, 112.1, 111.3, 103.7, 86.6, 55.9, 55.8, 52.5, 45.2, 36.3, 35.7, 28.5, 22.0, 14.0; IR (neat)*v*max: 3973, 3856, 3648, 3420, 2946, 2832, 2233, 2043, 1697, 1409, 1026 cm^{-1}; HRMS (ESI) *m/z* calcd for $C_{25}H_{30}N_4O_5$ $[M+Na]^+$: 489.2114; Found :489.2109.

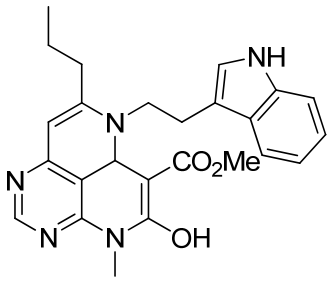

Compound 5e: Yield: 69%; Scarlet solid; mp: 169–173 °C; ^{1}H NMR (500 MHz, $CDCl_3$) δ 11.07 (brs, 1H), 8.64 (s, 1H), 8.23 (s, 1H), 8.12 (brs, 1H), 7.63 (d, *J* = 8.0 Hz, 1H), 7.42 (d, *J* = 8.0 Hz, 1H), 7.24 (t, *J* = 7.5 Hz, 1H), 7.16–7.12 (m, 2H), 5.41 (s, 1H), 3.95 (s, 3H), 3.74 (q, *J* = 6.8 Hz, 2H), 3.72 (s, 3H), 3.15 (t, *J* = 6.8 Hz, 2H), 2.33 (t, *J* = 8.0 Hz, 2H), 1.66–1.60 (m, 2H), 1.02 (t, *J* = 7.3 Hz, 3H); ^{13}C NMR (100 MHz, DMSO-*d*$_6$) δ; 165.6, 164.8, 161.6, 158.7, 157.3, 154.3, 137.0, 136.4, 127.0, 124.0, 121.0, 119.3, 118.33, 118.28, 111.5, 110.7, 102.5, 86.1, 52.0, 43.6, 34.9, 28.1, 25.4, 21.5, 13.8; IR (neat)*v*max: 3867, 3366, 2942, 2832, 2516, 2226, 2042, 1719, 1642, 1527, 1452, 1194, 1112, 1023, 738 cm^{-1}; HRMS (ESI) *m/z* calcd for $C_{25}H_{27}N_5O_3$ $[M+Na]^+$: 468.2012; Found: 468.2007.

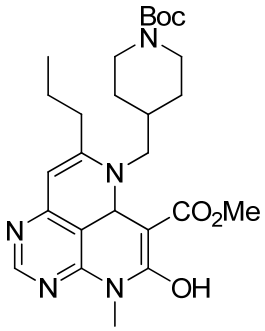

Compound 5f: Yield: 49%; Brown oil; ^{1}H NMR (400 MHz, $CDCl_3$) δ 11.14 (brs, 1H), 8.67 (s, 1H), 8.54 (s, 1H), 5.46 (s, 1H), 4.18 (brs ,2H), 3.96 (s, 3H), 3.74 (s, 3H), 3.29 (t, *J* = 5.6 Hz, 2H), 2.74 (s, 2H), 2.37 (t, *J* = 7.6 Hz, 2H), 1.82–1.76 (m, 3H), 1.73-1.64 (m, 2H), 1.47 (s, 9H), 1.30–1.24 (m, 2H), 1.06 (t, *J* = 7.2 Hz, 3H); ^{13}C NMR (100 MHz, $CDCl_3$) δ 165.9, 165.5, 162.7, 159.9, 157.7, 155.1, 154.7, 138.9, 119.0, 103.8, 86.7, 79.6, 52.6, 49.1, 37.4, 35.7, 29.9, 28.6, 28.4, 22.1, 14.0; IR (neat)*v*max: 3981, 3859, 3427, 2833, 2231, 2043, 1667, 1452, 1021 cm^{-1}; HRMS (ESI) *m/z* calcd for $C_{26}H_{37}N_5O_5$ $[M+Na]^+$: 522.2692; Found: 522.2685.

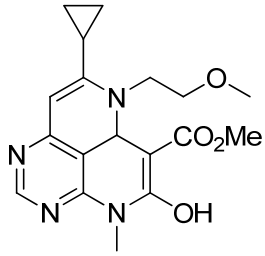

Compound 6a: Yield: 74%; Orange solid; mp: 144–148 ^{o}C; ^{1}H NMR (400 MHz, $CDCl_3$) δ 11.23 (brs, 1H), 8.63 (s, 1H), 8.58 (s, 1H), 5.34 (s, 1H), 3.96 (s, 3H), 3.78 (t, *J* = 5.6 Hz, 2H), 3.74 (s, 3H), 3.65 (t, *J* = 5.6 Hz, 22H), 3.46 (s, 3H), 1.77–1.72 (m, 1H), 1.05–1.01 (m, 2H), 0.89–0.85 (m, 2H); ^{13}C NMR (100 MHz, $CDCl_3$) δ 165.9, 165.4, 162.9, 159.9, 157.7, 155.1, 138.7, 119.0, 104.0, 83.4, 71.6, 59.1, 52.5, 43.2, 28.5, 13.9, 7.1; IR (neat)*v*max: 3855, 3566, 2947, 2830, 2392, 2043, 1765, 1650, 1471, 1112, 1023 cm^{-1}; HRMS (ESI) *m/z* calcd for $C_{18}H_{22}N_4O_4$ $[M+Na]^+$: 381.1539; Found: 381.1534.

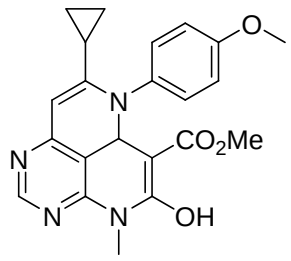

Compound 6b: Yield: 87%; Red solid; mp: 191–195 ^{o}C; ^{1}H NMR (400 MHz, $CDCl_3$) δ 12.79 (brs, 1H), 8.63 (s, 1H), 8.61 (s, 1H), 7.24 (d, *J* = 8.6 Hz, 2H), 6.94 (d, *J* = 8.6 Hz, 2H), 5.31 (s, 1H), 3.97 (s, 3H), 3.84 (s, 3H), 3.75 (s, 3H), 1.77–1.70 (m, 1H), 0.98 (d, *J* = 6.9 Hz, 4H); ^{13}C NMR (100 MHz, $CDCl_3$) δ 165.9, 164.8, 162.7, 159.8, 157.7, 157.5, 155.1, 138.5, 131.6, 126.8, 119.5, 114.3, 104.2, 82.2, 55.5, 52.6, 28.6, 14.2, 9.9;

IR (neat)*v*max: 3856, 3614, 3388, 2828, 2230, 2038, 1682, 1449, 1024 cm^{-1}; HRMS (ESI) *m/z* calcd for $C_{22}H_{22}N_4O_4$ $[M+Na]^+$: 429.1539; Found: 429.1535.

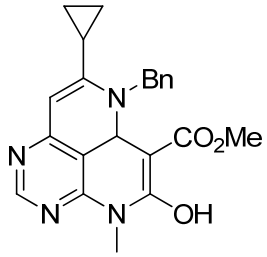

Compound 6c: Yield: 76%; Orange solid; mp: 137–141 ^oC; ^1H NMR (400 MHz, $CDCl_3$) δ 11.49 (brs, 1H), 8.64 (s, 1H), 8.55 (s, 1H), 7.40–7.31 (m, 5H), 5.39 (s, 1H), 4.84 (d, *J* = 5.9 Hz, 2H), 3.96 (s, 3H), 3.74 (s, 3H), 1.72–1.65 (m, 1H), 1.01–0.96 (m, 2H), 0.89-0.84 (m, 2H); ^{13}C NMR (100 MHz, $CDCl_3$) δ 165.8, 165.7, 163.0, 159.9, 157.7, 155.1, 138.7, 138.4, 128.8, 127.5, 126.6, 119.2, 104.2, 83.7, 52.6, 47.1, 28.6, 13.9, 7.3; IR (neat)*v*max: 3857, 3533, 2833, 2409, 2041, 1651, 1022 cm^{-1}; HRMS (ESI) *m/z* calcd for $C_{22}H_{22}N_4O_3$ $[M+Na]^+$: 413.1590; Found: 413.1583.

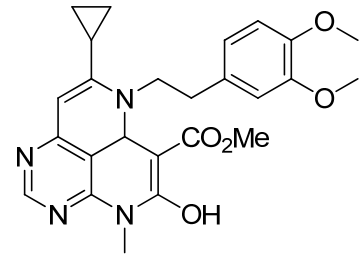

Compound 6d: Yield: 53%; Brown oil; ^1H NMR (400 MHz, $CDCl_3$) δ 11.13 (brs, 1H), 8.60 (s, 1H), 8.44 (s, 1H), 6.84 (s, 2H), 6.77 (s, 1H), 5.30 (s, 1H), 3.95 (s, 3H), 3.88 (s, 3H), 3.86 (t, *J* = 6.0 Hz, 2H), 3.83 (s, 3H), 3.73 (s, 3H), 2.95 (t, *J* = 6.8 Hz, 2H), 1.66–1.62 (m, 1H), 1.02–0.97 (m, 2H), 0.84–0.80 (m, 2H); ^{13}C NMR (100 MHz, $CDCl_3$) δ 165.9, 165.3, 162.8, 159.9, 157.6, 155.1, 149.0, 147.9, 138.7, 131.0, 120.9, 119.0, 112.1, 111.2, 103.9, 83.2, 55.9, 55.8, 52.6, 45.1, 36.3, 28.6, 13.9, 7.2; IR (neat)*v*max: 3856, 3543, 2833, 2438, 2042, 1518, 1114, 1022, 759 cm^{-1}; HRMS (ESI) *m/z* calcd for $C_{25}H_{28}N_4O_5$ $[M+Na]^+$: 487.1957; Found: 487.1953.

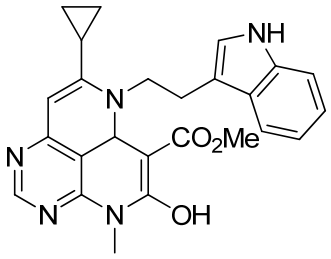

Compound 6e: Yield: 87%; Orange solid; mp: 170–174 °C; ^{1}H NMR (400 MHz, DMSO-d_6) δ 11.07 (brs, 1H), 10.96 (brs, 1H), 8.50 (s, 1H), 8.24 (s, 1H), 7.61 (d, J = 8.0 Hz, 1H), 7.37 (d, J = 7.2 Hz, 1H), 7.32 (s, 1H), 7.08 (t, J = 7.4 Hz, 1H), 6.98 (t, J = 7.4 Hz, 1H), 5.20 (s, 1H), 3.88 (d, J = 6.4 Hz, 2H), 3.78 (s, 3H), 3.33 (s, 3H), 3.09 (t, J = 6.4 Hz, 2H), 1.86 (brs, 1H), 0.95 (d, J = 8.4 Hz, 2H), 0.86 (d, J = 3.6 Hz, 2H); ^{13}C NMR (100 MHz, DMSO-d_6) δ 165.9, 165.0, 161.8, 158.8, 157.1, 154.2, 136.6, 136.4, 127.0, 123.9, 121.0, 119.8, 118.3, 111.5, 110.9, 102.7, 81.8, 52.1, 38.9, 28.1, 25.2, 13.5, 7.2; IR (neat)*ν*max: 3855, 3552, 2826, 2438, 2042, 1661, 1520, 1020 cm^{-1}; HRMS (ESI) *m/z* calcd for $C_{25}H_{25}N_5O_3$ $[M+Na]^+$: 466.1855; Found: 466.1849.

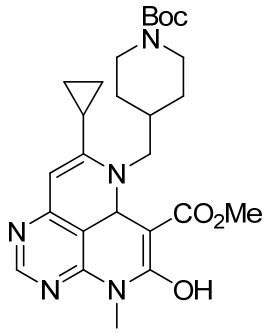

Compound 6f: Yield: 47%; Brown oil; ^{1}H NMR (400 MHz, $CDCl_3$) δ 11.23 (brs, 1H), 8.62 (s, 1H), 8.55 (s, 1H), 5.31 (s, 1H), 3.96 (brs, 2H), 3.82 (s, 3H), 3.74 (s, 3H), 3.50 (t, J = 6.0 Hz, 2H), 2.74 (brs, 2H), 1.81 (d, J = 10.8 Hz, 2H), 1.71–1.67 (m, 1H), 1.58 (brs, 1H), 1.47 (s, 9H), 1.31–1.24 (m, 2H), 1.04 (q, J = 5.6 Hz, 2H), 0.87 (q, J = 5.6 Hz, 2H); ^{13}C NMR (100 MHz, $CDCl_3$) δ 165.9, 165.3, 162.8, 159.9, 157.6, 155.1, 149.1, 148.0, 138.7, 131.0, 120.9, 119.0, 112.1, 111.3, 103.9, 83.2, 77.3, 56.0, 55.8, 52.6, 45.1, 36.3, 29.7, 28.6, 13.9, 7.2; IR (neat)*ν*max: 3976, 3856, 3611, 2980, 2824, 2476, 2231, 2043, 1680, 1625, 1539, 1024 cm^{-1}; HRMS (ESI) *m/z* calcd for $C_{26}H_{35}N_5O_5$ $[M+Na]^+$: 520.2536; Found: 520.2531.

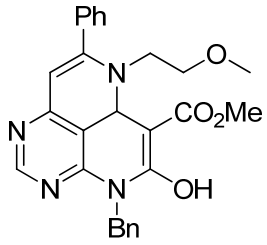

Compound 7a: Yield: 61%; Yellow solid; mp: 95–99 °C; ^{1}H NMR (400 MHz, $CDCl_3$) δ 11.12 (brs, 1H), 8.72 (s, 1H), 8.64 (s, 1H), 7.50–7.46 (m, 5H), 7.45–7.41 (m, 2H), 7.28–7.19 (m, 3H), 5.68 (s, 2H), 5.55 (s, 1H), 3.90 (s, 3H), 3.48 (t, *J* = 5.8 Hz, 2H), 3.41 (t, *J* = 5.8 Hz, 2H), 3.40 (s, 3H); ^{13}C NMR (100 MHz, $CDCl_3$) δ 165.5, 163.6, 163.0, 159.6, 158.0, 157.5, 155.1, 139.2, 137.1, 136.5, 129.5, 128.9, 128.6, 128.2, 127.8, 127.2, 119.9, 104.7, 89.4, 71.9, 59.1, 52.6, 45.0, 44.4; IR (neat)*ν*max: 3407, 2841, 2524, 2163, 1660, 1453, 1117, 1019 cm^{-1}; HRMS (ESI) *m/z* calcd for $C_{27}H_{26}N_4O_4$ $[M+Na]^+$: 493.1852; Found: 493.1845.

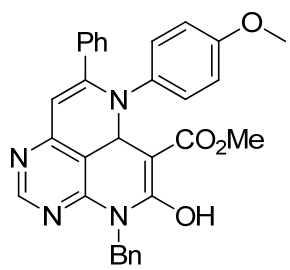

Compound 7b: Yield: 70%; Yellow solid; mp: 187–191 °C; ^{1}H NMR (400 MHz, $CDCl_3$) δ 12.57 (brs, 1H), 8.78 (s, 1H), 8.74 (s, 1H), 7.51 (d, *J* = 7.0 Hz, 2H), 7.40–7.31 (m, 5H), 7.28–7.19 (m, 3H), 6.75 (d, *J* = 9.0 Hz, 2H), 6.68 (d, *J* = 9.0 Hz, 2H), 5.84 (s, 1H), 5.69 (s, 2H), 3.93 (s, 3H), 3.72 (s, 3H); ^{13}C NMR (100 MHz, $CDCl_3$) δ 165.4, 162.7, 159.3, 158.8, 157.8, 156.4, 155.1, 138.8, 136.9, 136.6, 132.8, 129.5, 128.9, 128.5, 128.2, 127.3, 124.7, 120.7, 114.0, 105.4, 92.2, 55.3, 52.7, 44.5; IR (neat)*ν*max: 3418, 2951, 2838, 2522, 2147, 1664, 1453, 1114, 1020 cm^{-1}; HRMS (ESI) *m/z* calcd for $C_{31}H_{26}N_4O_4$ $[M+Na]^+$: 541.1852; Found: 541.1844.

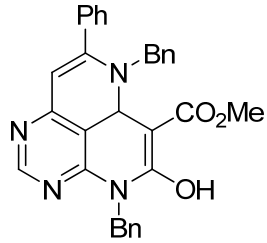

Compound 7c: Yield: 91%; Yellow solid; mp: 105–109 °C; ^{1}H NMR (400 MHz, $CDCl_3$) δ 11.33 (brs, 1H), 8.67 (s, 1H), 8.66 (s, 1H), 7.50 (d, *J* = 6.8 Hz, 2H), 7.48–7.39 (m, 5H), 7.34 (t, *J* = 7.6 Hz, 2H), 7.29–7.19 (m, 6H), 5.68 (s, 2H), 5.62 (s, 1H), 4.47 (d, *J* = 6.8 Hz, 2H), 3.91 (s, 3H); ^{13}C NMR (100 MHz, $CDCl_3$) δ 165.5, 163.8, 163.0, 159.5, 158.0, 155.1,

139.2, 138.8, 137.1, 136.2, 129.6, 128.9, 128.7, 128.6, 128.2, 127.8, 127.4, 127.3, 126.6, 120.1, 104.8, 89.8, 52.6, 48.9, 44.4; IR (neat)*v*max: 3861, 3609, 2498, 2038, 1681, 1024 cm^{-1}; HRMS (ESI) *m/z* calcd for $C_{31}H_{26}N_4O_3$ $[M+Na]^+$: 525.1903; Found: 525.1898.

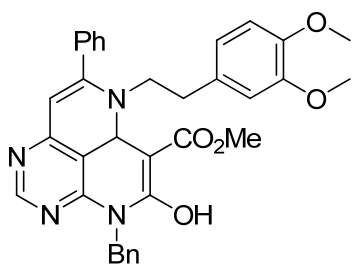

Compound 7d: Yield: 70%; Yellow solid; mp: 116–120 °C; ^{1}H NMR (500 MHz, $CDCl_3$) δ 10.95 (brs, 1H), 8.61 (s, 1H), 8.55 (s, 1H), 7.50 (d, *J* = 7.5 Hz, 2H), 7.47-7.42 (m, 3H), 7.30–7.21 (m, 5H), 6.79 (d, *J* = 8.5 Hz, 1H), 6.68 (dd, *J* = 8.5 Hz, *J* = 2.0 Hz, 1H), 6.59 (d, *J* = 2.0 Hz, 1H), 5.67 (s, 2H), 5.48 (s, 1H), 3.89 (s, 3H), 3.87 (s, 3H), 3.76 (s, 3H), 3.49 (q, *J* = 6.8 Hz, 2H), 2.77 (t, *J* = 6.8 Hz, 2H); ^{13}C NMR (100 MHz, $CDCl_3$) δ 165.5, 163.7, 162.8, 159.6, 157.8, 155.0, 149.0, 147.9, 139.1, 137.1, 136.4, 130.8, 129.4, 128.8, 128.5, 128.2, 127.7, 127.3, 121.0, 119.8, 112.0, 111.2, 104.5, 89.2, 56.0, 55.7, 52.6, 46.9, 44.4, 37.0; IR (neat)*v*max: 3547, 2947, 2836, 2407, 2040, 1644, 1113, 1019 cm^{-1}; HRMS (ESI) *m/z* calcd for $C_{34}H_{32}N_4O_5$ $[M+Na]^+$: 599.2270; Found: 599.2265.

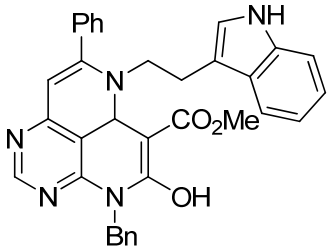

Compound 7e: Yield: 67%; Orange solid; mp: 199–203 °C; ^{1}H NMR (500 MHz, $CDCl_3$) δ 11.00 (brs, 1H), 8.60 (s, 1H), 8.39 (s, 1H), 8.30 (brs, 1H), 7.46–7.36 (m, 7H), 7.32 (dd, *J* = 7.8 Hz, *J* = 1.2 Hz, 2H), 7.25–7.15 (m, 4H), 7.05–7.01 (m, 2H), 5.64 (s, 2H), 5.46 (s, 1H), 3.87 (s, 3H), 3.57 (q, *J* = 6.6 Hz, 2H), 2.99 (t, *J* = 6.6 Hz, 2H); ^{13}C NMR (100 MHz, $CDCl_3$) δ 165.5, 163.7, 162.7, 159.6, 157.8, 155.0, 139.2, 137.1, 136.5, 136.3, 129.4, 128.7, 128.6, 128.2, 127.7, 127.2, 127.1, 122.6, 122.2, 119.6, 119.4, 118.5, 112.3, 111.3, 104.4, 89.1, 52.6, 45.8, 44.4, 27.0; IR (neat)*v*max: 3860, 3525, 2947, 2834, 2390, 2042, 1650, 1453, 1120, 1025 cm^{-1}; HRMS (ESI) *m/z* calcd for $C_{34}H_{29}N_5O_3$ $[M+Na]^+$: 578.2168; Found: 578.2165.

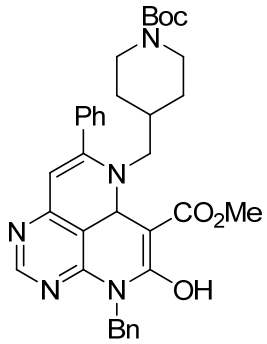

Compound 7f: Yield: 56%; Orange solid; mp: 161–165 ^{o}C; ^{1}H NMR (500 MHz, $CDCl_3$) δ 11.05 (brs, 1H), 8.69 (s, 1H), 8.64 (s, 1H), 7.51–7.48 (m, 5H), 7.40–7.38 (m, 2H), 7.28-7.19 (m, 3H), 5.68 (s, 2H), 5.53 (s, 1H), 4.10 (brs, 2H), 3.90 (s, 3H), 3.16 (t, *J* = 6.4 Hz, 2H), 2.66 (brs, 2H), 1.67 (d, *J* = 12.7 Hz, 2H), 1.64–1.60 (m, 1H), 1.43 (s, 9H), 1.12–1.09 (m, 2H); ^{13}C NMR (100 MHz, $CDCl_3$) δ 165.5, 164.0, 162.8, 159.5, 157.9, 155.1, 154.7, 139.1, 137.1, 136.3, 129.6, 128.9, 128.7, 128.2, 127.8, 127.3, 120.0, 104.6, 89.3, 79.5, 52.6, 50.8, 44.4, 37.8, 29.7, 28.4; IR (neat)*ν*max: 3745, 3409, 2976, 2139, 1738, 1683, 1559, 1452, 1427, 1345, 1251, 1141, 1019 cm^{-1}; HRMS (ESI) *m/z* calcd for $C_{35}H_{39}N_5O_5$ $[M+Na]^+$: 632.2849; Found: 632.2843.

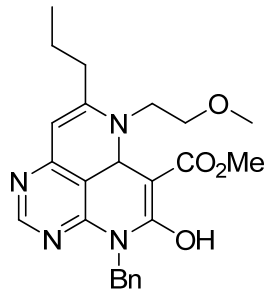

Compound 8a: Yield: 62%; Orange solid; mp: 112–116 ^{o}C; ^{1}H NMR (500 MHz, $CDCl_3$) δ 11.19 (brs, 1H), 8.70 (s, 1H), 8.58 (s, 1H), 7.47 (d, *J* = 7.4 Hz, 2H), 7.24–7.19 (m, 3H), 5.66 (s, 2H), 5.48 (s, 1H), 3.95 (s, 3H), 3.60 (t, *J* = 4.9 Hz, 2H), 3.57 (t, *J* = 4.9 Hz, 2H), 3.44 (s, 3H), 2.39 (t, *J* = 7.9 Hz, 2H), 1.71–1.63 (m, 2H), 1.06 (t, *J* = 7.4 Hz, 3H); ^{13}C NMR (100 MHz, $CDCl_3$) δ 165.9, 165.4, 162.9, 159.6, 157.9, 155.0, 139.5, 137.2, 128.8, 128.2, 127.2, 119.2, 103.9, 86.8, 71.6, 59.1, 52.6, 44.3, 43.2, 35.8, 22.1, 14.0; IR (neat)*ν*max: 3979, 3858, 3638, 2831, 2488, 2227, 2041, 1667, 1107, 1020 cm^{-1}; HRMS (ESI) *m/z* calcd for $C_{24}H_{28}N_4O_4$ $[M+Na]^+$: 459.2008; Found: 459.2003.

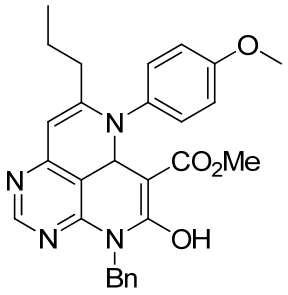

Compound 8b: Yield: 85%; Yellow solid; mp: 159–163 °C; ^{1}H NMR (400 MHz, $CDCl_3$) δ 12.51 (brs, 1H), 8.75 (s, 1H), 8.64 (s, 1H), 7.49 (d, *J* = 7.2 Hz, 2H), 7.27–7.20 (m, 3H), 7.12 (d, *J* = 8.8 Hz, 2H), 6.93 (d, *J* = 8.8 Hz, 2H), 5.68 (s, 2H), 5.66 (s, 1H), 3.96 (s, 3H), 3.84 (s, 3H), 2.39 (t, *J* = 8.0 Hz, 2H), 1.58–1.52 (m, 2H), 0.90 (t, *J* = 7.6 Hz, 3H); ^{13}C NMR (100 MHz, $CDCl_3$) δ 165.8, 164.2, 162.8, 159.5, 158.1, 157.8, 155.1, 139.2, 137.1, 131.4, 128.8, 128.2, 127.25, 127.21, 119.9, 116.4, 114.8, 114.4, 104.3, 87.9, 55.7, 55.5, 52.7, 44.4, 35.4, 29.7, 22.2, 13.9; IR (neat)*ν*max: 3861, 3654, 2950, 2829, 2494, 2233, 2042, 1650, 1024 cm^{-1}; HRMS (ESI) *m/z* calcd for $C_{28}H_{28}N_4O_4$ $[M+Na]^+$: 507.2008; Found: 507.2003.

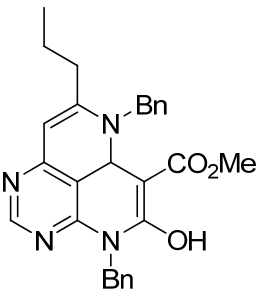

Compound 8c: Yield: 74%; Brown oil; ^{1}H NMR (400 MHz, $CDCl_3$) δ 11.41 (brs, 1H), 8.72 (s, 1H), 8.54 (s, 1H), 7.47 (d, *J* = 7.6 Hz, 2H), 7.40–7.36 (m, 2H), 7.33–7.29 (m, 3H), 7.25–7.18 (m, 3H), 5.66 (s, 2H), 5.55 (s, 1H), 4.63 (d, *J* = 6.0 Hz, 2H), 3.92 (s, 3H), 2.39 (t, *J* = 7.6 Hz, 2H), 1.70–1.64 (m, 2H), 1.03 (t, *J* = 7.6 Hz, 3H); ^{13}C NMR (100 MHz, $CDCl_3$) δ 165.9, 165.5, 163.0, 159.6, 157.9, 155.0, 139.4, 138.2, 137.2, 128.9, 128.8, 128.2, 127.6, 127.2, 126.5, 119.4, 104.0, 87.1, 52.6, 47.1, 44.4, 35.6, 29.6, 22.2, 14.0; IR (neat)*ν*max: 3975, 3856, 3652, 2942, 2826, 2493, 2230, 2041, 1682, 1452, 1110, 1023 cm^{-1}; HRMS (ESI) *m/z* calcd for $C_{28}H_{28}N_4O_3$ $[M+Na]^+$: 491.2059; Found: 491.2054.

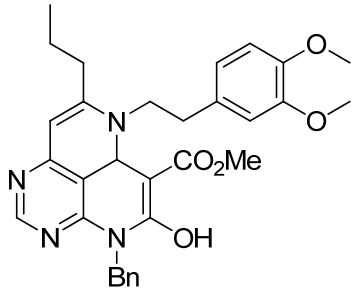

Compound 8d: Yield: 48%; Orange solid; mp: 129–133 °C; ^{1}H NMR (400 MHz, $CDCl_3$) δ 11.03 (brs, 1H), 8.67 (s, 1H), 8.41 (s, 1H), 7.47 (d, *J* = 6.8 Hz, 2H), 7.25–7.20 (m, 3H), 6.86–6.82 (m, 2H), 6.76 (s, 1H), 5.65 (s, 2H), 5.42 (s, 1H), 3.94 (s, 3H), 3.88 (s, 3H), 3.82 (s, 3H), 3.64 (q, *J* = 6.0 Hz, 2H), 2.90 (t, *J* = 6.8 Hz, 2H), 2.31 (t, *J* = 7.2 Hz, 2H), 1.66-1.60 (m, 2H), 1.03 (t, *J* = 7.2 Hz, 3H); ^{13}C NMR (100 MHz, $CDCl_3$) δ 165.9, 165.3, 162.7, 159.6, 157.7, 155.0, 149.0, 148.0, 139.4, 137.2, 130.7, 128.8, 128.2, 127.2, 121.0, 119.2, 112.1, 111.3, 103.7, 86.7, 56.0, 55.8, 52.6, 45.2, 44.3, 36.4, 35.7, 26.7, 22.0. 14.0; IR (neat)*ν*max: 3856, 3561, 2942, 2832, 2424, 2222, 2043, 1667, 1118, 1023 cm^{-1}; HRMS (ESI) *m/z* calcd for $C_{31}H_{34}N_4O_5$ $[M+Na]^+$: 565.2427; Found: 565.2421.

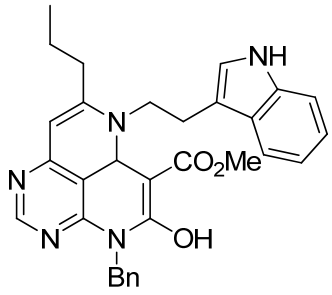

Compound 8e: Yield: 64%; Orange solid; mp: 214–218 °C; ^{1}H NMR (400 MHz, $CDCl_3$) δ 11.07 (t, *J* = 5.7 Hz, 1H), 8.67 (s, 1H), 8.26 (s, 1H), 8.14 (brs, 1H), 7.62 (d, *J* = 7.6 Hz, 1H), 7.45 (d, *J* = 7.6 Hz, 2H), 7.41 (d, *J* = 8.4 Hz, 1H), 7.25–7.20 (m, 4H), 7.15–7.12 (m, 2H), 5.63 (s, 2H), 5.41 (s, 1H), 3.94 (s, 3H), 3.73 (q, *J* = 6.4 Hz, 2H), 3.14 (t, *J* = 6.4 Hz, 2H), 2.33 (t, *J* = 7.6 Hz, 2H), 1.65-1.58 (m, 2H), 1.01 (t, *J* = 7.6 Hz, 3H); ^{13}C NMR (100 MHz, $CDCl_3$) δ 166.0, 165.4, 162.6, 159.7, 157.7, 155.0, 139.5, 137.2, 136.4, 128.7, 128.2, 127.2, 127.1, 122.6, 122.3, 119.6, 118.9, 118.5, 112.3, 111.4, 103.7, 86.6, 52.6, 44.3, 44.0, 35.8, 26.3, 22.1, 14.0; IR (neat)*ν*max: 3973, 3859, 3618, 2941, 2830, 2511, 2228, 2041, 1661, 1120, 1021 cm^{-1}; HRMS (ESI) *m/z* calcd for $C_{31}H_{31}N_5O_3$ $[M+Na]^+$: 544.2325; Found: 544.2319.

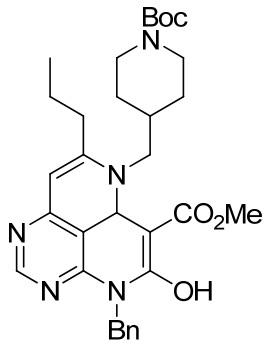

Compound 8f: Yield: 48%; Brown oil; ^{1}H NMR (400 MHz, $CDCl_3$) δ 11.16 (brs, 1H), 8.69 (s, 1H), 8.56 (s, 1H), 7.48 (d, *J* = 6.9 Hz, 2H), 7.25–7.18 (m, 3H), 5.66 (s, 2H), 5.46 (s, 1H), 4.18 (brs, 2H), 3.95 (s, 3H), 3.28 (t, *J* = 6.4 Hz, 2H), 2.73 (brs, 2H), 2.36 (t, *J* = 7.9 Hz, 2H), 1.79 (d, *J* = 12.7 Hz, 2H), 1.75–1.72 (m, 1H), 1.66 (q, *J* = 7.9 Hz, 2H), 1.46 (s, 9H), 1.43 (d, *J* = 8.8 Hz, 2H), 1.06 (t, *J* = 7.4 Hz, 3H); ^{13}C NMR (100 MHz, $CDCl_3$) δ 165.8, 165.5, 162.7, 159.6, 157.8, 155.0, 154.7, 139.4, 137.1, 128.8, 128.2, 127.2, 119.1, 103.8, 86.7, 79.5, 52.6, 49.1, 44.4, 37.4, 35.6, 29.8, 28.4, 22.1, 14.0; IR (neat)*ν*max: 3856, 3647, 2825, 2495, 2232, 2040, 1669, 1109, 1022 cm^{-1}; HRMS (ESI) *m/z* calcd for $C_{32}H_{41}N_5O_5$ $[M+Na]^+$: 598.3005; Found: 598.3000.

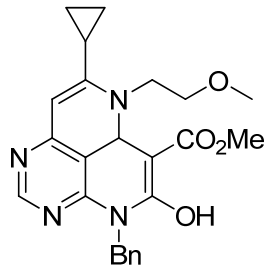

Compound 9a: Yield: 67%; Orange solid; mp: 121–125 ^{o}C; ^{1}H NMR (500 MHz, $CDCl_3$) δ 11.24 (brs, 1H), 8.65 (s, 1H), 8.59 (s, 1H), 7.47 (d, *J* = 6.9 Hz, 2H), 7.24–7.19 (m, 3H), 5.65 (s, 2H), 5.34 (s, 1H), 3.95 (s, 3H), 3.78 (q, *J* = 5.4 Hz, 2H), 3.64 (t, *J* = 5.4 Hz, 2H), 3.45 (s, 3H), 1.77–1.72 (m, 1H), 1.04–1.00 (m, 2H), 0.87–0.84 (m, 2H); ^{13}C NMR (100 MHz, $CDCl_3$) δ 165.9, 165.4, 163.0, 159.6, 157.8, 155.0, 139.2, 137.2, 128.8, 128.2, 127.1, 119.2, 104.0, 83.4, 71.6, 59.1, 52.6, 44.3, 43.1, 13.9, 7.1; IR (neat)*ν*max: 3983, 3856, 3652, 2942, 2829, 2501, 2233, 2041, 1681, 1453, 1102, 1021 cm^{-1}; HRMS (ESI) *m/z* calcd for $C_{24}H_{26}N_4O_4$ $[M+Na]^+$: 457.1852; Found: 457.1846.

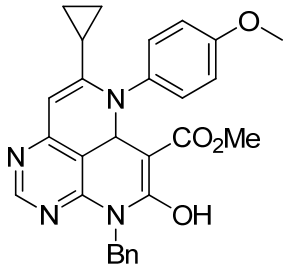

Compound 9b: Yield: 92%; Scarlet solid; mp: 176–180 ^{o}C; ^{1}H NMR (500 MHz, $CDCl_3$) δ 12.79 (brs, 1H), 8.67 (s, 1H), 8.62 (s, 1H), 7.48 (d, *J* = 7.4 Hz, 2H), 7.27–7.20 (m, 5H), 6.93 (d, *J* = 8.8 Hz, 2H), 5.67 (s, 2H), 5.31 (s, 1H), 3.96 (s, 3H), 3.84 (s, 3H), 1.75–1.69 (m, 1H), 0.99–0.97 (m, 4H); ^{13}C NMR (100 MHz, $CDCl_3$) δ 165.8, 164.8, 162.8, 159.5, 157.73, 157.65, 155.1, 139.0, 137.1, 131.6, 128.8, 128.2, 127.2, 126.8, 119.7, 114.3, 104.3, 82.2, 55.5, 52.7, 44.4, 14.2, 9.9; IR (neat)*ν*max: 3975, 3857, 3664, 2933, 2826, 2500, 2224, 2041, 1693, 1453, 1113, 1026, 669 cm^{-1}; HRMS (ESI) *m/z* calcd for $C_{28}H_{26}N_4O_4$ $[M+Na]^+$: 505.1852; Found: 505.1846.

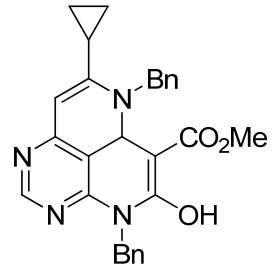

Compound 9c: Yield: 72%; Brown oil; ^{1}H NMR (400 MHz, $CDCl_3$) δ 11.50 (brs, 1H), 8.67 (s, 1H), 8.55 (s, 1H), 7.47 (d, *J* = 6.7 Hz, 2H), 7.39–7.19 (m, 8H), 5.64 (s, 2H), 5.39 (s, 1H), 4.83 (d, *J* = 5.1 Hz, 2H), 3.93 (s, 3H), 1.71-1.64 (m, 1H), 1.00–0.95 (m, 2H), 0.87–0.83 (m, 2H); ^{13}C NMR (100 MHz, $CDCl_3$) δ 165.7, 165.6, 163.1, 159.6, 157.8, 155.0, 139.2, 138.4, 137.1, 128.8, 128.7, 128.2, 127.4, 127.2, 126.6, 119.4, 104.2, 83.7, 52.6, 47.0, 44.4, 13.9, 7.3; IR (neat)*ν*max: 3981, 3857, 3645, 2829, 2513, 2226, 2042, 1680, 1417, 1113, 1026 cm^{-1}; HRMS (ESI) *m/z* calcd for $C_{28}H_{26}N_4O_3$ $[M+Na]^+$: 489.1903; Found: 489.1897.

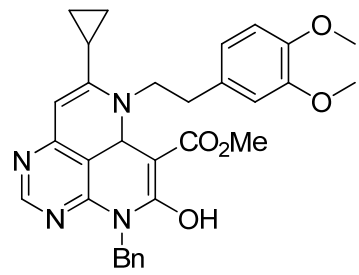

Compound 9d: Yield: 65%; Orange solid; mp: 134–138 ^{o}C; ^{1}H NMR (500 MHz, $CDCl_3$) δ 11.11 (brs, 1H), 8.63 (s, 1H), 8.44 (s, 1H), 7.47 (d, *J* = 7.4 Hz, 2H), 7.29–7.18 (m, 3H), 6.85–6.81 (m, 2H), 6.77 (d, *J* = 1.5 Hz, 1H), 5.64 (s, 2H), 5.28 (s, 1H), 3.94 (s, 3H), 3.88 (s, 3H), 3.85 (t, *J* = 6.9 Hz,

2H), 3.82 (s, 3H), 2.94 (t, *J* = 6.9 Hz, 2H), 1.66–1.60 (m, 1H), 1.01–0.97 (m, 2H), 0.82–0.79 (m, 2H); ^{13}C NMR (100 MHz, $CDCl_3$) δ 165.9, 165.3, 162.8, 159.6, 157.7, 155.0, 149.0, 147.9, 139.2, 137.2, 131.0, 128.8, 128.2, 127.2, 120.9, 119.2, 112.0, 111.3, 104.0, 83.2, 55.9, 55.8, 52.6, 45.1, 44.4, 36.3, 13.9, 7.2; IR (neat)*v*max: 3976, 3858, 3649, 2825, 2515, 2229, 2042, 1680, 1419, 1024 cm^{-1}; HRMS (ESI) *m/z* calcd for $C_{31}H_{32}N_4O_5$ $[M+Na]^+$: 563.2270; Found: 563.2265.

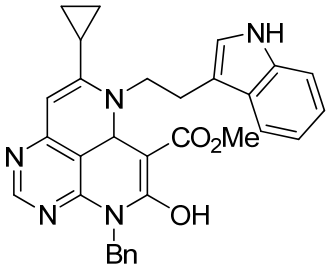

Compound 9e: Yield: 64%; Orange solid; mp: 191–195 °C; ^{1}H NMR (400 MHz, $CDCl_3$) δ 11.16 (brs, 1H), 8.62 (s, 1H), 8.29 (s, 1H), 8.09 (brs, 1H), 7.63 (d, *J* = 8.0 Hz, 1H), 7.45 (d, *J* = 7.6 Hz, 2H), 7.41 (d, *J* = 7.6 Hz, 1H), 7.26–7.11 (m, 6H), 5.63 (s, 2H), 5.26 (s, 1H), 3.95 (t, *J* = 6.8 Hz, 2H), 3.94 (s, 3H), 3.17 (t, *J* = 6.8 Hz, 2H), 1.68–1.64 (m, 1H), 0.96–0.92 (m, 2H), 0.82–0.78 (m, 2H); ^{13}C NMR (100 MHz, DMSO-*d*$_6$) δ 166.1, 164.9, 161.9, 158.4, 157.3, 154.1, 137.2, 136.4, 128.3, 127.2, 127.0, 126.9, 124.0, 121.0, 120.1, 118.3, 111.5, 110.8, 102.8, 81.9, 52.1, 43.63, 43.57, 25.2, 13.6, 7.3; IR (neat)*v*max: 3860, 3565, 2948, 2835, 2443, 2036, 1679, 1456, 1115, 1021 cm^{-1}; HRMS (ESI) *m/z* calcd for $C_{31}H_{29}N_5O_3$ $[M+Na]^+$: 542.2168; Found: 542.2163.

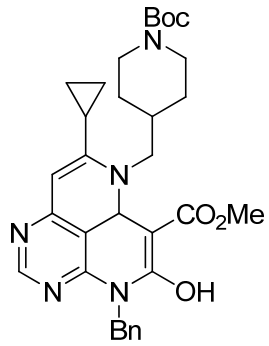

Compound 9f: Yield: 55%; Orange solid; mp: 139–143 °C; ^{1}H NMR (400 MHz, $CDCl_3$) δ 11.26 (brs, 1H), 8.64 (s, 1H), 8.56 (s, 1H), 7.48 (d, *J* = 7.0 Hz, 2H), 7.25–7.17 (m, 3H), 5.65 (s, 2H), 5.30 (s, 1H), 4.18 (brs, 2H), 3.95 (s, 3H), 3.49 (t, *J* = 5.5 Hz, 2H), 2.73 (t, *J* = 11.8 Hz, 2H), 1.80 (d, *J* = 11.4 Hz, 3H), 1.72–1.65 (m, 1H), 1.46 (s, 9H), 1.45 (d, *J* = 2.7 Hz, 2H), 1.06–1.01 (m, 2H), 0.90–0.84 (m, 2H); ^{13}C NMR (100 MHz, $CDCl_3$) δ 165.9, 165.6, 162.9, 159.6, 157.8, 155.0,

154.7, 139.2, 137.2, 128.8, 128.2, 127.2, 119.3, 104.0, 83.1, 79.5, 52.6, 49.0, 44.4, 37.3, 30.0, 28.4, 13.8, 7.4; IR (neat)*ν*max: 3975, 3858, 3651, 2941, 2828, 2499, 2226, 2041, 1668, 1021 cm^{-1}; HRMS (ESI) *m/z* calcd for $C_{32}H_{39}N_5O_5$ $[M+Na]^+$: 596.2849; Found: 596.2843.

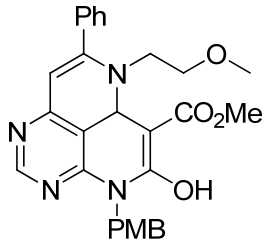

Compound 10a: Yield: 60%; Orange solid; mp: 133–137 °C; ^1H NMR (400 MHz, $CDCl_3$) δ 11.11 (brs, 1H), 8.74 (s, 1H), 8.62 (s, 1H), 7.52 (d, *J* = 8.4 Hz, 2H), 7.48–7.41 (m, 5H), 6.79 (d, *J* = 8.4 Hz, 2H), 5.61 (s, 2H), 5.54 (s, 1H), 3.90 (s, 3H), 3.75 (s, 3H), 3.48 (t, *J* = 5.2 Hz, 2H), 3.43 (t, *J* = 5.2 Hz, 2H), 3.40 (s, 3H); ^{13}C NMR (100 MHz, $CDCl_3$) δ 165.6, 163.6, 163.0, 159.6, 158.8, 158.0, 155.0, 139.1, 136.5, 130.7, 129.5, 129.4, 128.6, 127.9, 119.9, 113.6, 104.7, 89.4, 71.9, 59.0, 55.2, 52.6, 45.0, 43.8; IR (neat)*ν*max: 3855, 3648, 2831, 2517, 2220, 2040, 1669, 1414, 1114, 1019 cm^{-1}; HRMS (ESI) *m/z* calcd for $C_{28}H_{28}N_4O_5$ $[M+Na]^+$: 523.1957; Found: 523.1954.

5. General synthetic procedure for compounds 11a–13b

To a DCE solution of imine (**4á–4ḋ, 4f́, 4ǵ, 7á–7ḋ, 10á, 10ḃ**) (0.3 mmol), AgOTf (10 mol%) and AcOH (2.0 equiv.) were added. After stirring at 80 °C for 1 h, the reaction mixture was filtered under Na_2SO_4 pad and washed thrice with DCM. After the removal of solvent under the reduced pressure, the reaction mixture was dissolved with DMF and added with 1,8-diazabicyclo[5.4.0]undec-7-ene (DBU) (3.0 equiv.) and diethyl chloromalonate (3.0 equiv.). The resulting solution was stirred at 80 °C for 4 h. After the completion of reaction monitored by TLC, the reaction mixture was quenched with deionized water and extracted thrice with DCM. The combined organic layer was washed with brine and dried with anhydrous Na_2SO_4(s). After the solvent was removed under the reduced pressure, the residue was purified by silica-gel flash column chromatography to obtain **11a–13b**.

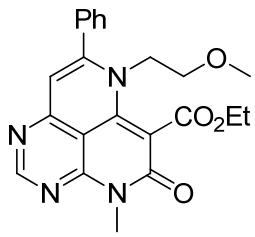

Compound 11a: Yield: 53%; Pale yellow solid; mp: 149–153 °C; ^{1}H NMR (400 MHz, $CDCl_3$) δ 8.84 (s, 1H), 7.52–7.44 (m, 5H), 6.49 (s, 1H), 4.42 (q, *J* = 7.0 Hz, 2H), 4.03 (t, *J* = 5.1 Hz, 2H), 3.72 (s, 3H), 3.42 (t, *J* = 5.1 Hz, 2H), 3.06 (s, 3H), 1.42 (t, *J* = 7.0 Hz, 3H); ^{13}C NMR (100 MHz, $CDCl_3$) δ 167.3, 161.2, 160.2, 156.0, 155.8, 153.9, 145.1, 135.5, 130.0, 129.0, 128.7, 110.8, 106.5, 102.4, 68.3, 62.1, 58.8, 51.2, 28.1, 14.1; IR (neat)*ν*max: 3856, 3647, 2784, 2508, 2221, 2040, 1717, 1553, 1448, 1113, 1021 cm^{-1}; HRMS (ESI) *m/z* calcd for $C_{22}H_{22}N_4O_4$ $[M+Na]^+$: 429.1539; Found: 429.1533.

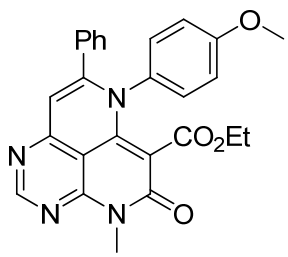

Compound 11b: Yield: 76%; Yellow solid; mp: 235–239 °C; ^{1}H NMR (400 MHz, $CDCl_3$) δ 8.85 (s, 1H), 7.22–7.16 (m, 3H), 7.04–7.01 (m, 4H), 6.69 (d, *J* = 8.6 Hz, 2H), 6.46 (s, 1H), 3.74 (s, 3H), 3.69 (s, 3H), 3.60 (d, *J* = 9.0 Hz, 2H), 1.28 (t, *J* = 7.0 Hz, 3H); ^{13}C NMR (100 MHz, $CDCl_3$) δ 165.3, 161.5, 160.2, 159.9, 156.5, 154.8, 153.7, 144.0, 134.7, 132.2, 130.5, 128.91, 128.86, 127.9, 113.7, 109.3, 106.1, 102.6, 61.3, 55.4, 28.1, 13.6; IR (neat)*ν*max: 3857, 3552, 2945, 2831, 2416, 2041, 1668, 1407, 1120, 1021, 766 cm^{-1}; HRMS (ESI) *m/z* calcd for $C_{26}H_{22}N_4O_4$ $[M+Na]^+$: 477.1539; Found: 477.1533.

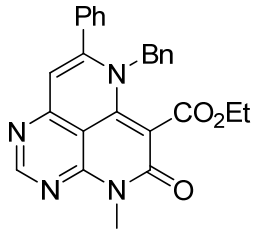

Compound 11c: Yield: 69%; Pale yellow solid; mp: 150–154 °C; ^{1}H NMR (400 MHz, $CDCl_3$) δ 8.89 (s, 1H), 7.41 (t, *J* = 7.4 Hz, 1H), 7.33 (t, *J* = 7.4 Hz, 2H), 7.18 (d, *J* = 8.2 Hz, 2H), 7.14 (d, *J* = 7.1 Hz, 1H), 7.09 (t, *J* = 7.4 Hz, 2H), 6.58 (d, *J* = 7.4 Hz, 2H), 6.55 (s, 1H), 4.95 (s, 2H), 4.33 (q, *J* = 7.0 Hz, 2H), 3.72 (s, 3H), 1.33 (t, *J* = 7.0 Hz, 3H); ^{13}C NMR (100 MHz, $CDCl_3$) δ 167.1, 161.2, 160.4, 156.0, 155.3, 154.0, 148.5, 135.5, 135.2,

130.0, 128.8, 128.5, 128.0, 127.8, 126.6, 112.0, 106.4, 101.9, 61.8, 58.1, 28.2, 14.0; IR (neat)*v*max: 3861, 3611, 2944, 2829, 2515, 2223, 2039, 1682, 1408, 1118, 1019 cm^{-1}; HRMS (ESI) *m/z* calcd for $C_{26}H_{22}N_4O_3$ $[M+Na]^+$: 461.1590; Found: 461.1584.

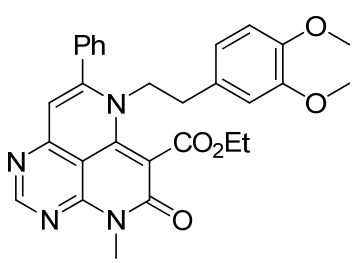

Compound 11d: Yield: 57%; Pale yellow solid; mp: 139–143 °C; ^{1}H NMR (400 MHz, $CDCl_3$) δ 8.82 (s, 1H), 7.53–7.47 (m, 3H), 7.30–7.28 (m, 2H), 6.54 (d, *J* = 8.6 Hz, 1H), 6.40 (s, 1H), 6.21 (d, *J* = 8.2 Hz, 1H), 6.20 (s, 1H), 4.42 (q, *J* = 7.0 Hz, 2H), 4.06 (t, *J* = 7.0 Hz, 2H), 3.79 (s, 3H), 3.73 (s, 3H), 3.64 (s, 3H), 2.72 (t, *J* = 7.0 Hz, 2H), 1.40 (t, *J* = 7.0 Hz, 3H); ^{13}C NMR (100 MHz, $CDCl_3$) δ 167.1, 161.2, 160.2, 155.8, 155.0, 153.8, 148.8, 148.0, 145.4, 135.2, 130.1, 129.0, 128.7, 128.5, 120.7, 111.6, 111.1, 110.9, 106.6, 102.5, 62.0, 55.8, 55.5, 53.5, 33.6, 28.2, 14.1; IR (neat)*v*max: 3862, 3524, 2944, 2832, 2518, 2223, 2044, 1668, 1572, 1418, 1115, 1021 cm^{-1}; HRMS (ESI) *m/z* calcd for $C_{29}H_{28}N_4O_5$ $[M+Na]^+$: 535.1957; Found: 535.1952.

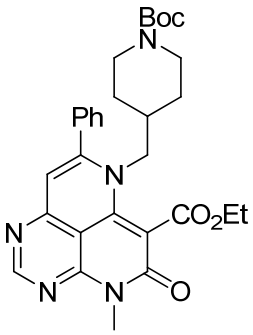

Compound 11f: Yield: 53%; Pale yellow solid; mp: 119–123 °C; ^{1}H NMR (400 MHz, $CDCl_3$) δ 8.86 (s, 1H), 7.53 (t, *J* = 3.5 Hz, 3H), 7.46 (brs, 2H), 6.54 (s, 1H), 4.44 (brs, 2H), 3.95 (brs, 2H), 3.73 (s, 3H), 3.70 (d, *J* = 7.0 Hz, 2H), 2.48 (brs, 2H), 2.10–1.99 (m, 1H), 1.45 (t, *J* = 7.0 Hz, 3H), 1.39 (s, 9H), 1.21 (brs, 2H), 0.76 (d, *J* = 11.0 Hz, 2H); ^{13}C NMR (100 MHz, $CDCl_3$) δ 167.0, 161.1, 160.4, 156.0, 155.7, 154.4, 154.0, 145.7, 135.3, 130.4, 129.4, 128.5, 111.0, 106.5, 79.6, 62.2, 57.5, 31.0, 28.8, 28.3, 28.2, 14.2; IR (neat)*v*max: 3971, 3857, 3650, 2942, 2827, 2503, 2229, 2040, 1681, 1414, 1025, 691 cm^{-1}; HRMS (ESI) *m/z* calcd for $C_{30}H_{35}N_5O_5$ $[M+Na]^+$: 568.2536; Found: 568.2530.

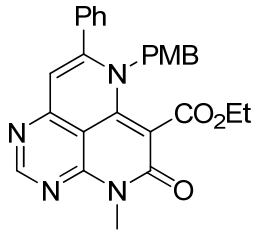

Compound 11g: Yield: 60%; Off-white solid; mp: 160–164 °C; ^{1}H NMR (400 MHz, $CDCl_3$) δ 8.88 (s, 1H), 7.43 (t, *J* = 7.4 Hz, 1H), 7.36 (t, *J* = 7.4 Hz, 2H), 7.21 (d, *J* = 6.7 Hz, 2H), 6.60 (d, *J* = 9.0 Hz, 2H), 6.55 (s, 1H), 6.47 (d, *J* = 8.6 Hz, 2H), 4.87 (s, 2H), 4.38 (q, *J* = 7.0 Hz, 2H), 3.72 (s, 3H), 3.71 (s, 3H), 1.37 (t, *J* = 7.0 Hz, 3H); ^{13}C NMR (100 MHz, $CDCl_3$) δ 167.1, 161.1, 160.4, 159.1, 156.0, 155.3, 154.0, 148.8, 135.4, 130.0, 128.8, 128.1, 127.9, 127.5, 113.9, 112.2, 106.5, 101.9, 61.8, 58.1, 55.2, 28.2, 14.1; IR (neat)*ν*max: 3858, 3652, 2940, 2830, 2498, 2223, 2041, 1668, 1022 cm^{-1}; HRMS (ESI) *m/z* calcd for $C_{27}H_{24}N_4O_4$ $[M+Na]^+$: 491.1965; Found: 491.1969.

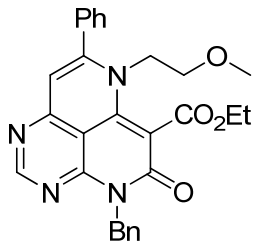

Compound 12a: Yield: 52%; Pale yellow solid; mp: 129–133 °C; ^{1}H NMR (400 MHz, $CDCl_3$) δ 8.84 (s, 1H), 7.56 (d, *J* = 7.0 Hz, 2H), 7.51–7.49 (m, 3H), 7.46–7.43 (m, 2H), 7.30–7.22 (m, 3H), 6.47 (s, 1H), 5.60 (s, 2H), 4.41 (q, *J* = 7.2 Hz, 2H), 4.01 (t, *J* = 5.2 Hz, 2H), 3.41 (t, *J* = 5.2 Hz, 2H), 3.06 (s, 3H), 1.40 (t, *J* = 7.2 Hz, 3H); ^{13}C NMR (100 MHz, $CDCl_3$) δ 167.3, 160.9, 160.3, 156.1, 155.8, 153.9, 145.4, 136.6, 130.0, 129.07, 129.05, 128.6, 128.3, 127.4, 111.0, 106.6, 102.5, 68.3, 58.8, 51.2, 44.3, 14.1; IR (neat)*ν*max: 3979, 3857, 3648, 2938, 2828, 2502, 2224, 2041, 1695, 1416, 1109, 1023 cm^{-1}; HRMS (ESI) *m/z* calcd for $C_{28}H_{26}N_4O_4$ $[M+Na]^+$: 505.1852; Found: 505.1846.

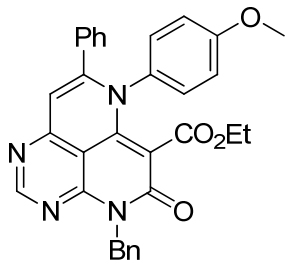

Compound 12b: Yield: 53%; Yellow solid; mp: 205–209 °C; ^{1}H NMR (400 MHz, $CDCl_3$) δ 8.85 (s, 1H), 7.54 (d, *J* = 7.2 Hz, 2H), 7.30–7.15 (m, 6H), 7.04–6.99 (m, 4H), 6.69 (d, *J* = 8.8 Hz, 2H), 6.43 (s, 1H), 5.57 (s, 2H), 3.73 (s, 3H), 3.59 (s, 2H), 1.12 (t, *J* = 7.6 Hz, 3H); ^{13}C NMR (100 MHz, $CDCl_3$) δ 165.3, 161.2, 160.2, 159.9, 156.6, 154.7, 153.6, 144.2, 136.6, 134.7, 132.3, 130.5, 129.0, 128.92, 128.86, 128.3, 127.9, 127.4,

113.7, 109.3, 106.2, 102.7, 61.3, 55.4, 44.2, 13.5; IR (neat)*ν*max: 3980, 3858, 3648, 2498, 2229, 2042, 1695, 1447, 1114, 1021 cm^{-1}; HRMS (ESI) *m/z* calcd for $C_{32}H_{26}N_4O_4$ $[M+Na]^+$: 553.1852; Found: 553.1846.

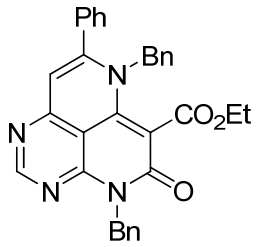

Compound 12c: Yield: 53%; Pale yellow solid; mp: 182–186 °C; ^1H NMR (500 MHz, $CDCl_3$) δ 8.89 (s, 1H), 7.57 (d, *J* = 7.4 Hz, 2H), 7.39 (t, *J* = 7.4 Hz, 1H), 7.33–7.22 (m, 5H), 7.14 (t, *J* = 6.6 Hz, 3H), 7.07 (t, *J* = 7.6 Hz, 2H), 6.56 (d, *J* = 7.4 Hz, 2H), 6.53 (s, 1H), 5.61 (s, 2H), 4.92 (s, 2H), 4.34 (q, *J* = 7.1 Hz, 2H), 1.32 (t, *J* = 7.1 Hz, 3H); ^{13}C NMR (100 MHz, $CDCl_3$) δ 167.1, 160.9, 160.4, 156.1, 155.2, 153.9, 149.0, 136.6, 135.5, 135.2, 129.9, 129.0, 128.8, 128.5, 128.3, 127.9, 127.8, 127.4, 126.7, 112.2, 106.5, 101.9, 61.9, 58.5, 44.3, 14.1; IR (neat)*ν*max: 3857, 3552, 2945, 2833, 2417, 2041, 1673, 1415, 1116, 1023 cm^{-1}; HRMS (ESI) *m/z* calcd for $C_{32}H_{26}N_4O_3$ $[M+Na]^+$: 537.1903; Found: 537.1897.

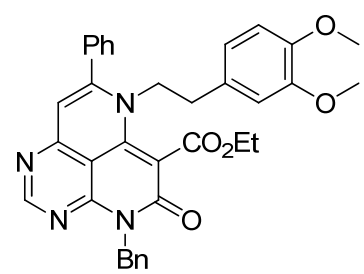

Compound 12d: Yield: 52%; Pale yellow solid; mp: 196–200 °C; ^1H NMR (500 MHz, $CDCl_3$) δ 8.82 (s, 1H), 7.57 (d, *J* = 7.4 Hz, 2H), 7.53–7.48 (m, 3H), 7.32–7.24 (m, 5H), 6.55 (d, *J* = 7.9 Hz, 1H), 6.50 (brs, 1H), 6.22–6.20 (m, 2H), 5.62 (s, 2H), 4.42 (q, *J* = 7.4 Hz, 2H), 4.07 (t, *J* = 7.1 Hz, 2H), 3.79 (s, 3H), 3.62 (s, 3H), 2.73 (t, *J* = 7.1 Hz, 2H), 1.39 (t, *J* = 7.4 Hz, 3H); ^{13}C NMR (100 MHz, $CDCl_3$) δ 166.9, 160.7, 158.9, 153.7, 148.8, 148.0, 145.3, 136.3, 135.0, 130.3, 129.1, 128.5, 128.4, 128.3, 127.5, 120.6, 111.5, 110.9, 110.1, 106.4, 102.9, 62.1, 55.8, 55.5, 53.6, 44.5, 33.6, 14.1; IR (neat)*ν*max: 3859, 3545, 2944, 2833, 2432, 2225, 2042, 1669, 1408, 1116, 1022 cm^{-1}; HRMS (ESI) *m/z* calcd for $C_{35}H_{32}N_4O_5$ $[M+Na]^+$: 611.2270; Found: 611.2265.

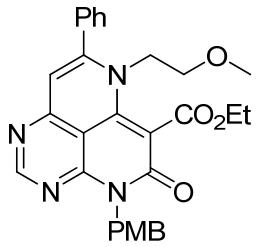

Compound 13a: Yield: 48%; Pale yellow solid; mp: 141–145 °C; ^{1}H NMR (400 MHz, $CDCl_3$) δ 8.85 (s, 1H), 7.57 (d, *J* = 9.0 Hz, 2H), 7.50–7.44 (m, 5H), 6.82 (d, *J* = 8.6 Hz, 2H), 6.46 (s, 1H), 5.53 (s, 2H), 4.41 (q, *J* = 7.0 Hz, 2H), 4.00 (t, *J* = 5.1 Hz, 2H), 3.77 (s, 3H), 3.40 (t, *J* = 5.5 Hz, 2H), 3.05 (s, 3H), 1.40 (t, *J* = 7.4 Hz, 3H); ^{13}C NMR (100 MHz, $CDCl_3$) δ 167.3, 160.9, 160.2, 159.0, 156.1, 155.7, 153.8, 145.3, 135.5, 130.8, 130.0, 129.0, 128.9, 128.6, 113.6, 110.9, 106.6, 102.6, 68.3, 62.1, 58.8, 55.2, 51.2, 43.7, 14.1; IR (neat)*v*max: 3859, 3616, 2941, 2830, 2443, 2224, 2039, 15334, 1114, 1018 cm^{-1}; HRMS (ESI) *m/z* calcd for $C_{29}H_{28}N_4O_5$ $[M+Na]^+$: 535.1957; Found: 535.1952.

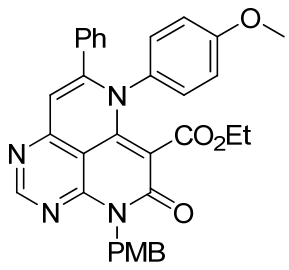

Compound 13b: Yield: 57%; Yellow solid; mp: 204–208 °C; ^{1}H NMR (400 MHz, $CDCl_3$) δ 8.86 (s, 1H), 7.54 (d, *J* = 8.8 Hz, 2H), 7.21–7.15 (m, 4H), 7.02 (d, *J* = 6.8 Hz, 2H), 7.00 (d, *J* = 6.8 Hz, 2H), 6.80 (d, J = 8.8 Hz, 2H), 6.68 (d, *J* = 9.2 Hz, 2H), 6.42 (s, 1H), 5.50 (s, 2H), 3.77 (s, 3H), 3.73 (s, 3H), 3.58 (s, 2H), 1.12 (t, J = 7.6 Hz, 3H); ^{13}C NMR (100 MHz, $CDCl_3$) δ 165.4, 161.2, 160.2, 159.9, 158.9, 156.6, 154.7, 153.5, 144.1, 134.7, 132.3, 130.7, 130.5, 129.3, 128.89, 128.84, 128.1, 127.9, 113.65, 113.58, 109.3, 106.2, 102.8, 61.3, 55.4, 55.2, 43.6, 13.5; IR (neat)*v*max: 3857, 3628, 2947, 2828, 2463 2226, 2042, 1666, 1112, 1024 cm^{-1}; HRMS (ESI) *m/z* calcd for $C_{33}H_{28}N_4O_5$ $[M+Na]^+$: 583.1957; Found: 583.1952.

6. General synthetic procedure for compounds 14 and 18

10a or **13a** (0.2 mmol) was dissolved with trifluoroacetic acid (1.0 mL) and stirred at room temperature for 4 h. The reaction mixture was neutralized with aqueous sodium bicarbonate and extracted thrice with DCM. After drying with anhydrous Na_2SO_4(s), the solvent was removed under reduced pressure. The

residue was purified by silica-gel flash column chromatography to obtain **14** and **18**.

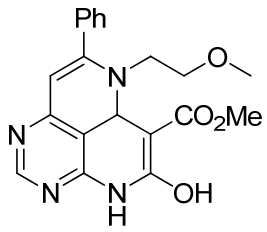

Compound 14: Yield: 77%; Orange solid; mp: 195–199 ^{o}C; ^{1}H NMR (400 MHz, $CDCl_3$) δ 11.25 (brs, 1H), 8.77 (s, 1H), 8.68 (s, 1H), 7.56–7.49 (m, 3H), 7.45–7.43 (m ,2H), 5.54 (s, 1H), 3.93 (s, 3H), 3.50 (t, *J* = 5.6 Hz, 2H), 3.43 (t, *J* = 5.2 Hz, 2H), 3.42 (s, 3H); ^{13}C NMR (100 MHz, $CDCl_3$) δ 165.1, 164.4, 162.5, 159.9, 158.5, 154.7, 141.3, 136.3, 129.7, 128.7, 127.8, 120.4, 104.0, 89.5, 71.7, 59.1, 52.6, 45.2; IR (neat)*ν*max: 3859, 3653, 2941, 2827, 2480, 2224, 2042, 1680, 1111, 1022 cm^{-1}; HRMS (ESI) *m/z* calcd for $C_{20}H_{20}N_4O_4$ $[M+Na]^+$: 403.1382; Found: 403.1377.

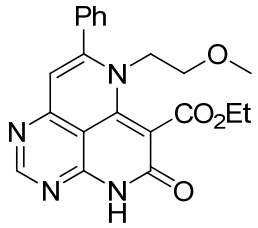

Compound 18: Yield: 76%; Pale yellow solid; mp: 211–215 ^{o}C; ^{1}H NMR (400 MHz, $CDCl_3$) δ 10.74 (brs, 1H), 8.87 (s, 1H), 7.52–7.51 (m, 3H), 7.48 (s, 2H), 6.54 (s, 1H), 4.43 (q, *J* = 7.2 Hz, 2H), 4.04 (t, *J* = 5.2 Hz, 2H), 3.41 (t, *J* = 5.2 Hz, 2H), 3.07 (s, 3H), 1.41 (t, *J* = 7.2 Hz, 3H); ^{13}C NMR (100 MHz, $CDCl_3$) δ 166.7, 161.2, 160.6, 156.6, 156.2, 153.6, 147.5, 135.5, 130.2, 129.2, 128.6, 111.2, 106.3, 102.6, 68.2, 62.1, 58.9, 51.9, 14.2; IR (neat)*ν*max: 3856, 3671, 3352, 2831, 2508, 2231, 2040, 1682, 1414, 1113, 1022 cm^{-1}; HRMS (ESI) *m/z* calcd for $C_{21}H_{20}N_4O_4$ $[M+Na]^+$: 415.1382; Found: 415.1377.

7. General synthetic procedure for compounds 15 and 19

To a solution of **4a** or **11a** (0.2 mmol) in MeOH (2.0 mL), NaOH (3.0 equiv.) was added. After stirring at 60 ^{o}C for 3 h (the reaction completion was monitored by TLC), the solvent was removed under the reduced pressure. The reaction mixture was dissolved with deionized water and extracted thrice with DCM.

After drying with anhydrous Na_2SO_4(s), the solvent was removed under the reduced pressure. The residue was purified by silica-gel flash column chromatography to obtain **15** and **19**.

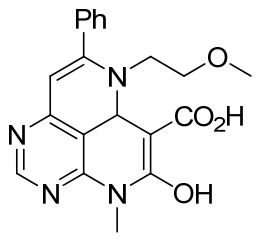

Compound 15: Yield: 80%; Yellow solid; mp: 223–227 ^{o}C; ^{1}H NMR (500 MHz, DMSO-*d*$_6$) δ 12.4 (brs, 1H), 11.06 (brs, 1H), 8.60 (s, 1H), 8.57 (s, 1H), 7.51 (s, 5H), 5.57 (s, 1H), 3.74 (s, 3H), 3.42 (s, 2H), 3.34 (s, 2H), 3.27 (s, 3H); ^{13}C NMR (100 MHz, DMSO-*d*$_6$) δ 164.5, 163.1, 161.7, 159.5, 158.1, 154.7, 138.9, 136.1, 129.5, 128.6, 127.9, 121.5, 103.2, 88.6, 71.2, 58.2, 52.0, 44.4, 40.1; IR (neat)*v*max: 3986, 3857, 3649, 2941, 2830, 2503, 2227, 2040, 1666, 1114, 1021 cm^{-1}; HRMS (ESI) *m/z* calcd for $C_{20}H_{20}N_4O_4$ $[M+Na]^+$: 403.1382; Found: 403.1377.

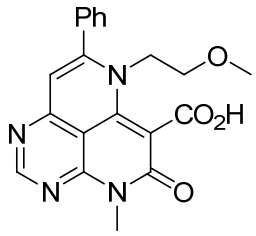

Compound 19: Yield: 70%; Off-white solid; mp: 172–176 ^{o}C; ^{1}H NMR (400 MHz, $CDCl_3$) δ 9.04 (s, 1H), 7.75–7.73 (m, 2H), 7.58–7.56 (m, 3H), 7.03 (s, 1H), 4.38 (s, 2H), 3.84 (s, 3H), 3.15 (t, *J* = 5.2 Hz, 2H), 2.94 (s, 3H); ^{13}C NMR (100 MHz, $CDCl_3$) δ 166.9, 165.0, 161.0, 156.0, 155.9, 154.0, 153.7, 134.9, 130.9, 129.5, 129.0, 128.6, 128.2, 125.3, 113.9, 97.1, 69.5, 59.3, 58.7, 28.8; IR (neat)*v*max: 3972, 3857, 3358, 2943, 2827, 2507, 2225, 2040, 1680, 153, 1023 cm^{-1}; HRMS (ESI) *m/z* calcd for $C_{20}H_{18}N_4O_4$ $[M+Na]^+$: 401.1226; Found: 401.1220.

8. General synthetic procedure for compounds 16 and 20

To a solution of **4a** or **11a** (0.2 mmol) in DMF (2.0 mL), NaOH (3.0 equiv.) was added. After stirring at 120 ^{o}C for 12 h (the reaction completion was monitored by TLC), the reaction mixture was quenched with deionized water. The resultant was extracted with DCM (10 mL × 3) and the combined organic

layer was washed with brine (10 mL). After drying with anhydrous Na_2SO_4(s), the solvent was removed under the reduced pressure. The residue was purified by silica-gel flash column chromatography to obtain **16** and **20**.

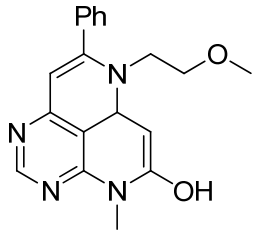

Compound 16: Yield: 64%; Pale yellow solid; mp: 155–159 °C; ^{1}H NMR (400 MHz, $CDCl_3$) δ 10.85 (brs, 1H), 8,.73 (s, 1H), 7.84 (d, *J* = 9.6 Hz, 1H), 7.45 (s, 5H), 6.59 (d, *J* = 9.6 Hz, 1H), 5.46 (s, 1H), 3.77 (s, 3H), 3.48 (t, *J* = 5.6 Hz, 2H), 3.39 (s, 3H), 3.38 (t, *J* = 5.2 Hz, 2H); ^{13}C NMR (100 MHz, $CDCl_3$) δ 163.4, 162.2, 162.0, 156.1, 153.8, 136.9, 133.1, 132.8, 129.8, 129.2, 128.5, 128.2, 127.9, 120.0, 106.1, 89.3, 72.1, 59.0, 44.8, 28.2; IR (neat)*v*max: 3857, 3646, 2941, 2831, 2495, 2230, 2041, 1680, 1453, 1114, 1023 cm^{-1}; HRMS (ESI) *m/z* calcd for $C_{19}H_{20}N_4O_2$ $[M+Na]^+$: 359.1484; Found: 359.1478.

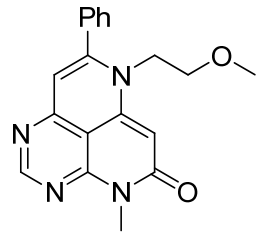

Compound 20: Yield: 74%; Brown solid; mp: 120–124 °C; ^{1}H NMR (400 MHz, $CDCl_3$) δ 8.80 (s, 1H), 7.52–7.50 (m, 3H), 7.40–7.37 (m, 2H), 6.24 (s, 1H), 5.86 (s, 1H), 3.91 (t, *J* = 5.6 Hz, 2H), 3.71 (s, 3H), 3.53 (t, *J* = 5.6 Hz, 2H), 3.17 (s, 3H); ^{13}C NMR (100 MHz, $CDCl_3$) δ 163.5, 160.1, 155.8, 154.4, 154.3, 146.3, 134.7, 130.8, 129.8, 128.8, 128.5, 108.3, 106.5, 91.7, 66.8, 58.9, 47.3, 27.8; IR (neat)*v*max: 3978, 3858, 3674, 3300, 2827, 2495, 2232, 2041, 1454, 1024 cm^{-1}; HRMS (ESI) *m/z* calcd for $C_{19}H_{18}N_4O_2$ $[M+Na]^+$: 357.1327; Found: 357.1322.

9. General synthetic procedure for compounds 17 and 21

4g or **11g** (0.2 mmol) was dissolved with trifluoroacetic acid (1.0 mL) and stirred at 50 °C for 4 h. The reaction mixture was neutralized with aqueous sodium bicarbonate and extracted thrice with DCM. After drying with

anhydrous Na_2SO_4(s), the solvent was removed under the reduced pressure. The residue was purified by silica-gel flash column chromatography to obtain **17** and **21**.

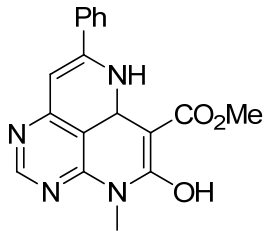

Compound 17: Yield: 86%; Orange solid; mp: 181–185; ^{1}H NMR (400 MHz, $CDCl_3$) δ 10.29 (brs, 1H), 8.79 (s, 1H), 8.76 (s, 1H), 7.68–7.66 (m, 2H), 7.53–7.48 (m, 3H), 5.93 (s, 1H), 3.96 (s, 3H), 3.79 (s, 3H); ^{13}C NMR (100 MHz, $CDCl_3$) δ 165.6, 164.0, 160.0, 159.8, 157.9, 155.3, 138.6, 138.5, 130.6, 129.1, 128.7, 126.5, 120.5, 105.5, 87.9, 52.7, 28.7; IR (neat)*ν*max: 3859, 3646, 2945, 2830, 2508, 2229, 2039, 1695, 1452, 1115, 1022 cm^{-1}; HRMS (ESI) *m/z* calcd for $C_{18}H_{16}N_4O_3$ $[M+Na]^+$: 359.1120; Found: 359.1115.

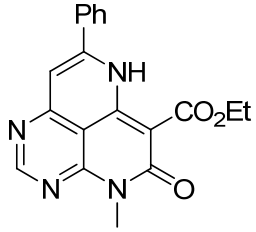

Compound 21: Yield: 67%; Off-white solid; mp: 209–213 °C; ^{1}H NMR (400 MHz, $CDCl_3$) δ 13.79 (brs, 1H), 8.93 (s, 1H), 7.83–7.81 (m, 2H), 7.63–7.60 (m, 3H), 4.47 (q, *J* = 7.2 Hz, 2H), 3.78 (s, 3H), 1.49 (t, *J* = 7.2 Hz, 3H); ^{13}C NMR (100 MHz, $CDCl_3$) δ 170.3, 161.8, 160.4, 157.3, 155.8, 150.0, 148.4, 132.6, 131.6, 129.9, 126.1, 106.6, 104.5, 90.6, 61.3, 27.9, 14.4; IR (neat)*ν*max: 3858, 3687, 3432, 2942, 2830, 2508, 2225, 2043, 1450, 1113, 1024 cm^{-1}; HRMS (ESI) *m/z* calcd for $C_{19}H_{16}N_4O_3$ $[M+Na]^+$: 371.1120; Found: 371.1115.

IV. Experimental Procedures for Cell Viability Test and LD screening

1. Reagents and materials

SF44, a fluorescent bioprobe for lipid droplets, was prepared by following the reported procedure.[1,2] Hoechst 33342 was purchased from Invitrogen. Micro BCA™ Protein Assay Kit was purchased from PIERCE. Ez-cytox kit was purchased from Daeil Co. (Korea). Cell culture reagents including fatal bovine serum, culture media, and antibiotic-antimycotic solution were purchased from GIBCO, Invitrogen. The culturing dish or screening plates were purchased from CORNING. Antibodies for western blot analyses were purchased from Abcam and Cell Signaling. Amersham ECL Prime Western Blotting Detection System was purchased from GE Healthcare Life Science.

2. Instruments for biological assays

High-contents screening was performed by InCell Analyzer 2000 (GE Healthcare). Data were analyzed by InCell Analyzer 1000 workstation 3.6 program according to the manufacturer's protocol. Fluorescence microscopic images were taken by Olympus Inverted Microscope Model IX71, equipped for epi-illumination using a halogen bulb (Philips No. 7724). Emission signal of each experiment was observed at the indicated spectral setting: green channel, using a 450–480 band pass exciter filter, a 500 nm center wavelength chromatic beam splitter, a 515 nm-long pass barrier filter (Olympus filter set U-MWB2). Emission signals of each experiment were detected with 12.5 M pixel recording digital color camera (Olympus, DP71). For western blots, chemiluminescent signal was monitored by ChemiDocTM MP imaging system (Bio-Rad) and quantified by ImageLab 4.0.1 program. For the EZ-cytox-based cell cytotoxicity test, the absorbance of 96-well plate was measured by BioTek Synergy HT Microplate reader.

3. Cell culture

HeLa and HEK293T were obtained from American Type Culture Collection [ATCC, Manassas, VA, USA]. HeLa cell lines were cultured in RPMI 1640 [GIBCO, Invitrogen] supplemented with heat-inactivated 10% (v/v) fetal bovine serum [GIBCO, Invitrogen] and 1% (v/v) antibiotic-antimycotic solution [GIBCO, Invitrogen]. HEK293T cells were maintained in DMEM [GIBCO, Invitrogen] supplemented with heat-inactivated 10% (v/v) calf serum [GIBCO, Invitrogen] and 1% (v/v) antibiotic-antimycotic solution [GIBCO, Invitrogen]. Cells were maintained in a humidified atmosphere of 5% CO_2 incubator at 37 °C, and cultured in 100 mm cell culture dish [CORNING].

4. Cell viability assay

In vitro cytotoxicity was measured by using EZ-cytox assay kit, and the experimental procedure was based on the manufacturer's manual. Briefly, HeLa or HEK293T cells were cultured on 96-well plates at a density of 3×10^3 cells/well for 24 h, and then cells were treated with compounds in various concentrations. After incubating for 24 h in presence of compounds, 10 μL of WST-1 solution containing (2-(4-nitrophenyl)-5-(2-sulfophenyl)-3-[4-(4-sulfophenylazo)-2-sulfophenyl]-2H-tetrazolium disodium salt was added to each well, and the plates were incubated for additional 1 h at 37 °C. Absorbance in 455 nm was measured by a microplate reader. The percentage of cell viability was calculated by following formula: % cell viability = (mean absorbance in test wells)/(mean absorbance in control well)×100. Each experiment was performed in triplicate experiments.

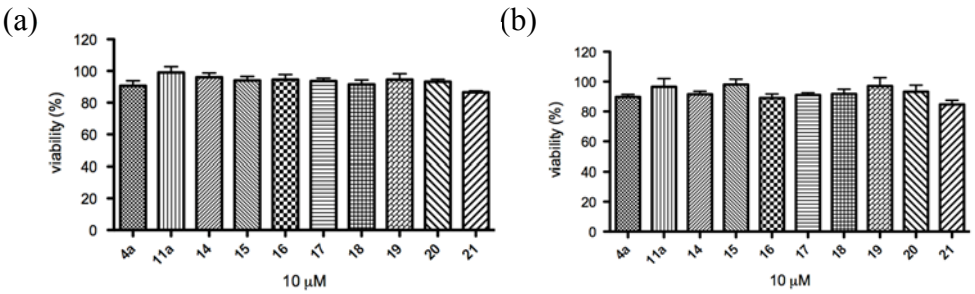

Figure S1. Cell cytotoxicity of pyrimidine-embedded compounds. (a) HeLa and (b) HEK293T cells were incubated with each compound (10 μM) for 24 h, and the cell viability was measured using WST-1 solution. Data were normalized to the viability data from the cells treated with DMSO.

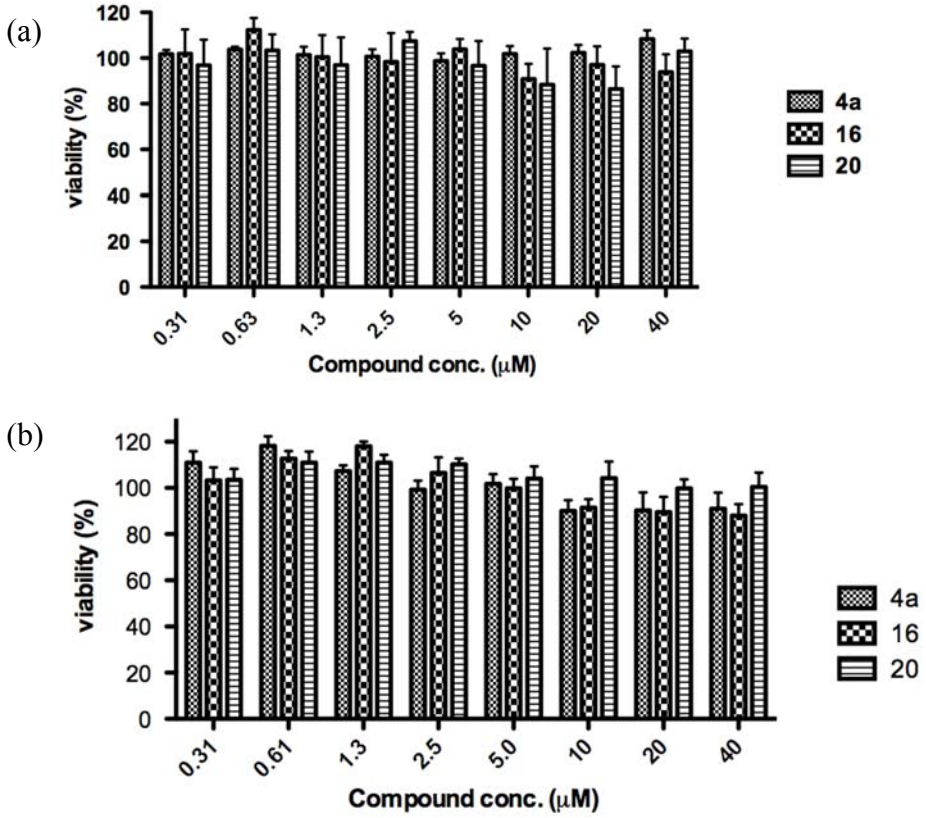

Figure S2. Cell viability test of pyrimidine-embedded compounds with various concentrations ranging from 0.3 to 40 μM. (a) HeLa and (b) HEK293T cells were incubated with **4a**, **16**, and **20** for 24 h, and the cell viability was measured

using WST-1 solution. Data were normalized to the viability data from the cells treated with DMSO.

5. High-content screening for cellular lipid droplets

The image-based high-throughput screening for cellular LDs was carried out by following the reported protocol.[1,2] Briefly, HeLa cells were seeded on 96-well plates at a density of 3×10^3 cells/well and incubated for 24 h at 5% CO_2, 37 °C. After the incubation, compounds were treated to the cells on each well of the plates with their final concentration as 10 μM (for the initial screening) or with various concentrations (for dose-dependency test), for 24 h in 5% CO_2 incubator at 37 °C. Individual screening plates contained the reference wells as a control such as DMSO for the normalization, oleic acid (5 μM) as a positive control, and serum-free condition as a negative control. SF44 (5 μM) and Hoechst 33342 (2 μg/mL) was added to cells for probing lipid droplets and nuclei, respectively, and incubated for 30 min at 37 °C. LD-staining patterns in live cells were measured using automated fluorescence microscopy (InCell Analyzer 2000) directly without additional washing steps. Four different fields in each well of a 96-well plate were randomly selected for the automatic image capturing in auto-focusing mode (20 nm scale) with indicated filter setting; Excitation filter: 430/24 nm and Emission filter 605/64 nm for LD; Excitation filter: 350/50 nm and Emission filter: 455/50 nm for nuclei.

(a)

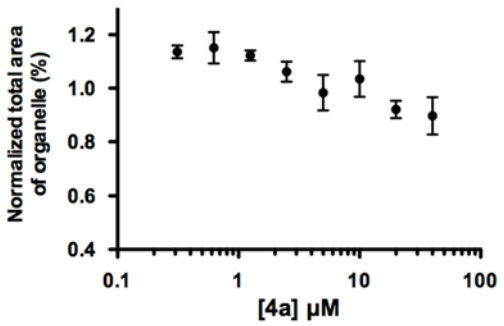

(b)

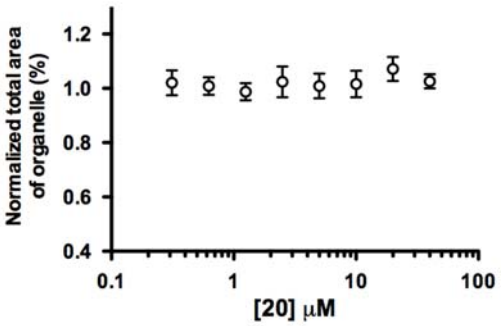

Figure S3. Dose-dependent analysis of the cellular LDs in HeLa cells upon treatment with (a) **4a** and (b) **20**. Experiments were triplicated.

6. Fluorescence imaging

HeLa cells were seeded on cover glass bottom dish and incubated for 24 h at 5% CO_2, 37 °C. Compounds (**4a**, **16**, **20** and oleic acid) were added to the cells in media, and incubated for 24 h. SF44 (5 μM, 30 min) and Hoechst 33342 (2 μg/mL, 20 min) were added to cells in normal growth media. Fluorescence, and bright-field images were taken under a fluorescence microscopy (Olympus Inverted Microscope Model IX71) in PBS buffer.

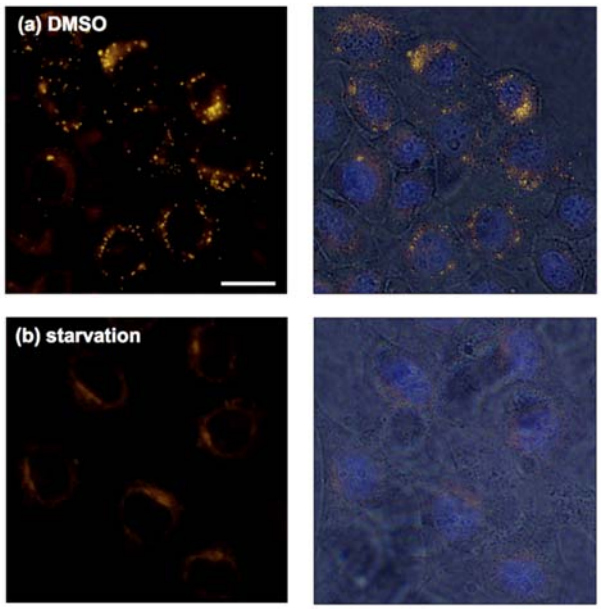

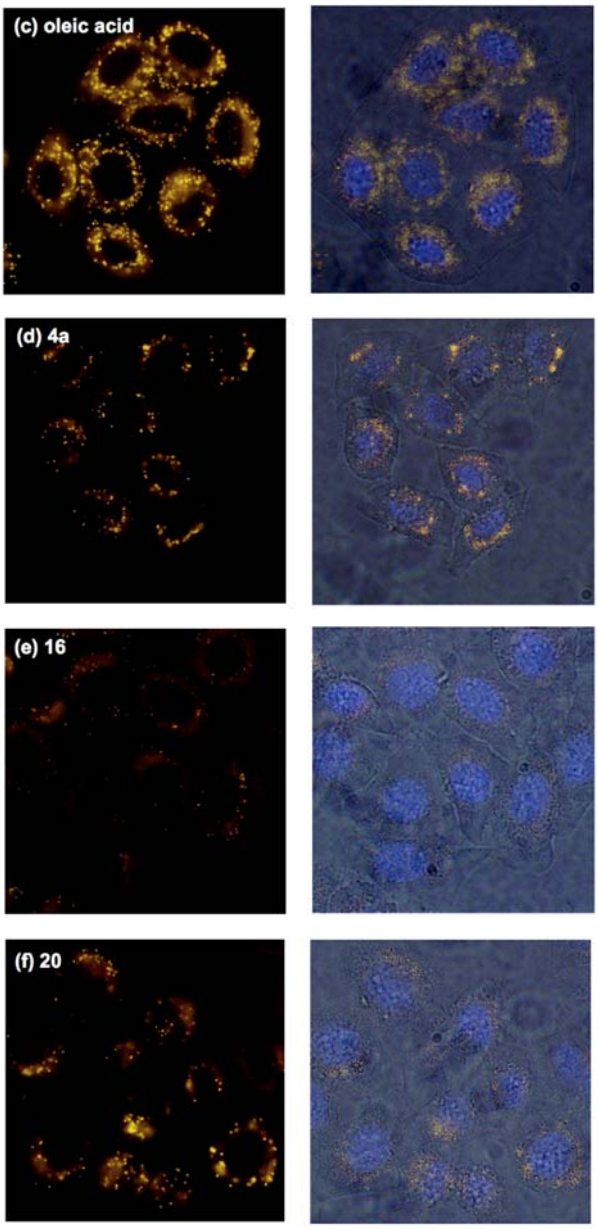

Figure S4. Fluorescence (LDs) and merged (fluorescence and bright field) images of live HeLa cells presenting different cellular LD levels. Cells were incubated with (a) DMSO; (b) serum-free media; (c) oleic acid, 5 μM; (d) **4a**, 10 μM; (e) **16**, 10 μM; (f) **20**, 10 μM for 24 h. Scale bar: 20 μm.

6. Western blot analysis

HeLa cells were seeded on 6-well plate and incubated for 24 h at 5% CO_2, 37 °C. Cells were treated with compounds (10 μM for **4a**, **16** and **20**, 10 nM for bafilomycin A1 and 200 nM for rapamycin). After 12 h of incubation, cells were harvested and frozen at −80 °C. Cells were lysed in RIPA buffer containing protease inhibitors and phosphatase inhibitors on ice for 30 min. After centrifuging down the cell lysates (14,000 rpm and 4 °C for 10 min), the supernatant was transferred and the total protein concentrations were measured by BCA assay. The resulting proteome were analyzed by SDS-PAGE and transferred into PVDF membrane, followed by 2% BSA blocking in TBST over 1 h. The samples were subjected to immunoblotting to detect the conversion of LC3-I to LC3-II and the degradation of p62 with specific primary antibodies, e.g. anti-LC3 (abcam), anti-p62 (cell signaling), and β-actin (cell signaling) antibodies for overnight at 4 °C, followed by washing with TBST for 1 h. The resulting membrane was exposed into HRP-conjugated secondary antibody for 1 h at room temperature. After washing membranes with TBST for 1 h, the membrane was developed by ECL prime solution and the chemiluminescent signal was measured by ChemiDocTM MP imaging system.

2-5. Reference

[1] Swinney, D. C. *Clin. Pharmacol. Ther.*, **2013**, *93*, 299.

[2] Swinney, D. C.; Anthony, J. *Nat. Rev. Drug Disc.*, **2011**, *10*, 507.

[3] Schreiber, S. L. *Nature*, **2009**, *457*, 153.

[4] Lipinski, C.; Hopkins, A. *Nature*, **2004**, *432*, 855.

[5] Galloway, W. R. J. D.;
Spring, D. R. *Expert Opin. Drug Discovery*, **2009**, *4*, 467.

[6] Tan, D. S. *Nat. Chem. Biol.*, **2005**, *1*, 74.

[7] Galloway, W. R. J. D.; Isidro-Llobet, A.; Spring, D. R. *Nat. Commun.*, **2010**, *1*, 80.

[8] O'Connor, C. J.; Beckmann, H. S. G.; Spring, D. R. *Chem. Soc. Rev.*, 2012, **41**, 4444.

[9] Oh, S.-M.; Park, S. B. *Chem. Commun.*, **2011**, *47*, 12754.

[10] Kim, J.; Kim, H. ; Park, S. B. *J. Am. Chem. Soc.*, **2014**, *136*, 14629.

[11] Lee, S.; Nam, Y.; Koo, J. Y.; Lim, D.; Park, J.; Ock, J.; Suk, K.; Park, S. B. *Nat. Chem. Biol*, **2014**, *10*, 1055.

[12] Oh, S.; Kim, J.; Hwang, J. H.; Lee, H. Y.; Ryu, M. J.; Park, J.; Kim, S. J.; Jo, Y. S.; Kim, Y. K.; Lee, C. H.; Kweon, K. R.; Shong, M.; Park, S. B. *J. Med. Chem.*, 2010, **53**, 7405.

[13] Kim, J.; Cho, T.–J.; Kwon, S.-K.; Oh, K.; Lee, J.-A.; Lee, D.-S.; Cho, J.; Park, S. B. *Chem. Sci.*, **2012**, *3*, 3071.

[14] Park, J.; Oh, S.; Park, S. B. *Angew. Chem. Int. Ed.*, **2012**, *51*, 5447.

[15] Ko, S. K.; Jang, H. J.; Kim, E.; Park, S. B. *Chem. Commun.*, **2006**, *28*, 2962.

[16] Kim, H.; Tung, T. T.; Park, S. B. *Org. Lett.*, **2013**, *15*, 5814.

[17] Larghi, E. L.; Bohn, M. L.; Kaufman, T. S. *Tetrahedron*, **2009**, *65*, 4257.

[18] Shen, Y.-C.; Lin, T.-T.; Sheu, J.-H.; Duh, C.-Y. *J. Nat. Prod.*, **1999**, *62*, 1264

[19] SouZa, T. M.; Abrantes, J. L.; Epifanio, R. A.; Fontes, C. F. L.; Fruguhetti,

I. C. P. *Planta Med.*, **2007**, *73*, 200.

[20] Fugmann, B.; Steffan, B.; Steglich, W. *Tetrahedron Lett*., **1984**, *25*, 3575.

[21] Naoki, A.; Salprima, Y. S.; Tsutomu, N.; Yoshinori, Y. *Angew. Chem. Int. Ed.*, **2005**, *44*, 5526.

[22] Inga, C.; Rita, B.; Simonas, R.; Marius, M.; Dainius, M. *Tetrahedron*, **2010**, *66*, 251.

[23] Lee, S.; Kim, E.; Park, S. B. *Chem. Sci.*, **2013**, *4*, 3282–3287.

[24] Kim, E.; Lee, S.; Park, S. B. *Chem. Commun.*, **2012**, *48*, 2331.

Part 3. Discovery of Pyrazolo[1,5-*a*]pyridine-Fused Pyrimidine Based Novel Fluorophore and Its Bioapplication to Probing Lipid Droplets

Chem. Commun. **2016**, *52*, 7822–7825.

3-1. Introduction

Fluorescent small molecules play significant roles in the biomedical and life sciences as research tools for monitoring spatiotemporal change in certain biological processes.[1,2] The development of novel fluorescent probes for specific analytes, such as chemokines, metabolites, and ions, might initiate new research topics or fields. Therefore, identifying novel fluorescent core skeletons is important for the development of new bioprobes. In addition, understanding the structural features of fluorescent materials toward their photophysical properties for biological applications is essential. For last decade, our group has developed indolizine-based new fluorescent core skeleton, named Seoul-Fluor (SF),[3] which has been studied to unprecedentedly predict its photophysical properties, such as emission wavelength (λ_{em}),[4] quantum yield (Φ),[5] and molar absorptivity (ε)[6] with its structural information. On the basis of the systematic investigations of structure–photophysical property relationship in SF, a variety of SF-based bioprobes were rationally designed and applied to monitor the specific biological events, such as selective phosphatase activity,[7] lipid droplets (LDs),[8] or mitochondria.[6] Thus, the identification of new fluorescent core skeletons along with a thorough study of structure-photophysical property relationship may shed light on productive progresses to dissect and understand valuable biological processes.

Pyrimidine has been recognized as a useful core structure not only in the development of therapeutic agents,[9] but also light-emitting materials such as organic light-emitting diodes,[10] luminescent sensors,[11] and nonlinear optical

materials.[12] However, pyrimidine-containing fluorescent heteroaromatic materials have not been explored extensively explored due to difficult syntheses. Thus, there has been no systematic study regarding the structure-photophysical property relationship in pyrimidine-embedded heterocyclic fluorescent molecules and no subsequent bioprobe development. We recently developed a new privileged substructure-based diversity-oriented synthesis (pDOS) strategy for the preparation of a series of pyrimidine-embedded distinct polyheterocycles with high biological relevancy.[13]

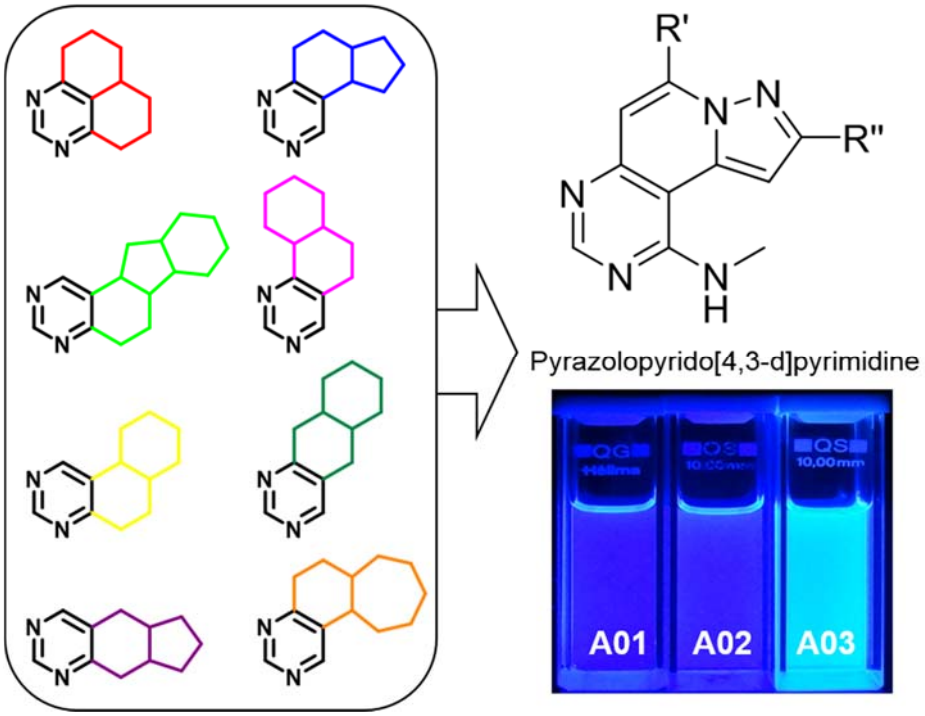

Figure 3-1. Unexpected fluorescence of pyrazolo[1,5-*a*]pyridiopyrimidine among various pyrimidine-containing polyheterocyclic core skeletons generated by the pDOS strategy

As shown in **Figure 3-1**, we synthesized pyrazolo[1′,5′:1,2]pyrido[4,3-*d*]pyrimidine, and found that analogues of this core skeleton emit violet and blue fluorescence. Herein, we report pyrazolo[1,5-*a*]pyridine-fused pyrimidines, named fluoremidine (FD), a novel fluorescent core skeleton with unique photophysical properties and applicability in bioimaging. Based on the observed absorption and emission spectra of A01–A03, we hypothesized that the phenyl

moiety at the R′ and R″ position could be essential for controlling the emission wavelength and brightness of fluoremidine (see **Table S1**). To test this hypothesis, we introduced various substituents at the R^1 and R^2 positions in order to change the electronic character of the phenyl rings and systematically understand structure-photophysical property relationships in fluoremidine.

3-2. Results and discussion

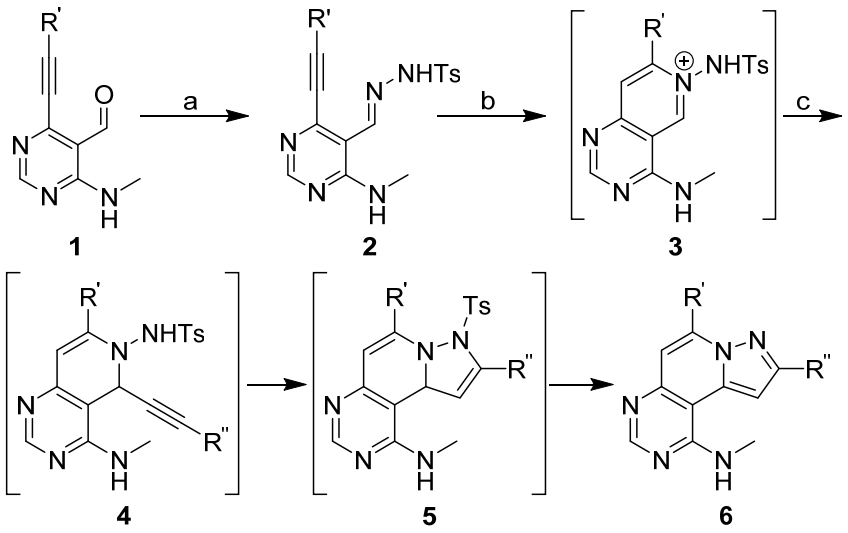

Scheme 3-1. Synthetic Scheme of Fluoremidine (FD). *Reagents and conditions*: (a) tosyl hydrazide, AcOH, MeOH, 40 °C; (b) AgOTf, DCE, 80 °C; (c) terminal alkynes, DBU, r.t.

For the efficient preparation of FD analogues, we employed the silver-promoted domino cyclization of pyrimidine containing *p*-tosylhydrazone (**2**), prepared from *ortho*-alkynylpyrimidine carbaldehyde (**1**) and *p*-tosylhydrazide. As shown in **Scheme 3-1**, **2** was first converted to bicyclic pyridinium (**3**) via Ag-catalyzed 6-*endo* cyclization. After the formation of cyclic intermediates (**4**) from the nucleophilic attack of terminal alkynes at the iminium moiety, the desired fluoremidine core skeleton (**6)** afforded by the 5-*endo* cyclization of **4** followed by spontaneous aromatization via removal of the *p*-tosyl group in intermediate **5**. This four-step transformation allowed the efficient preparation

of FD analogues with moderate yields (average 62%) in a one-pot process (see **Table S2**).

Table 3-2. Photophysical properties of fluoremidine (FD) fluorophores

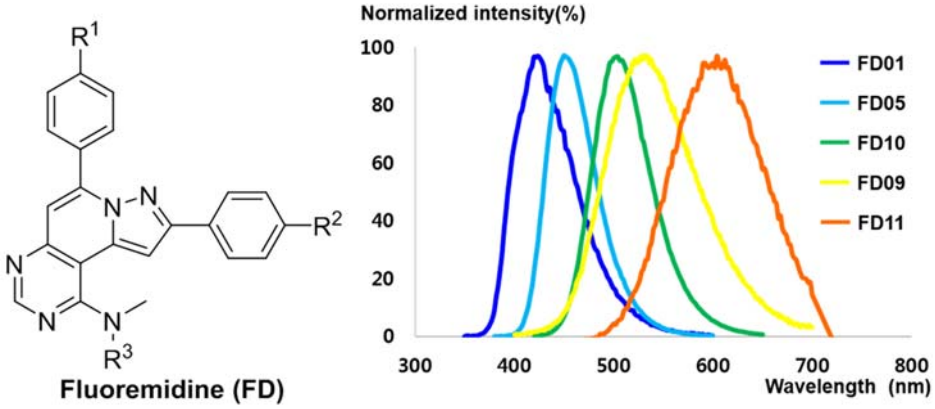

cpd	R^1	R^2	R^3	λ_{abs} [a]	λ_{em} [b]	ε	Q.Y. [c]
FD01	H	H	H	330	424	13000	0.12
FD02	CN	H	H	329	456	9000	0.15
FD03	CF_3	H	H	333	438	14000	0.14
FD04	OCH_3	H	H	324	420	20000	0.16
FD05	$N(CH_3)_2$	H	H	367	452	28000	0.73
FD06	H	CN	H	337	422	13000	0.10
FD07	H	CF_3	H	333	420	12000	0.12
FD08	H	OCH_3	H	328	424	16000	0.13
FD09	H	$N(CH_3)_2$	H	348	532	22000	0.41
FD10	$N(CH_3)_2$	H	Ac	403	504	24000	0.72
FD11	H	$N(CH_3)_2$	Ac	393	604	12000	0.15

All experiment data obtained in dichloromethane (DCM). [a]Only the longest absorption maxima are shown. [b]Excited at the maximum excitation wavelength. [c] Absolute quantum yield.

Using this synthetic strategy, 11 FD analogues were prepared and their photophysical properties were measured. When R^1 was changed from an electron-donating group (EDG) to an electron-withdrawing group (EWG) with

identical proton substituent at the R^2 position (**FD01**–**FD05**), the emission wavelength changed marginally. However, a *N*,*N*-dimethylamino group at the R^1 position (**FD05**) resulted in a considerably enhanced quantum yield, from 12% to 73%, and a two-fold enhancement in molar absorptivity, which was consistent with reports that *N*,*N*-dialkylamino groups at the 4- or 6-positions connected with π-conjugation in pyrimidine cores make it possible to increase their quantum yield and molar absorptivity.[14-16] This implied that our new fluorophore, fluoremidine, had behavior similar to a single pyrimidine motif in terms of managing fluorescent brightness. When the R^1 position was fixed as a proton, FD derivatives containing various substituents at the R^2 position (**FD06**–**FD09**) did not show any difference in fluorescent characteristics, except **FD09**, which had an *N*,*N*-dimethylamino group and emitted 532 nm light with a 108 nm bathochromic shift relative to **FD01**, along with a slightly improved quantum yield and molar absorptivity. This significant red shift in emission wavelength might have been due to intramolecular charge transfer (ICT) between the *N*,*N*-dimethylamino group in the R^2 position and nitrogens in the FD molecular framework. The electronic push-pull system could reduce the energy gap between the highest occupied molecular orbital (HOMO) and the lowest unoccupied molecular orbital (LUMO). Based on the HOMO–LUMO energy gap and changes in their lobe shapes, we concluded that an ICT process was highly probable in the **FD09** molecular structure (see **Figure S1**).

We then explored controlling the emission wavelength over a wider range because the emission wavelengths of **FD01–FD09** were either blue or green. The π-electron donating ability of amino groups in the pyrimidine motif might influence the emission wavelength, which was expected due to stabilization of the LUMO state (see **Figure S2**); **FD10** and **FD11**, *N*-acetylated analogues at the R^3 position of **FD05** and **FD09**, showed 50 nm and 70 nm-red shifts in emission wavelength, respectively. This observation was consistent with the predicted decrease in energy gap between HOMO and LUMO, mainly due to

lowering LUMO state by diminishing the electron-donating character of amino group by *N*-acetylation in the pyrimidine moiety. Consequently, an *N*,*N*-dimethylamino group at the R^2 position and *N*-acetylation of the amino group in the pyrimidine moiety significantly influenced the emission wavelength of the fluoremidine system, allowing a wider spectrum of emission wavelengths (424–604 nm) compared with those of known pyrazolo[1,5-*a*]pyridine-based fluorescent compounds (421–444 nm).[17]

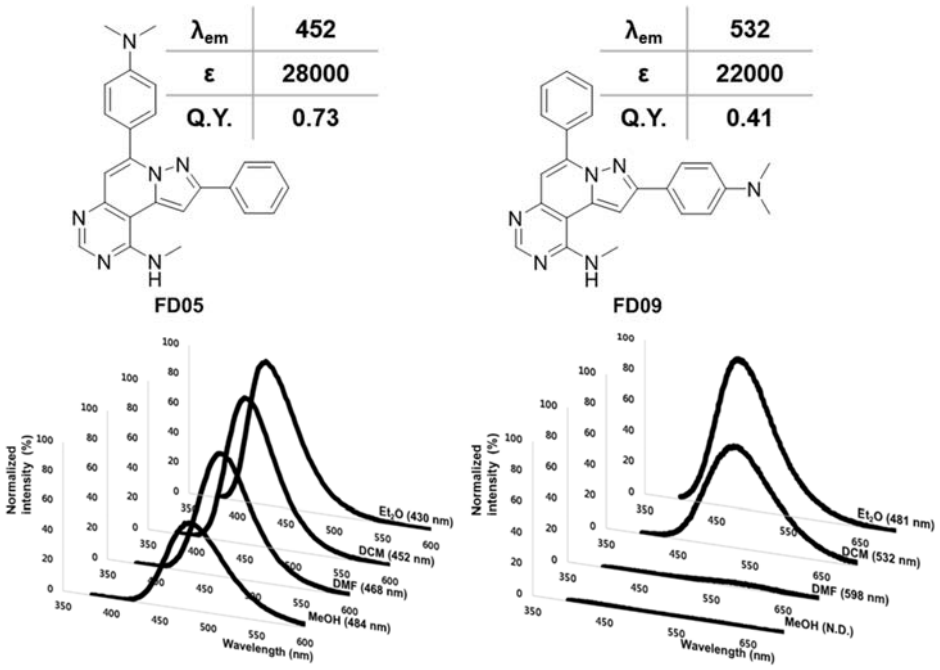

Figure 3-2. Chemical structure, photophysical property, solvatochromism of **FD05** and **FD09**

Next, we investigated the photophysical properties of **FD01**–**FD11** resulting from environmental changes, such as solvent polarity. As shown in **Figure 2**, solvatochromism was clearly observed in *N*,*N*-dimethylamino-containing FD analogues (**FD05**, **FD09**, **FD10**, and **FD11**), but was not observed in other analogues (see **Table S3**). This solvatochromism might have been caused by changes in the electronic push-pull system (ICT process) of *N*,*N*-dimethylamino group with other nitrogens in the FD core skeleton. Moreover, these FD analogues showed turn-on fluorescence in nonpolar solvents (Et_2O and DCM),

allowing the rational sensor design of lipophilic organelles or biopolymers in cellular systems as new bioprobes. Thus, we treated **FD05**, **FD09**, **FD10**, and **FD11** in the A549 human lung carcinoma cell line to test whether they could selectively stain certain lipophilic organelles in living cells. Unfortunately, the tested compounds produced no clear fluorescence images due to their weak fluorescent intensity or high background signal (see **Figure S3**).

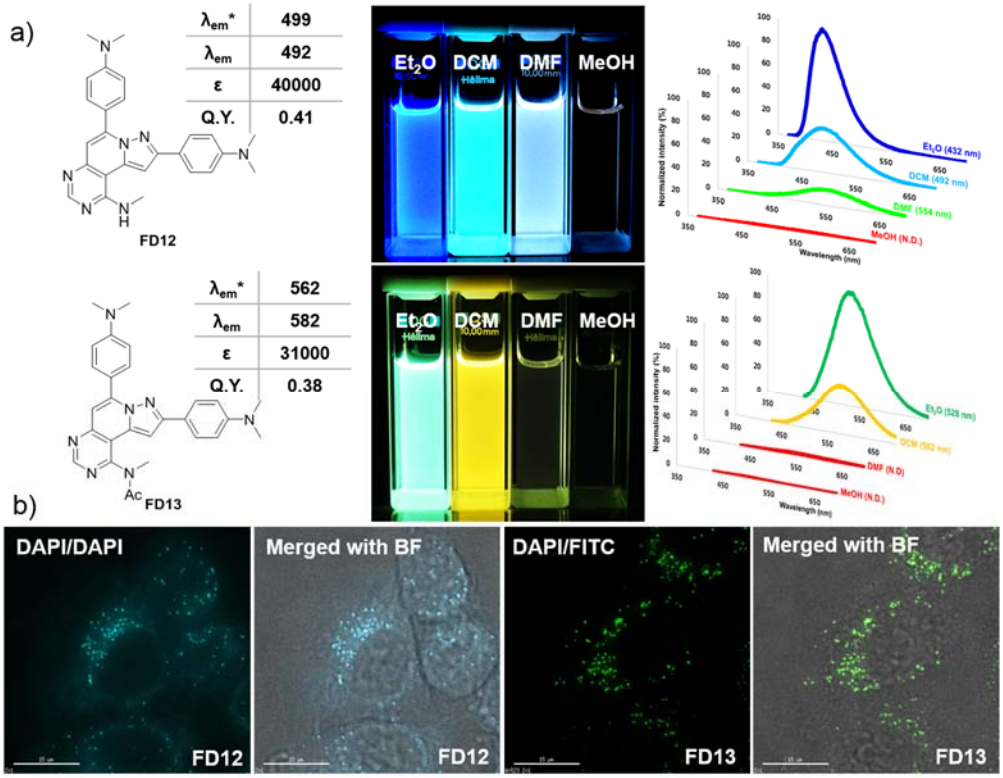

Figure 3-3. a) Structure and solvatochromism of **FD12** and **FD13**. Estimated values (*); b) Live cell imaging after staining A549 cells with **FD12** and **FD13**. A549 cells were treated with 20 μM of either **FD12** or **FD13** in a 5% CO_2 incubator. After 1 h, cells were washed with PBS, and fluorescence images were taken using a DeltaVision imaging system. Scale bars, 15 μm.

Based on this observation, we designed new molecules **FD12** and **FD13** to improve the brightness and staining specificity in live cell imaging by introducing *N*,*N*-dimethylamino group at the both R^1 and R^2 positions, and differentiating with the absence or presence of an acetyl moiety on the pyrimidine amino group, respectively. Based on *in silico* analysis of the

HOMO–LUMO energy gap, we were able to predict their emission wavelengths. As shown in **Figure 3-3a**, **FD12** and **FD13** showed high molar absorptivity with two different emission wavelengths, 492 nm (sky blue) and 582 nm (green), respectively, which were consistent with predicted emission wavelengths (see **Figure S4**). Moreover, we observed clear solvatochromism with excellent turn-on/off ratios upon changes in polarity (see **Table S4**). When A549 cells were treated with either **FD12** or **FD13**, we could monitor the cellular staining patterns in two different channels, DAPI and FITC, respectively. Based on their cellular staining images shown in **Figure 3-3b**, we selected **FD13** for further biological evaluation due to its selective staining pattern, clear turn-on fluorescence in the lipophilic environment, and low background signal caused by endogenous cellular fluorescence.

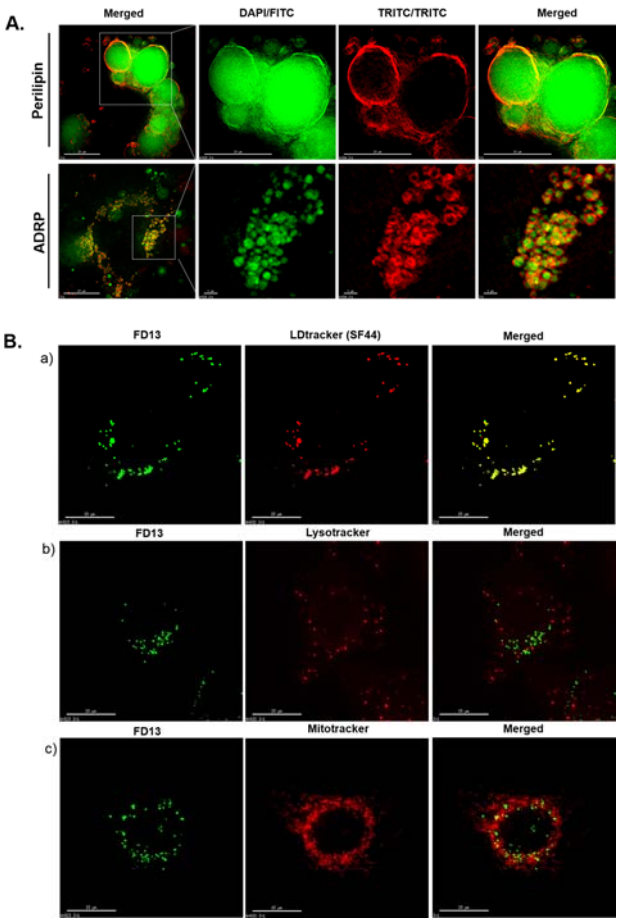

Figure 3-4. (A) Immunofluorescent images of perilipin and adipose differentiation-related protein (ADRP) in differentiated 3T3-L1 adipocyte. TRITC-conjugated secondary antibody is used to detect each primary antibody. After the antibody labeling, cells are treated with 20 μM of **FD13** for 1 h at room temperature. Then, cells are washed with PBS, and the fluorescence images were taken by DeltaVision imaging system. Fluorescence signal were obtained using DAPI/FITC filter set for **FD13** and TRITC/TRICT filter set for antibody labeling. Scale bars are shown in each figure. (B) Colocalization of **FD13** and lipid droplet tracker (LD tracker, SF44). A549 cells were treated with 20 μM **FD13** for 1 h. Cellular lipid droplet, lysosome, and mitochondria were stained with SF44 (20 μM), Lysotracker Red (50 nM), and Mitotracker Red (20 nM), respectively, for 30 min. After washing, live cell images were obtained using DeltaVision imaging system equipped with a 60× lens. Merged images show specific colocalization of **FD13** and LD tracker (yellow). Scale bars, 15 μm. Images of a) **FD13** and LD tracker; b) **FD13** and Lysotracker; and c) **FD13** and Mitotracker.

Lipid droplets (LDs) have been known as the cellular storehouse of lipids such as cholesterol and triglycerides, but recent studies have shown that LDs are dynamic subcellular organelles with various sizes and quantities, which can be closely related to metabolic syndromes, such as cardiovascular diseases, type 2 diabetes, cancer, and Alzheimer's disease.[18,19] Along with the increasing scientific interest, image-based high-content screening system of cellular LDs was developed.[20] Thus, we focused on the lipophilic nature of LDs and presumed that the specific staining pattern of **FD13** might be matched with the subcellular location of LDs. In order to verify this assumption, immunohistochemistry using adipose differentiated-related protein (ADRP) and perilipin—the surface markers of early-stage and late-stage lipid droplets, respectively—with **FD13** in the differentiated 3T3-L1 cells was performed. As shown in **Figure 3-4A**, the specific LD staining property of **FD13** was clearly confirmed via co-staining experiment of ADRP and perilipin. Besides, **FD13** was co-treated with SF44, a well-studied LD tracing turn-on probe developed by our group.[8] As shown in **Figure 3-4B**, the cellular images of **FD13** and SF44 are well merged. However, the staining image of **FD13** does not match with that of the Lysotracker or the Mitotracker. Consequently, we concluded that **FD13** could be a new fluorescent bioprobe for tracing the subcellular location of LDs with their size and quantity in living cells through its turn-on fluorescence property in a hydrophobic environment.

3-3. Conclusion

In this study, we discovered a novel fluorescent skeleton containing pyrazolo[1,5-*a*]pyridine-fused pyrimidine, named fluoremidine. Based on our efficient preparation of core skeletons via silver-promoted tandem cyclization, we readily synthesized a collection of fluoremidine analogues with various substituents at the R^1, R^2, and R^3 positions. In terms of brightness, *N*,*N*-dimethylamino group at the R^1 position significantly increased the quantum yield and molar absorptivity. Regarding the specific tuning of emission wavelength, *N*,*N*-dimethylamino group at the R^2 position and *N*-acetyl group at the R^3 position significantly contributed to a large bathochromic shift. Moreover, we observed a fluorescent turn-on property in FD analogues containing *N*,*N*-dimethylamino group in the lipophilic environment. On the basis of the unique fluorescent properties, we designed a new fluorescent probe for real-time monitoring of cellular changes in LDs, important organelles related to lipid biogenesis or autophagy. We demonstrated that **FD13** selectively stained cellular LDs, confirmed by successful co-staining experiments with LD tracker (SF44), but did not when co-stained with Lysotracker or Mitotracker. Based on the development of **FD13**, a real-time LD-specific bioprobe, we can state that fluoremidine, a new pyrimidine-embedded heteroaromatic fluorescent core skeleton, serves as a template for the development of novel and practical bioprobes for enlightening unexplored biological systems.

3-4. Supporting information

I. General Information

All commercially available reagents and solvents were used without further purification unless noted otherwise. All the solvents were purchased from commercial venders. ^{1}H and ^{13}C NMR spectra were obtained using Agilent 400–MR DD2 [Agilent, USA] or Varian Inova–500 [Varian Assoc., Palo Alto, USA] instruments. Chemical shifts were reported in ppm from tetramethylsilane (TMS) as internal standard or the residual solvent peak ($CDCl_3$; ^{1}H: δ = 7.26 ppm; ^{13}C: δ = 77.23 ppm). Multiplicity was indicated as follows: s (singlet), d (doublet), t (triplet), q (quartet), m (multiplet), dd (doublet of doublet), dt (doublet of triplet), td (triplet of doublet), brs (broad singlet), and so on. Coupling constants are reported in hertz. Mass spectrometric analysis was performed using a Finnigan Surveyor MSQ Plus LC/MS [Thermo] or 6120 Quadrupole LC/MS [Agilent Technologies] with electrospray ionization (ESI). High resolution mass spectrometric analyses were conducted by Ultra High Resolution ESI Q-TOF mass spectrometer [Bruker]. The conversion of starting materials was monitored by thin–layer chromatography (TLC) using pre–coated glass–backed plates (silica gel 60; F_{254}=0.25 mm), and the reaction components were visualized by observation under UV light (254 and 365 nm) or by treatment of TLC plates with visualizing agents such as $KMnO_4$, phosphomolybdic acid, and ninhydrin followed by heating. Products were purified by flash column chromatography on silica gel (230–400 mesh) using a mixture of EtOAc/hexane or MeOH/CH_2Cl_2 as eluents. Absorption spectra and molar absorption coefficient at the absorption maxima of fluorescence compounds were measured by UV-VIS spectrophotometer UV-1650PC [Shimadzu, Japan]. Emission spectra was measured by Cary Eclipse Fluorescence spectrophotometer [Varian Associates] and absolute quantum yield was measured by QE-2000 [Otsuka Electronics]. All quantum mechanical calculations were performed in Gaussin09W. The

ground state structures of fluoremidine compounds were optimized using density functional theory (DFT) at the B3LYP/6-31G* level. The energy of HOMO and LUMO values were calculated through time dependent density functional theory (TD-DFT) with the optimized structures of the ground state compare with experimental emission properties. Cell culture reagents including fetal bovine serum, calf serum, culture media, and antibiotic-antimycotic solution were purchased from GIBCO. Lysotracker Red DND-99 and MitoTracker Red CMXRos were purchased from Molecular Probes. The culture dish was purchased from CORNING. Insulin was purchased from Sigma Aldrich. Glass bottom chamber slide was purchased from Thermo scientific. All antibodies for immunofluorescence imaging were purchased from Abcam. Fluorescence microscopy studies were carried with DeltaVision Elite imaging system [GE Healthcare] equipped with a sCMOS camera. Objective lenses are supported by Olympus IX-71 [Olympus] inverted microscope equipped with Plan APO 60×/Oil, 1.42 NA, WD 0.15 mm or Super-Plan APO 100×/Oil, 1.4 NA, WD 0.13 mm. DeltaVision Elite uses a solid state illumination system, InSightSSI fluorescence illumination module. Four-color standard filter set [GE Healthcare, 52-852113-003] and Seven-color combined filter set [GE Healthcare, 52-852113-024] were used to detect fluorescence signals.

II. Supporting Figures and Tables

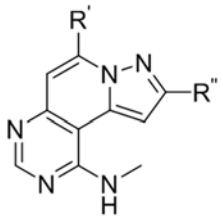

cpd	R`	R``	λ_{abs} (nm)[a]	λ_{em} (nm)[b]	ε
A01	*n*-propyl	cyclopropyl	325	386	4,000
A02	*n*-propyl	phenyl	324	388	8,000
A03	phenyl	phenyl	330	424	13,000

All experiment data obtained in dichloromethane (DCM). [a] Only the longest absorption maxima are shown. [b] Excited at the maximum excitation wavelength.

Table S1. Photophysical properties of A01–A03.

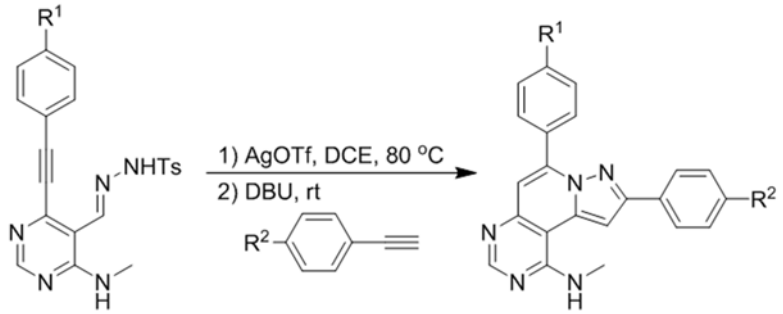

2a-2e **FD01-FD09**

cpd	R^1	R^2	yield(%)[a]
FD01	H	H	70
FD02	CN	H	51
FD03	CF_3	H	77
FD04	OCH_3	H	72
FD05	$N(CH_3)_2$	H	77
FD06	H	CN	40
FD07	H	CF_3	55
FD08	H	OCH_3	53
FD09	H	$N(CH_3)_2$	64

[a] Isolated yield

Table S2. Synthetic yield results of key transformation for **FD01–FD09**.

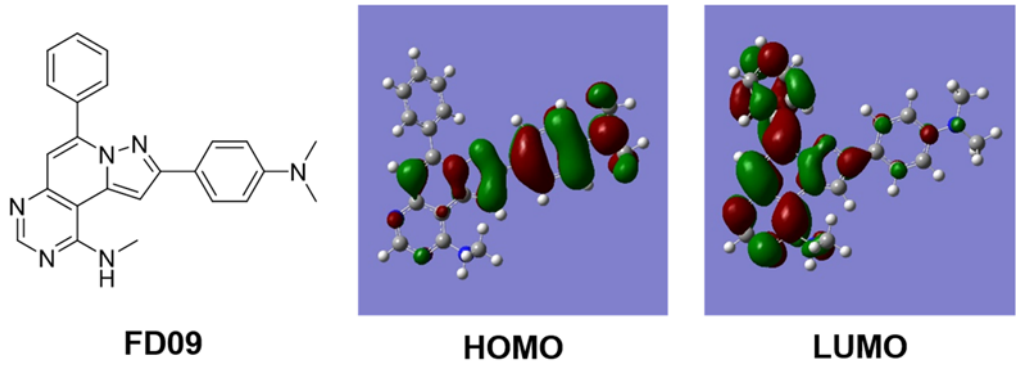

Figure S1. Chemical structure and electron density distribution of the HOMO and the LUMO for *N*,*N*-dimethylamino group at the R^2 position (**FD09**), calculated through DFT at the B3LYP/6-31G*level.

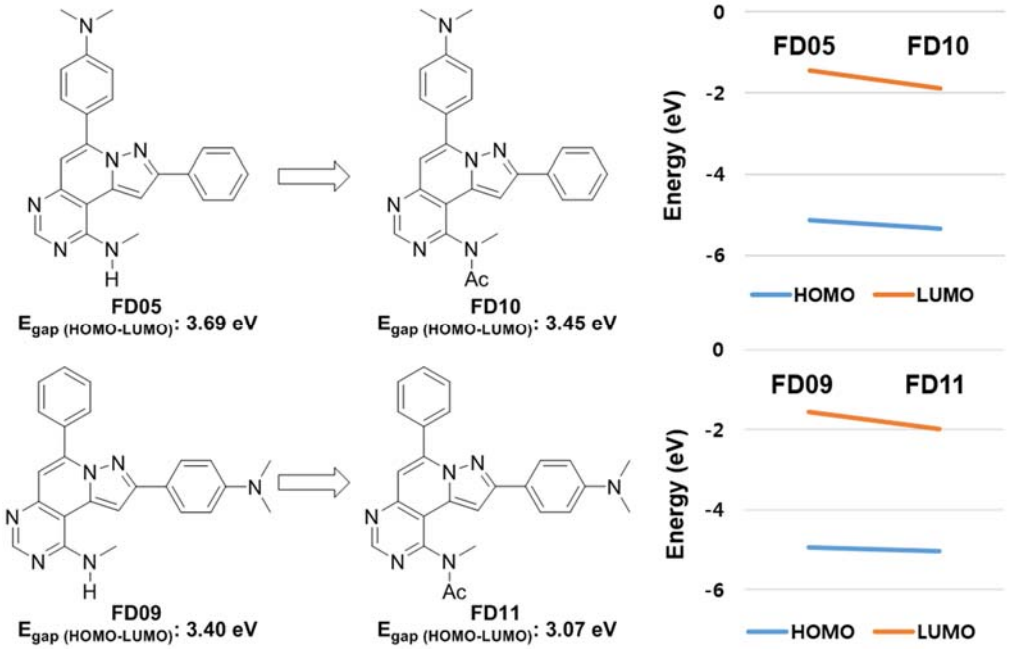

Figure S2. Chemical structures and energy levels of the HOMO and the LUMO of **FD05**, **FD09**, **FD10**, and **FD11**.

Cpd	R^1	R^2	R^3	Ether (nm)	DCM (nm)	DMF (nm)	MeOH (nm)
FD01	H	H	H	420	424	434	434
FD02	CN	H	H	452	456	476	472
FD03	CF_3	H	H	432	438	458	454
FD04	OCH_3	H	H	410	420	428	432
FD05	$N(CH_3)_2$	H	H	430	450	468	484
FD06	H	CN	H	416	422	432	430
FD07	H	CF_3	H	416	420	434	430
FD08	H	OCH_3	H	420	424	438	436
FD09	H	$N(CH_3)_2$	H	481	532	598	N.D.
FD10	$N(CH_3)_2$	H	Ac	474	504	542	N.D.
FD11	H	$N(CH_3)_2$	Ac	560	604	N.D.	N.D.
FD12	$N(CH_3)_2$	$N(CH_3)_2$	H	432	492	554	N.D.
FD13	$N(CH_3)_2$	$N(CH_3)_2$	Ac	528	582	N.D.	N.D.

Table S3. Emission wavelengths of **FD01–FD13** upon polarity changes at the different organic solvents.

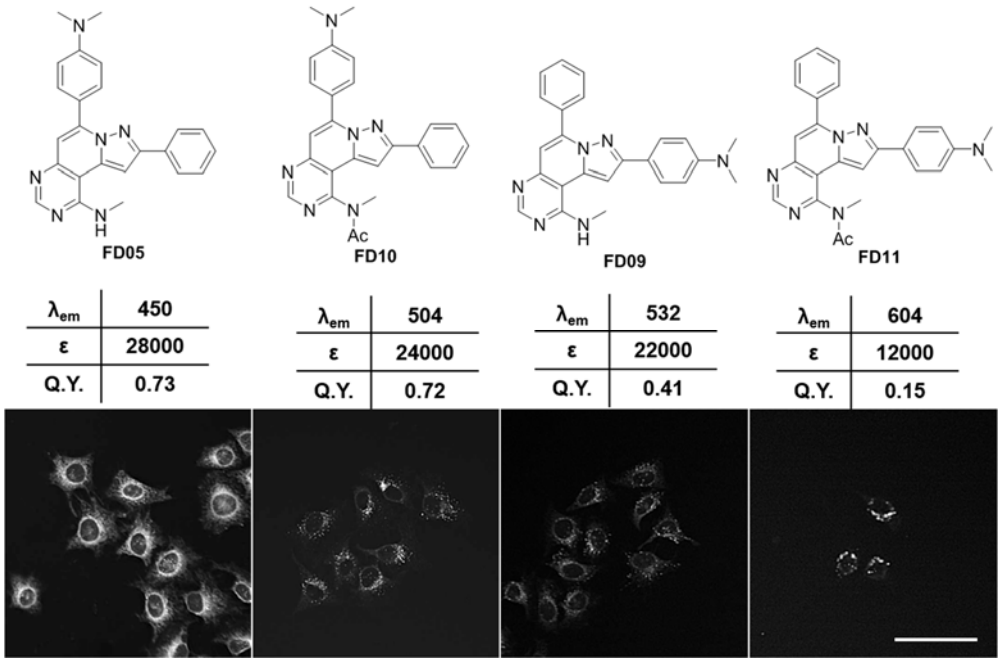

Figure S3. Live cell imaging after staining of A549 cells with probes. 20 μM of each probe was treated to A549 cells. After 1 h, cells were washed with PBS. Fluorescence images were taken by InCell Analyzer 2000 [GE Healthcare]

equipped with 20× lens. Fluorescence signals of each probe were obtained using the following filter sets; **FD05** (DAPI/DAPI), **FD09** (DAPI/DAPI), **FD10** (DAPI/FITC), **FD11** (DAPI/FITC). Scale bars, 100 μm.

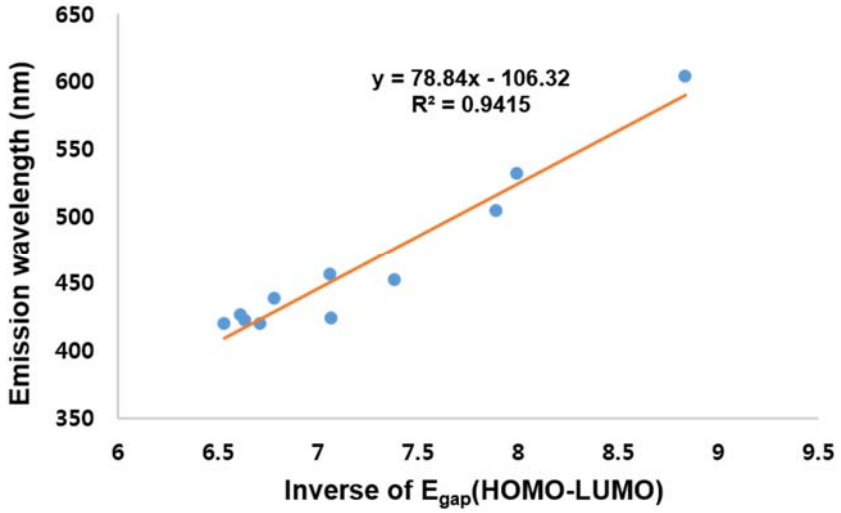

Figure S4. Correlation between the calculated HOMO-LUMO energy gap and the measured emission wavelength of **FD01–FD11**.

☞ Prediction of λ_{em} of for **FD12** and **FD13**

The estimation of emission wavelength (λ_{em}) = 78.84x – 106.32 (x: calculated 1/eV)

cpd	x (calculated 1/eV)	Estimated λ_{em}
FD12	7.6834422	499 nm
FD13	8.47745	562 nm

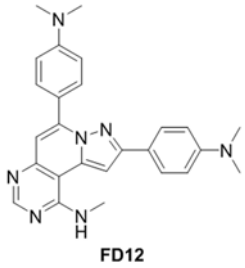

FD12

solvent	Abs (nm)[a]	Em (nm)[b]	ε	Q. Y.[c]
Ether	337	432	33000	0.45
DCM	352	492	40000	0.41
DMF	348	554	33000	0.23
MeOH	360	N.D.	31000	0.05

[a]Only the longest absorption maxima are shown. [b]Excited at the maximum excitation wavelength. [c]Absolute quantum yield.

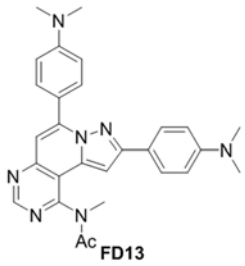

FD13

solvent	Abs (nm)[a]	Em (nm)[b]	ε	Q. Y.[c]
Ether	392	528	35000	0.43
DCM	404	582	31000	0.38
DMF	400	N.D.	24000	0.06
MeOH	400	N.D.	24000	< 0.01

[a]Only the longest absorption maxima are shown. [b]Excited at the maximum excitation wavelength. [c]Absolute quantum yield.

Table S4. Photophysical properties of **FD12** and **FD13**

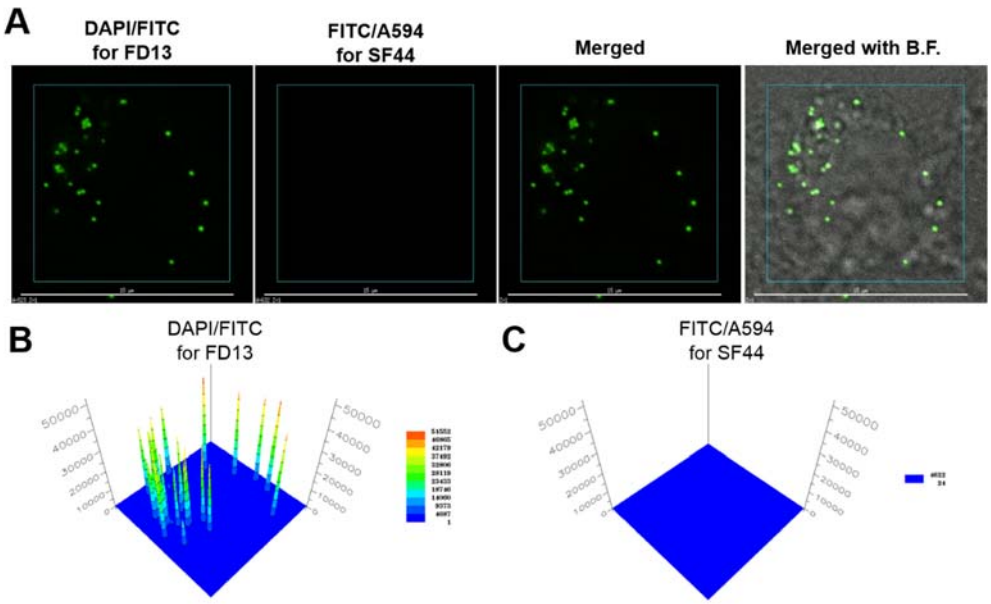

Figure S5. Single treatment of FD13 in Hela cells for fluorescence imaging. A) 20 μM of **FD13** is treated to Hela cells for 1 h in 5% CO_2 incubator. After 1 h, fluorescent images are taken without washing of probe within media. Fluorescence images are taken by DeltaVision imaging system equipped with

60× lens. Scale bars, 15 μm. B) Calculated DAPI/FITC fluorescence intensity (for **FD13**) within selected area (blue square) of cells. The color scale indicates the fluorescence intensity, from low (blue) to high (red). C) Calculated FITC/A594 fluorescence intensity (for **SF44**) within selected area (blue square) of cells. The color scale indicates the fluorescence intensity, from low (blue) to high (red).

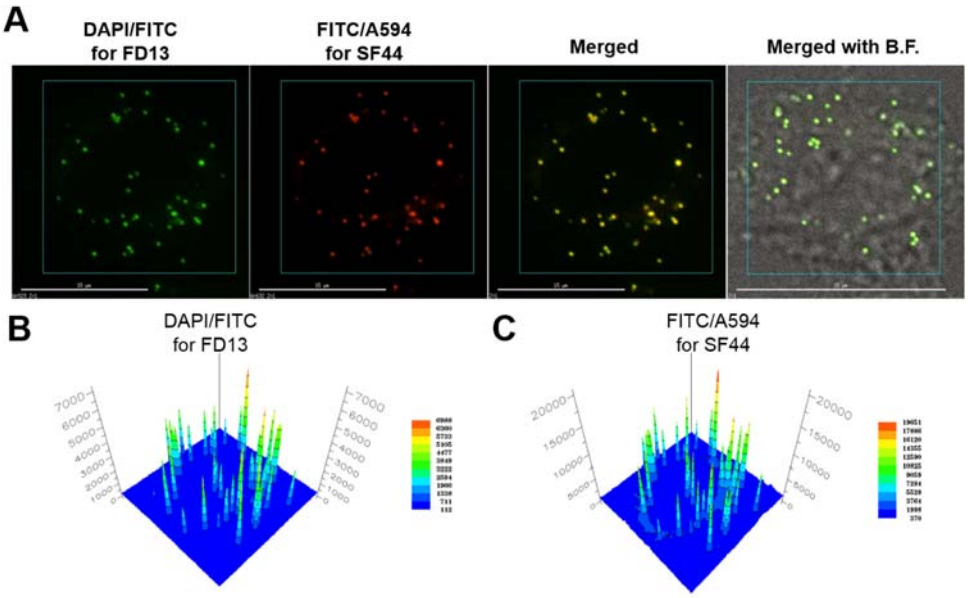

Figure S6. Dual treatment of FD13 and SF44 for fluorescence imaging. A) 20 μM of **FD13** is treated to Hela cells for 1 h in 5% CO_2 incubator. After 1 h, add 20 μM of SF44 and incubate for 30 min. Fluorescent images are taken without washing of probes within media. Fluorescence images are taken by DeltaVision imaging system equipped with 60× lens. Scale bars, 15 μm. B) Calculated DAPI/FITC fluorescence intensity (for **FD13**) within selected area (blue square) of cells. The color scale indicates the fluorescence intensity, from low (blue) to high (red). C) Calculated FITC/A594 fluorescence intensity (for

SF44) within selected area (blue square) of cells. The color scale indicates the fluorescence intensity, from low (blue) to high (red).

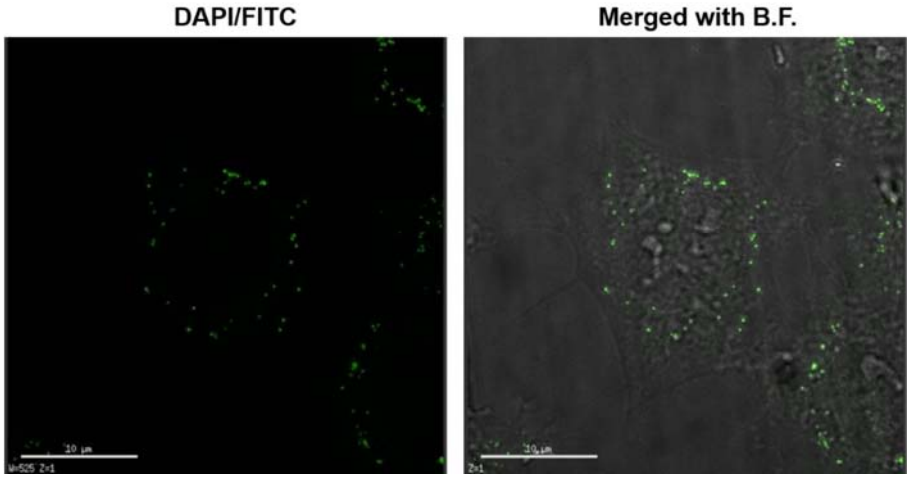

Figure S7. Hela cells are fixed with 3.7% para-formaldehyde for 15 min at r.t. After the fixation of cells, 20 μM of **FD13** is treated for 1 h at r.t. After washing with PBS buffer for three times, fluorescence images are taken by DeltaVision imaging system equipped with 60× lens. Scale bars, 10 μm.

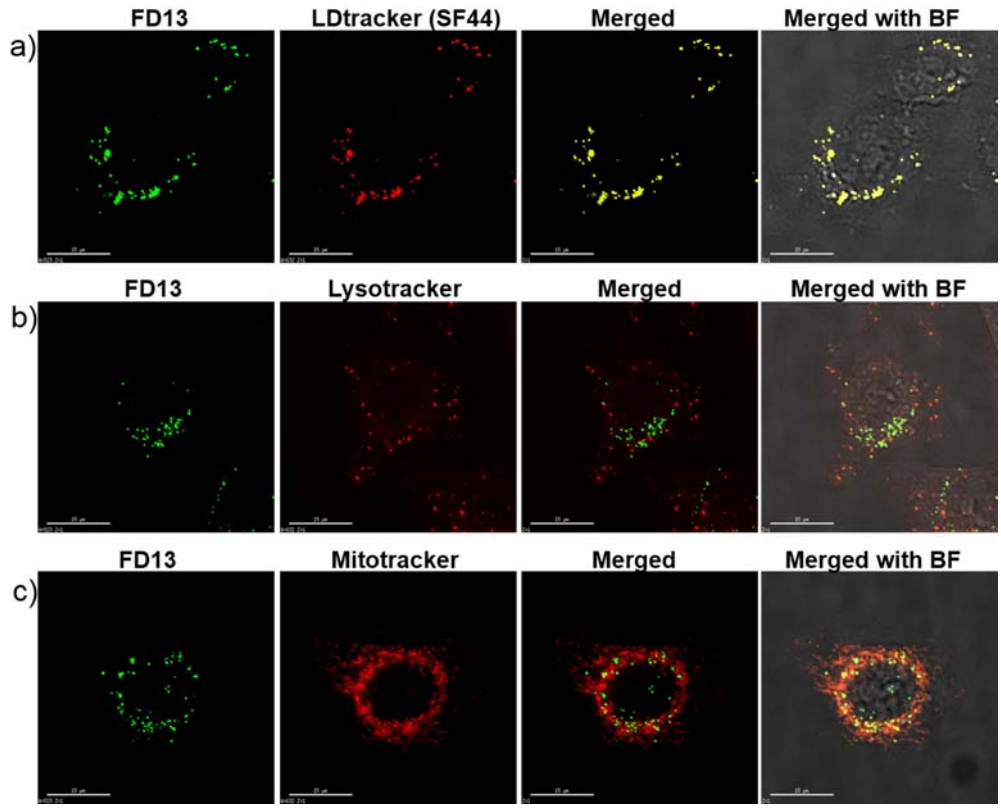

Figure S8. Colocalization of **FD13** and lipid droplet tracker (LD tracker, SF44). A549 cells were treated with 20 μM **FD13** for 1 h. Cellular lipid droplet, lysosome, and mitochondria were stained with SF44 (20 μM), Lysotracker Red (50 nM), and Mitotracker Red (20 nM), respectively, for 30 min. After washing, live cell images were obtained using DeltaVision imaging system equipped with a 60× lens. Merged images show specific colocalization of **FD13** and LD tracker (yellow). Scale bars, 15 μm. Images of a) **FD13** and LD tracker; b) FD13 and Lysotracker; and c) **FD13** and Mitotracker.

III. General Experimental Procedures and Spectroscopic Data

1. General synthetic procedure for compounds 1a–1e

To the anhydrous DMF solution (60 mL) of 4-chloro-6-(methylamino)pyrimidine-5-carbaldehyde (1.0 g), $Pd(PPh_3)Cl_2$ (5 mol%), and CuI (20 mol%), terminal alkynes (2.0 equiv.), and triethylamine (1.6 mL, 2.0 equiv.) were added under argon atmosphere. After being stirred at room temperature for 4 h, the reaction mixture was quenched with deionized water (200 mL). The resultant was extracted with EtOAc (100 mL × 3) and combined organic layer was washed with brine (100 mL). After drying with anhydrous Na_2SO_4(s), the solvent was removed under the reduced pressure. The residue was purified by silica-gel flash column chromatography to obtain **1a–1e**.

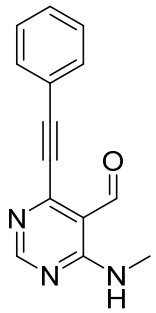

Compound 1a: Yield: 98%; pale-yellow solid; ^{1}H NMR (400 MHz, $CDCl_3$) δ 10.55 (s, 1H), 8.91 (brs, 1H), 8.67 (s, 1H), 7.65–7.62 (m, 2H), 7.47–7.38 (m, 3H), 3.14 (d, J = 5.2 Hz, 3H); ^{13}C NMR (100 MHz, $CDCl_3$) δ 192.5, 161.5, 160.4, 155.0, 132.4, 130.3, 128.6, 120.6, 98.3, 83.8, 27.4; IR (neat) ν_{max}: 3337, 3076, 2934, 2859, 2214, 1764, 1652, 1582, 1538, 1400, 969, 878; LRMS (ESI) *m/z* calcd for $C_{14}H_{11}N_3O$ $[M+H]^+$: 238.09; Found: 237.99; Registration No.: 1477472-98-2.

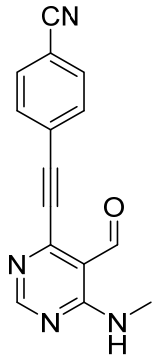

Compound 1b: Yield: 79%; brown solid; ^{1}H NMR (500 MHz, $CDCl_3$) δ 10.52 (s, 1H), 8.91 (brs, 1H), 8.70 (s, 1H), 7.71–7.73 (m, 4H), 3.17 (d, J = 5.0 Hz, 3H); ^{13}C NMR (100 MHz, $CDCl_3$) δ 192.0, 161.6, 160.4, 154.2, 132.8, 132.3, 125.4, 117.9, 113.7, 112.1, 95.1, 87.1, 27.5; IR (neat) ν_{max}: 3331, 2925, 2848, 2229, 1660, 1603, 1546, 1443, 1260, 1099, 966, 839; LRMS (ESI) *m/z* calcd for $C_{15}H_{10}N_4O$ $[M+H]^+$: 263.09; Found: 263.2.

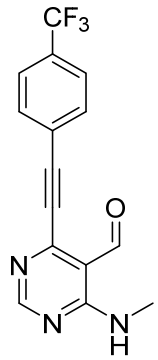

Compound 1c: Yield: 91%; brown solid; ^{1}H NMR (400 MHz, $CDCl_3$) δ 10.52 (s, 1H), 8.89 (brs, 1H), 8.67 (s, 1H), 7.73 (d, *J* = 8.4 Hz, 2H), 7.66 (d, *J* = 8.4 Hz, 2H), 3.14 (d, *J* = 4.8 Hz, 3H); ^{13}C NMR (100 MHz, $CDCl_3$) δ 192.2, 161.6, 160.4, 154.4, 132.6, 125.7, 125.61, 125.58, 124.4, 112.0, 95.9, 85.5, 27.5; IR (neat) ν_{max}: 3334, 3052, 2943, 2857, 2218, 1657, 1608, 1543, 1394, 1327, 1173, 1108, 967, 841; LRMS (ESI) *m/z* calcd for $C_{15}H_{10}F_3N_3O$ $[M+H]^+$: 306.08; Found: 306.1.

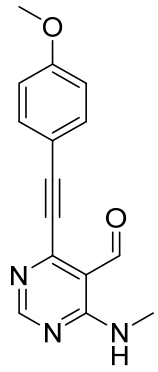

Compound 1d: Yield: 75%; brown solid; ^{1}H NMR (400 MHz, $CDCl_3$) δ 10.53 (s, 1H), 8.90 (d, *J* = 4.0 Hz, 1H), 8.64 (s, 1H), 7.57 (d, *J* = 8.8 Hz, 2H), 6.91 (d, *J* = 8.8 Hz, 2H), 3.85 (s, 3H), 3.13 (d, *J* = 5.2 Hz, 3H); ^{13}C NMR (100 MHz, $CDCl_3$) δ 192.7, 161.5, 161.3, 160.4, 155.3, 134.3, 114.3, 112.6, 111.5, 99.2, 83.3, 55.4, 27.4; IR (neat) ν_{max}: 3334, 2924, 2856, 2207, 1663, 1539, 1396, 1255, 1173, 1027, 967, 832; LRMS (ESI) *m/z* calcd for $C_{15}H_{13}N_3O_2$ $[M+H]^+$: 268.10; Found: 268.2.

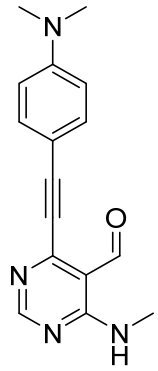

Compound 1e: Yield: 96%; reddish brown solid; ^{1}H NMR (400 MHz, $CDCl_3$) δ 10.55 (s, 1H), 8.90 (brs, 1H), 8.62 (s, 1H), 7.50 (d, *J* = 8.8 Hz, 2H), 6.66 (d, *J* = 8.8 Hz, 2H), 3.12 (d, *J* = 5.2 Hz, 3H), 3.04 (s, 6H); ^{13}C NMR (100 MHz, $CDCl_3$) δ 192.9, 161.4, 160.5, 155.7, 151.3, 134.1, 111.5, 111.0, 106.5, 102.0, 83.5, 40.0, 27.4; IR (neat) ν_{max}: 3329, 2955, 2927, 2912, 2853, 2197, 1658, 1582, 1526, 1396, 1371, 1184, 967, 814; LRMS (ESI) *m/z* calcd for $C_{16}H_{16}N_4O$ $[M+H]^+$: 281.13; Found: 281.2.

2. General synthetic procedure for compounds 2a–2e

To a methanol solution of **1a–1e**, tosylhydrazide (2.0 equiv.), and AcOH were added. After stirring at 40 °C until starting materials were consumed, the reaction mixture was quenched with deionized water. The resultant was extracted with dichloromethane (DCM) twice and dried with anhydrous Na_2SO_4(s). After the solvent was removed under the reduced pressure, the residue was purified by silica-gel flash column chromatography to obtain **2a–2e**.

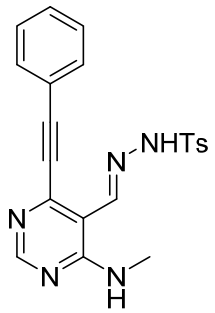

Compound 2a: Yield: 80%; yellow solid; ^{1}H NMR (400 MHz, $CDCl_3$) δ 8.45 (s, 1H), 8.38 (s, 2H), 7.83 (d, *J* = 6.8 Hz, 2H), 7.30 (d, *J* = 7.6 Hz, 2H), 7.20 (t, *J* = 6.8 Hz, 1H), 7.12–7.06 (m, 4H), 3.04 (d, *J* = 5.2 Hz, 3H), 2.38 (s, 3H); ^{13}C NMR (100 MHz, $CDCl_3$) δ 158.8, 157.5, 147.9, 145.5, 144.6, 135.1, 131.7, 129.8, 129.7, 128.1, 127.8, 120.5, 110.2, 97.7, 84.2, 27.7, 21.6; IR (neat) ν_{max}: 3295, 3181, 3057, 2864, 2752, 2214, 1608, 1544, 1267, 1074, 971; LRMS (ESI) *m/z* calcd for $C_{21}H_{19}N_5O_2S$ $[M+H]^+$: 406.13; Found: 405.93; Registration No.: 1477473-18-9.

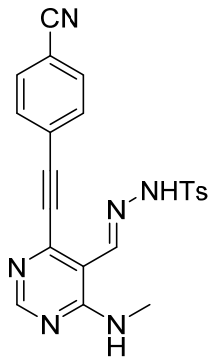

Compound 2b: Yield: 45%; yellowish brown solid; ^{1}H NMR (500 MHz, DMSO-d_6) δ 8.52 (s, 1H), 8.49 (brs, 1H), 8.46 (s, 1H), 7.99 (d, *J* = 6.0 Hz, 2H), 7.86 (d, *J* = 6.8 Hz, 2H), 7.78 (d, *J* = 6.8 Hz, 2H), 7.46 (d, *J* = 6.0 Hz, 2H), 3.03 (d, *J* = 4.0 Hz, 3H), 2.46 (s, 3H); ^{13}C NMR (100 MHz, $CDCl_3$) δ 158.8, 158.1, 147.7, 145.4, 145.2, 134.6, 132.5, 132.1, 130.1, 127.8, 125.6, 118.0, 113.1, 110.5, 94.5, 88.0, 27.9, 21.7; IR (neat) ν_{max}: 3230, 3062, 2230, 1608. 1581, 1545, 1440, 1168, 1075, 970; LRMS (ESI) *m/z* calcd for $C_{22}H_{18}N_6O_2S$ $[M+H]^+$: 431.12; Found: 431.2.

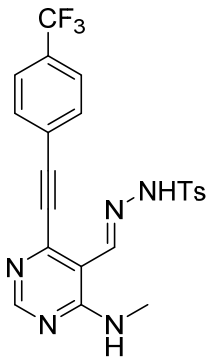

Compound 2c: Yield: 39%; yellow solid; ^{1}H NMR (400 MHz, $CDCl_3$) δ 8.46 (s, 1H), 8.35 (s, 1H), 8.27 (d, *J* = 4.8 Hz, 1H), 7.82 (d, *J* = 8.0 Hz, 2H), 7.30–7.21 (m, 6H), 2.97 (d, *J* = 5.2 Hz, 3H), 2.36 (s, 3H); ^{13}C NMR (100 MHz, $CDCl_3$) δ 158.6, 157.5, 147.2, 145.0, 144.9, 134.9, 132.0, 131.3, 131.0, 129.9, 127.8, 125.0, 124.1, 122.1, 95.6, 86.0, 27.6, 21.5; IR (neat) ν_{max}: 3219, 2923, 2218, 1609, 1545, 1324, 1165, 1130, 1086, 1066, 969; LRMS (ESI) *m/z* calcd for $C_{22}H_{18}F_3N_5O_2S$ $[M+H]^+$: 474.11; Found: 474.2.

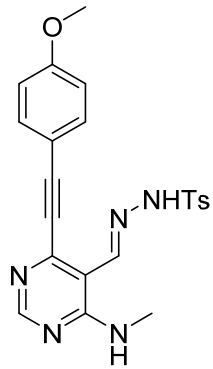

Compound 2d: Yield: 76%; pale yellow solid; ^{1}H NMR (400 MHz, CD_2Cl_2) δ 8.44 (s, 1H), 8.36 (brs, 1H), 8.34 (s, 1H), 7.81 (d, *J* = 8.4 Hz, 2H), 7.31 (d, *J* = 8.0 Hz, 2H), 7.02 (d, *J* = 8.8 Hz, 2H), 6.61 (d, *J* = 8.8 Hz, 2H), 3.77 (s, 3H), 3.03 (d, *J* = 4.8 Hz, 3H), 2.36 (s, 3H); ^{13}C NMR (100 MHz, CD_2Cl_2) δ 161.2, 159.2, 157.7, 148.5, 146.3, 145.2, 135.6, 133.7, 130.2, 128.1, 114.2, 112.8, 110.2, 98.6, 83.9, 55.7, 27.9, 21.7; IR (neat) ν_{max}: 2966, 2207, 1604, 1581, 1544, 1511, 1304, 1254, 1168, 1075, 970; LRMS (ESI) *m/z* calcd for $C_{22}H_{21}N_5O_3S$ $[M+H]^+$: 436.14; Found: 436.2.

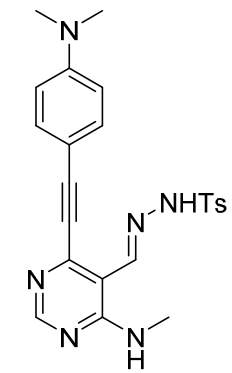

Compound 2e: Yield: 56%; yellow solid; ^{1}H NMR (400 MHz, DMSO-*d*$_6$) δ 11.91 (brs, 1H), 8.54 (s, 1H), 8.40–8.39 (m, 2H), 7.79 (d, *J* = 8.4 Hz, 2H), 7.49–7.45 (m, 4H), 6.74 (d, *J* = 9.2 Hz, 2H), 3.01 (d, *J* = 4.8 Hz, 3H), 2.98 (s, 6H), 2.38 (s, 3H); ^{13}C NMR (100 MHz, DMSO-*d*$_6$) δ 158.3, 157.6, 151.1, 148.5, 144.8, 144.1, 135.3, 133.5, 130.0, 127.2, 111.7, 108.9, 105.9, 99.3, 84.0, 48.6, 27.4, 21.1; IR (neat) ν_{max}: 3301, 3039, 2193, 1605, 1534, 1447, 1368, 1339, 1165, 1072, 969; LRMS (ESI) *m/z* calcd for $C_{23}H_{24}N_6O_2S$ $[M+H]^+$: 449.17; Found: 449.1.

3. General procedure for the preparation of FD01–FD09

To the DCE solution of **2a–2e**, AgOTf (20 mol%) was added. After stirring at 80 °C for 2 h, the reaction mixture was cooled to room temperature. After the addition of DBU (3.0 equiv.) and terminal alkyne (3.0 equiv.), the reaction mixture was stirred at room temperature for 16 h. The resultant was quenched with water and extracted with DCM in two times. After drying with anhydrous Na_2SO_4(s), the solvent was removed under the reduced pressure. The residue was purified by silica-gel flash column chromatography to obtain **FD01–FD09**.

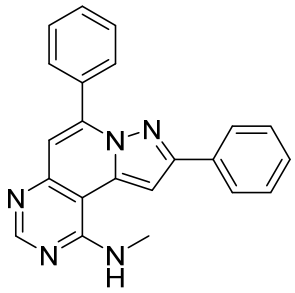

Compound FD01: Yield: 70%; off-white solid; ^{1}H NMR (400 MHz, $CDCl_3$) δ 8.76 (s, 1H), 8.00–7.97 (m, 2H), 7.92 (d, *J* = 8.0, 2H), 7.55–7.53 (m, 3H), 7.41 (t, *J* = 7.2 Hz, 2H), 7.35 (t, *J* = 7.6 Hz, 1H), 7.13 (s, 1H), 7.07 (s, 1H), 5.77 (d, *J* = 5.6 Hz, 1H), 3.29 (d, *J* = 4.4 Hz, 3H); ^{13}C NMR (100 MHz, $CDCl_3$) δ 158.3, 156.8, 153.6, 150.3, 144.8, 136.3, 132.7, 130.0, 129.7, 128.8, 128.7, 128.3, 126.4, 112.6, 103.7, 95.8, 28.7; IR (neat) ν_{max}: 3430, 3061, 2932, 1722, 1630, 1578, 1444, 1417, 1313, 1292, 740; HRMS (FAB+) *m/z* calcd for $C_{22}H_{17}N_5$ $[M+H]^+$: 352.1562; Found: 352.1556; Registration No.: 1477473-78-1.

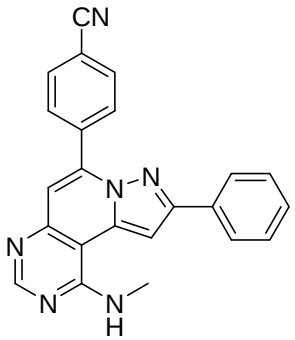

Compound FD02: Yield: 51%; yellowish brown solid; ^{1}H NMR (400 MHz, DMSO-d_6) δ 8.67 (s, 1H), 8.24 (d, *J* = 8.0 Hz, 2H), 8.12 (s, 1H), 8.07 (d, *J* = 8.4 Hz, 2H), 8.01 (d, *J* = 7.2 Hz, 2H), 7.53–7.52 (m, 2H), 7.45–7.41 (m, 1H), 7.27 (d, *J* = 4.4 Hz, 1H), 7.21 (s, 1H), 3.19 (d, *J* = 4.4 Hz, 3H); ^{13}C NMR (100 MHz, DMSO-d_6) δ 157.3, 156.9, 153.0, 149.6, 142.0, 136.9, 136.1, 132.2, 130.6, 129.0, 128.9, 126.2, 118.5, 113.3, 112.5, 103.6, 97.7, 28.7; IR (neat) ν_{max}:

3468, 3050, 2927, 2853, 2230, 1735, 1633, 1585, 1548, 1442, 1294, 743; HRMS (ESI) *m/z* calcd for $C_{23}H_{16}N_6$ $[M+H]^+$: 377.1509; Found: 377.1511.

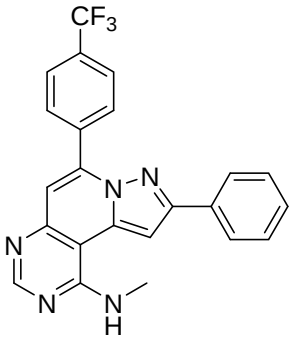

Compound FD03: Yield: 77%; pale brown solid; ^{1}H NMR (400 MHz, $CDCl_3$) δ 8.78 (s, 1H), 8.12 (d, *J* = 7.6 Hz, 2H), 7.95 (d, *J* = 7.6 Hz, 2H), 7.81 (d, *J* = 8.0 Hz, 2H), 7.47–7.43 (m, 2H), 7.41–7.38 (m, 1H), 7.17 (s, 1H), 7.13 (s, 1H), 5.80 (brs, 1H), 3.34 (d, *J* = 4.0 Hz, 3H); ^{13}C NMR (100 MHz, $CDCl_3$) δ 158.4, 157.0, 154.0, 150.1, 143.3, 136.3, 136.1, 132.1, 132.0, 131.7, 130.1 129.1, 128.8, 126.5, 125.3, 113.3, 104.1, 96.1, 28.8; IR (neat) ν_{max}: 3492, 3049, 2925, 2855, 1732, 1634, 1587, 1553, 1443, 1323, 1112, 1068, 843; HRMS (ESI) *m/z* calcd for $C_{23}H_{16}F_3N_5$ $[M+H]^+$: 420.1431; Found: 420.1430.

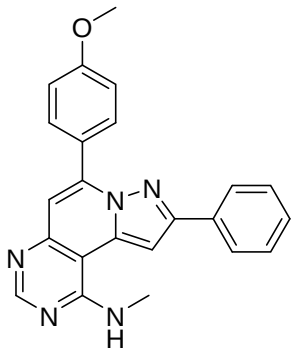

Compound FD04: Yield: 72%; orange solid; ^{1}H NMR (400 MHz, $CDCl_3$) δ 8.75 (s, 1H), 8.00 (d, *J* = 9.2 Hz, 2H), 7.97 (d, *J* = 7.2 Hz, 2H), 7.46–7.42 (m, 2H), 7.39–7.37 (m, 1H), 7.12 (s, 1H), 7.01 (s, 1H), 7.07 (d, *J* = 8.8 Hz, 2H), 5.79 (d, *J* = 4.4 Hz, 1H), 3.91 (s, 1H), 3.31 (d, *J* = 4.8 Hz, 3H); ^{13}C NMR (100 MHz, DMSO-d_6) δ 160.6, 157.2, 156.6, 152.7, 149.8, 143.6, 136.1, 132.5, 131.2, 128.9, 128.8, 126.1, 124.6, 113.7, 111.4, 102.7, 97.4, 55.4, 28.6; IR (neat) ν_{max}: 3346, 3117, 2923, 2852, 1734, 1628, 1561, 1510, 1443, 1258, 1180, 1034, 750; HRMS (ESI) *m/z* calcd for $C_{23}H_{19}N_5O$ $[M+H]^+$: 382.1662; Found: 382.1664.

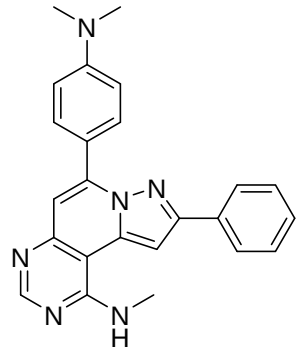

Compound FD05: Yield: 77%; orange solid; ^{1}H NMR (400 MHz, $CDCl_3$) δ 8.75 (s, 1H), 8.05–8.02 (m, 4H), 7.46–7.44 (m, 2H), 7.40–7.39 (m, 1H), 7.15 (s, 1H), 7.11 (s, 1H), 6.86 (d, *J* = 8.4 Hz, 2H), 5.76 (brs, 1H), 3.34 (d, *J* = 4.0 Hz, 3H), 3.01 (s, 6H); ^{13}C NMR (100 MHz, $CDCl_3$) δ 158.4, 156.7, 153.3, 151.5, 150.5, 145.4, 136.5, 132.7, 130.9, 128.7, 128.5, 128.4, 126.5, 119.7, 111.3, 110.7, 95.6, 40.2, 28.7; IR (neat) ν_{max}: 3409, 3049, 2930, 2813, 1732, 1574, 1522, 1460, 1365, 1265, 1167, 742; HRMS (ESI) *m/z* calcd for $C_{24}H_{22}N_6$ $[M+H]^+$: 395.1979; Found: 395.1978.

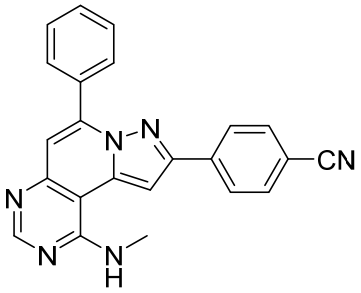

Compound FD06: Yield: 40%; pale brown solid; ^{1}H NMR (400 MHz, $CDCl_3$) δ 8.81 (s, 1H), 8.10 (d, *J* = 8.4 Hz, 2H), 8.01–7.98 (m, 2H), 7.74 (d, *J* = 8.0 Hz, 2H), 7.60–7.58 (m, 3H), 7.24 (s, 1H), 7.20 (s, 1H), 5.75 (brs, 1H), 3.37 (d, *J* = 5.2 Hz, 3H); ^{13}C NMR (100 MHz, DMSO-d_6) δ 157.23, 157.22, 156.9, 151.0, 149.8, 143.8, 136.8, 136.3, 133.0, 132.3, 130.2, 129.6, 128.4, 126.6, 118.8, 113.1, 111.0, 103.1, 98.4, 28.7; IR (neat) ν_{max}: 3458, 3054, 2987, 2930, 2853, 2220, 1631, 1588, 1547, 1450, 1265, 749; HRMS (ESI) *m/z* calcd for $C_{23}H_{16}N_6$ $[M+H]^+$: 377.1509; Found: 377.1510.

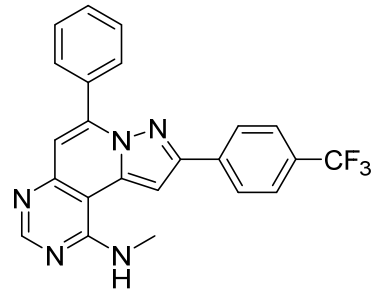

Compound FD07: Yield: 55%; pale orange solid; ^{1}H NMR (400 MHz, $CDCl_3$) δ 8.78 (s, 1H), 8.04 (d, *J* = 8.4 Hz, 2H), 7.98–7.96 (m, 2H), 7.66 (d, *J* = 8.0 Hz, 2H), 7.56–7.54 (m, 3H), 7.18 (s, 1H), 7.15 (s, 1H), 5.79 (d, *J* = 4.4 Hz, 1H), 3.33 (d, *J* = 4.8 Hz, 3H); ^{13}C NMR (100 MHz, $CDCl_3$) δ 158.4, 157.0, 152.1, 150.4, 144.8, 136.5, 135.8, 132.4, 130.7, 130.4, 130.2,

129.6, 128.3, 126.7, 125.72, 125.68, 125.64, 125.61, 113.3, 103.7, 96.2, 28.8 ; IR (neat) ν_{max}: 3385, 3115, 2926, 2848, 1738, 1622, 1563, 1539, 1409, 1330, 1173, 1117, 1068, 769; HRMS (ESI) *m/z* calcd for $C_{23}H_{16}F_3N_5$ $[M+H]^+$: 420.1431; Found: 420.1433.

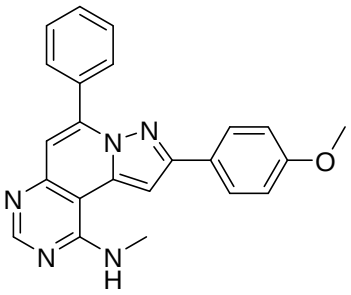

Compound FD08: Yield: 53%; white solid; ^{1}H NMR (400 MHz, $CDCl_3$) δ 8.78 (s, 1H), 8.04–8.02 (m, 2H), 7.92 (d, *J* = 9.2 Hz, 2H), 7.57–7.56 (m, 3H), 7.15 (s, 1H), 7.06 (s, 1H), 6.98 (d, *J* = 8.8 Hz, 2H), 5.77 (brs, 1H), 3.87 (s, 1H), 3.35 (d, *J* = 4.4 Hz, 3H); ^{13}C NMR (100 MHz, $CDCl_3$) δ 160.2, 158.4, 156.7, 153.6, 150.2, 144.8, 136.3, 132.8, 132.1, 130.0, 129.7, 128.2, 127.8, 125.1, 114.1, 112.2, 103.7, 95.4, 55.3, 28.8; IR (neat) ν_{max}: 2959, 2922, 2859, 1724, 1629, 1578, 1541, 1454, 1275, 1176, 749; HRMS (ESI) *m/z* calcd for $C_{23}H_{19}N_5O$ $[M+H]^+$: 382.1662; Found: 382.1664.

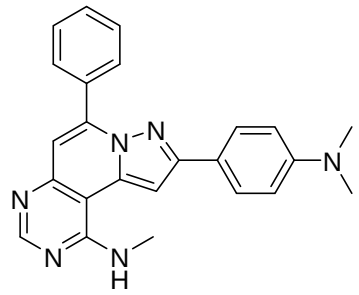

Compound FD09: Yield: 64%; yellow solid; ^{1}H NMR (500 MHz, $CDCl_3$) δ 8.76 (s, 1H), 8.04–8.03 (m, 2H), 7.87–7.85 (m, 2H), 7.56–7.55 (m, 3H), 7.12 (s, 1H), 7.02 (s, 1H), 6.78 (d, *J* = 8.8 Hz, 2H), 5.79 (brs, 1H), 3.35 (d, *J* = 4.8 Hz, 3H), 3.02 (s, 6H); ^{13}C NMR (100 MHz, $CDCl_3$) δ 158.4, 156.6, 154.3, 150.9, 150.2, 144.8, 136.2, 132.9, 129.9, 129.8, 128.2, 127.4, 120.3, 112.1, 111.7, 103.6, 95.0, 40.4, 28.7; IR (neat) ν_{max}: 3436, 3036, 2925, 2850, 2812, 1730, 1614, 1577, 1542, 1494, 1362, 1265, 1197, 736; HRMS (ESI) *m/z* calcd for $C_{24}H_{22}N_6$ $[M+H]^+$: 395.1979; Found: 395.1979.

4. General Procedure for the Preparation of FD10 and FD11

To freshly distilled DMF solution of sodium hydride (1.5 equiv.), **FD05** or **FD09** in anhydrous DMF was slowly added at 0 ºC. After the addition of acetic anhydride (3.0 equiv.), the reaction mixture was stirred at room temperature for 2 h. The resultant was extracted with EtOAc in three times and the combined organic layer was washed with brine. After drying with anhydrous Na_2SO_4(s), the solvent was removed under the reduced pressure. The residue was purified by silica-gel flash column chromatography to obtain **FD10** and **FD11**.

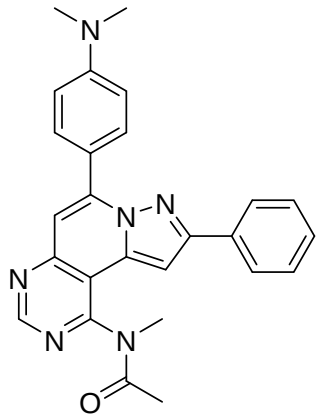

Compound FD10: Yield: 82%; orange solid; ^{1}H NMR (400 MHz, CD_2Cl_2) δ 9.20 (s, 1H), 8.07 (d, *J* = 8.8 Hz, 2H), 8.00 (d, *J* = 7.2 Hz, 2H), 7.50–7.46 (m, 2H), 7.43–7.39 (m, 1H), 7.30 (s, 1H), 7.27 (s, 1H), 6.88 (d, *J* = 9.2 Hz, 2H), 3.37 (s, 3H), 3.11 (s, 6H), 1.88 (s, 3H); ^{13}C NMR (100 MHz, $CDCl_3$) δ 170.1, 158.9, 157.3, 154.7, 154.5, 152.0, 148.2, 135.6, 132.1, 131.2, 129.1, 128.8, 126.7, 118.8, 112.7, 111.6, 111.3, 109.2, 99.9, 40.2, 33.5, 22.4; IR (neat) ν_{max}: 3056, 2929, 2854, 1677, 1613, 1563, 1441, 1358, 1297, 1168, 736; HRMS (ESI) *m/z* calcd for $C_{26}H_{24}N_6O$ $[M+Na]^+$: 459.1904; Found: 459.1902.

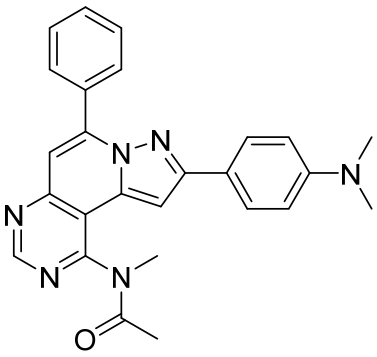

Compound FD11: Yield: 74%; yellowish orange solid; ^{1}H NMR (400 MHz, $CDCl_3$) δ 9.25 (s, 1H), 8.08–8.07 (m, 2H), 7.85 (d, *J* = 8.0 Hz, 2H), 7.61–7.59 (m, 3H), 7.28 (s, 1H), 7.18 (s, 1H), 6.77 (d, *J* = 8.8 Hz, 2 H), 3.42 (s, 3H), 3.02 (s, 6H) 1.94 (s, 3H); ^{13}C NMR (100 MHz, $CDCl_3$) δ 170.1, 159.1, 157.2, 155.5, 154.5, 151.1, 147.6, 135.3, 132.3, 130.6, 129.8, 128.4, 127.7, 119.6, 113.4, 112.2, 110.5, 99.4, 40.3,

33.5, 22.4; IR (neat) ν_{max}: 2925, 2855, 1678, 1606, 1563, 1546, 1519, 1444, 1369, 1295, 1170, 766; LRMS (ESI) *m/z* calcd for $C_{26}H_{24}N_6O$ $[M+H]^+$: 459.1904; Found: 459.1906.

5. Designed probe FD12 and FD13

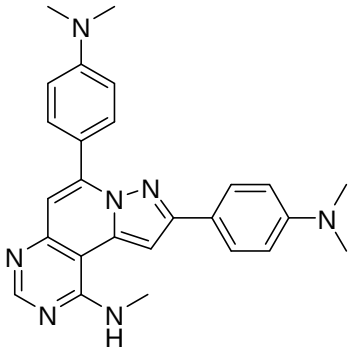

Compound FD12 was prepared using the general procedure of section 3 from compound **2e**.; Yield: 71%; yellow solid; ^{1}H NMR (400 MHz, $CDCl_3$) δ 8.71 (s, 1H), 8.05 (d, *J* = 8.8 Hz, 2H), 7.88 (d, *J* = 8.4 Hz, 2H), 7.08 (s, 1H), 6.99 (s, 1H), 6.84 (d, *J* = 8.8 Hz, 2H), 6.77 (d, *J* = 8.8 Hz, 2H), 5.81 (brs, 1H), 3.33 (d, *J* = 4.8 Hz, 3H), 3.08 (s, 6H), 3.02 (s, 6H); ^{13}C NMR (100 MHz, DMSO-d_6) δ 157.7, 156.9, 153.8, 151.1, 150.4, 144.7, 136.6, 131.1, 127.5, 120.7, 119.9, 112.6, 111.6, 109.6, 102.4, 96.6, 40.4, 40.3, 29.1; IR (neat) ν_{max}: 3411, 3032, 2925, 2806, 1735, 1670, 1614, 1571, 1520, 1441, 1364, 1197, 1121, 819, 736; HRMS (ESI) *m/z* calcd for $C_{26}H_{27}N_7$ $[M+H]^+$: 438.2401; Found: 438.2402.

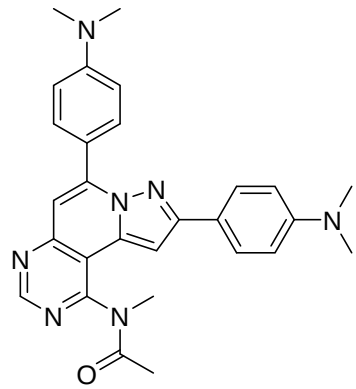

Compound FD13 was prepared using the general procedure of section 4 from **FD12**.; Yield: 82%; yellowish orange solid; ^{1}H NMR (500 MHz, CD_2Cl_2) δ 9.15 (s, 1H), 8.05 (d, *J* = 6.4 Hz, 2H), 7.84 (d, *J* = 7.2 Hz, 2H), 7.21 (s, 1H), 7.13 (s, 1H), 6.86 (d, *J* = 6.8 Hz, 2H), 6.77 (d, *J* = 7.2 Hz, 2H), 3.34 (s, 3H), 3.09 (s, 6H), 3.00 (s, 6H), 1.86 (s, 3H); ^{13}C NMR (100 MHz, $CDCl_3$) δ 170.1, 158.8, 157.1, 155.1, 154.6, 151.9, 151.0, 148.1, 135.5, 131.2, 127.7, 119.9, 119.1, 112.5, 112.2, 111.2, 108.3, 99.0, 40.4, 40.2, 33.4, 22.3; IR (neat) ν_{max}: 3053,

2928, 2854, 1724, 1677, 1610, 1562, 1522, 1440, 1265, 748; HRMS (ESI) *m/z* calcd for $C_{28}H_{29}N_7O$ $[M+H]^+$: 480.2506; Found: 480.2508

IV Experimental Procedures for Cell-based Fluorescence Image

1. Cell culture

A549 (human lung carcinoma) and Hela (human cervical cancer cell) cell lines were obtained from American Type Culture Collection [ATCC]. Cells were cultured in RPMI 1640 [GIBCO] supplemented with heat-inactivated 10% (v/v) fetal bovine serum [FBS, GIBCO] and 1% (v/v) antibiotic-antimycotic agent [GIBCO]. Cell lines were maintained in humidified atmosphere of 5% CO_2 and 95% air at 37 °C, and cultured in 100 mm cell culture dish [CORNING].

2. Live cell imaging of FD12 and FD13 in A549 cells

A549 cells were seeded on glass bottom chamber slide and incubated at 5 % CO_2, 37 °C for overnight. Cells were treated with **FD12** (20 μM) or **FD13** (20 μM) in media for 1 h. Then, probes were washed with PBS buffer for 3 times and fluorescence images were taken by fluorescence microscopy under PBS buffer with DeltaVision Elite imaging system [GE Healthcare] equipped with 60×/1.42 NA oil lens. Fluorescence signals of each probe were obtained using following filter sets; **FD12** (Ex; 390 nm with 18 nm bandwidth, Em; 435 nm with 48 bandwidth), **FD13** (Ex; 390 nm with 18 nm bandwidth, Em; 525 nm with 48 nm bandwidth).

3. Co-staining of FD13 with organelle staining markers

A549 cells were seeded on glass bottom chamber slide and incubated at 5 % CO_2, 37 °C for overnight. Cells were treated with 20 μM of **FD13** for 1 h. Then, 20 μM of LD tracker (SF44), 50 nM of Lysotracker Red or 20 nM of Mitotracker Red were treated to each well and incubated for 30 min. After treatment of each

probe, cells were washed with PBS buffer for 3 times and then fluorescence images were taken by fluorescence microscopy under PBS buffer with DeltaVision Elite imaging system [GE Healthcare] equipped with 60×/1.42 NA oil lens. Fluorescence signals of each probe were obtained using following filter sets; **FD13** (Ex; 390 nm with 18 nm bandwidth, Em; 525 nm with 48 nm bandwidth), SF44 (Ex; 475 nm with 28 nm bandwidth, Em; 625 nm with 45 nm bandwidth), Lysotracker Red and Mitotracker Red (Ex; 575 nm with 25 nm bandwidth, Em; 625 nm with 45 nm bandwidth).

4. Differentiation of 3T3-L1 cell lines

3T3-L1 cells were cultured to seeded on glass bottom chamber slide and incubated with DMEM, [Dulbecco's modified Eagle's medium] supplemented with heat inactivated 10% (v/v) calf serum and 1% (v/v) FBS (fetal bovine serum), 1 μM dexamethasone, 10 μM rosiglitazone, 5 μg/ml insulin. 2 days later, replaced the media to the DMEM supplemented with 10% (v/v) FBS, and 5 μg/ml insulin and refreshed the media with same condition every 2 day.

5. Immunohistochemistry with anti-ADRP and anti-perilipin antibodies

3T3-L1 cells were seeded on glass bottom chamber slide and differentiated by protocol as stated above. When the differentiation was completed, cells were fixed with 3.7% paraformaldehyde in PBS for 15 min at r.t., and washed with ice cold PBS for twice, decanted from glass bottom dish. Fixed cells on dish were introduced with diluted primary antibody solution (1:200) in PBST with 1% BSA, and incubated at 4 ^{o}C for overnight. Primary antibody was decanted and washed with PBS for 3 times. Diluted secondary antibody, conjugated with TRICT fluorescent dye, solution (1:100) was added, followed **FD13** (20 μM) was treated to the cell in PBS for 1 h at r.t., followed by PBS washing for 3 min twice. Fluorescence images were taken by Deltavision imaging system [GE Healthcare] equipped with 100×/1.4 NA oil lens. Fluorescence signal of **FD13**

and TRITC-conjugated secondary antibody were obtained using following filter sets; **FD13** (Ex; 390 nm with 18 nm bandwidth, Em; 525 nm with 48 nm bandwidth), TRITC-conjugated secondary antibody (Ex; 542 nm with 27 nm bandwidth, Em; 597 nm with 45 nm bandwidth).

3-5. Reference

[1] Koboyashi, H.; Ogawa, M.; Alford, R.; Choyke, P. L.; Urano, Y. *Chem. Rev.*, **2013**, *93*, 2640.

[2] Yun, S.-W.; Kang, N.-Y.; Park, S.-J.; Ha, H.-H.; Kim, Y. K.; Lee, J.-S.; Chang, Y.-T. *Acc. Chem. Res.*, **2014**, *47*, 1277.

[3] Kim, E.; Koh, M.; Ryu, J.; Park, S. B. *J. Am. Chem. Soc.*, **2008**, *130*, 12206.

[4] Kim, E.; Koh, M.; Lim, B. J.; Park, S. B. *J. Am. Chem. Soc.*, **2011**, *133*, 6642.

[5] Choi, E. J.; Kim, E.; Lee. Y.; Jo, A.; Park, S. B. *Angew. Chem. Int. Ed.*, **2014**, *53*, 1346.

[6] Lee. Y.; Jo, A.; Park, S. B. *Angew. Chem. Int. Ed.*, **2015**, *54*, 15689.

[7] Jeong, M. S.; Kim, E.; Kang, H. J.; Choi, E. J.; Cho, A. R.; Chung, S. J.; Park, S. B. *Chem. Commun.*, **2012**, *48*, 6553.

[8] Kim, E.; Lee, S.; Park, S. B. *Chem. Commun.*, **2012**, *48*, 2331.

[9] (a) Ribble, W.; Hill, W. E.; Ochsner, U. A.; Jarvis, T. C.; Guiles, J. W.; Janjic, N.; Bullard, J. M. *Antimicrob. Agents. Chemother*, **2010**, *54*, 4648. (b) Giblin, M. P.; O'Shaughenessy, C. T.; Naylor, A.; Mitchell, W. L.; Eatherton, A. J.; Slingsby, B. P.; Rawlings, A.; Goldsmith, P.; Brown, A. J.; Haslam, C. P.; Clayton, N. M.; Wilson, A. W.; Chessell, I. P.; Wittington, A. R.; Green, R. *J. Med. Chem.,* **2007**, *50*, 2597. (c) Yaziji, V.; Rodriquez, D.; Gutierrez-de-Teran, H.; Coelho, A.; Caamano, O.; Garcia-Mera, X.; Brea, J.; Loza, M. I.; Cadavid, M. I.; Sotelo, E. *J. Med. Chem.,* **2011**, *54*, 457. (d) Meng, W.; Brigance, R. P.; Chao, H. J.; Fura, A.; Harrity, T.; Marcikeviciene, J.; O'Connor, S. P.; Tamura, J. K.; Xie, D.; Zhang, Y.; Klei, H. E.; Kish, K.; Weigelt, C. A.; Turdi, H.; Wang,

A.; Zahler, R.; Kirby, M. S.; Hamann, L. G.; *J. Med. Chem.,* **2010**, *53*, 5620.

[10] Wong, K.-Y.; Hung, T. S.; Lin, Y.; Wu, C.-C.; Lee, G.-H.; Peng, S.-M.; Chou, C. H.; Su, Y. O. *Org. Lett.*, **2002**, *4*, 513.

[11] Hadad, C.; Achelle, S.; Garcia-Martinez, J. C.; Rdoriguez-Lopez, J. *J. Org. Chem.*, **2011**, *76*, 3837.

[12] Malval, J.-P.; Achelle, S.; Bodiou, L.; Spangenberg, A.; Gomez, L. C.; Soppera, O.; Robin-le Guen, F. *J. Mater. Chem. C*, **2014**, *2*, 7869.

[13] Kim, H.; Tung, T. T.; Park, S. B. *Org. Lett.*, **2013**, *15*, 5814.

[14] Itami, K.; Yamazaki, D.; Yoshida, J. *J. Am. Chem. Soc.*, **2004**, *126*, 15396.

[15] Achelle, S.; Ramondenc, Y.; Marsais, F.; Ple', N. *Eur. J. Org. Chem.*, **2008**, 3129.

[16] Yamada, S. Y.; Hiyoshi, H.; Umezu, K.; Nakamura, Y. *J. Org. Chem.*, **2015**, *80*, 9076.

[17] Yang, H.; Mu, J.; Chen, X.; Feng, L.; Jia, J.; Wang, J. *Dye and Pigments*, **2011**, *91*, 446.

[18] Maring, S.; Parton, R. G. *Nat. Rev. Mol. Cell Biol.,* **2006**, *7*, 373.

[19] Greenberg, A. S.; Coleman, R. A.; Kraemer, F. B.; McManaman, J. L.; Obin, M. S.; Puri, B.; Yan, Q.-W.; Miyoshi, H.; Mashek, D. G. *J. Clin. Invest.,* **2011**, *121*, 2102.

[20] Lee, S.; Kim, E.; Park, S. B. *Chem. Sci.,* **2013**, *4*, 3282.

국문 초록

새로운 생리활성 저분자 물질을 발굴하는 것은 화학생물학과 신약개발 연구에 있어서 필수불가결한 연구주제이다. 이에 새롭고 다양한 유기저분자 화합물군을 확보하기 위한 합성경로를 개발 연구가 주목 받고 있다. 이러한 연구 흐름에 하나로 독점적 구조 기반의 다양성 추구조합화학 (Privileged substructure-based diversity-oriented synthesis, pDOS)이 개발되었다. 독점적 구조는 하나 이상의 서로 다른 생체고분자에 대해서 높은 결합친화도를 나타내는 단일 구조체를 말한다. 독점적 구조를 기반으로 새로운 중심골격들을 효과적으로 합성할 수 있는 pDOS 전략을 수립하여 독특하고 다양한 화합물군을 합성하였다. 구축한 pDOS 화합물군을 이용하여 다방면의 생리활성 테스트와 검증을 통하여 새로운 생리활성 저분자 물질들이 발굴하였다. 본 연구에서는 pyrimidine이라는 독점적 구조를 기반으로 독특하고 다양한 다중고리골격화합물들을 합성하기 위하여 새로운 pDOS 합성경로를 개발하였으며, 합성한 화합물들을 이용하여 새로운 생리활성 저분자의 발굴 및 특정 생명현상의 변화를 관찰할 수 있는 형광 바이오프로브의 개발을 수행하였다.

Part 1에서는 pyrimidine이 포함된 새로운 다중고리골격화합들의 합성을 위한 새로운 pDOS 합성경로의 개발에 대해 다루고 있다. 알려진 pyrimidine 기반의 생리활성 저분자물질들의 구조적 특성과의 차별화를 위하여 *ortho*-alkynylpyrimidine carbaldehydes 중간체를 고안하여 은촉매 혹은 요오드에 의해 촉진되는 연속고리화반응을 주요 합성전략으로 독특한 5개의 pyrimidine-embedded polyehterocycle을 합성하였다. 5개의 중심골격들은 고리가 퓨전된 위치 및 고리의

크기가 체계적으로 다양화된 형태로써 3 차원적 구조 및 헤테로원자의 배향의 다양성을 지니고 있다.

Part 2 에서는 pyrimidine 이 포함된 새로운 아자트라이사이클의 화합물군을 구축하여 세포내의 지방방울의 변화를 유도하는 새로운 생리활성 저분자물질의 발굴한 연구를 서술하였다. 은촉매하에서의 연속고리화 반응을 통하여 효과적으로 화합물군을 합성하였으며, 극성 비공유결합의 요소를 체계적으로 다양화하였다. 지방방울의 크기 및 양의 변화를 형광이미지를 기반으로 관찰할 수 있는 표현형 기반 스크리닝을 이용하여 지방방울의 감소를 효과적으로 유도하는 새로운 생리활성 저분자 물질을 도출하였다.

Part 3 에서는 새로운 형광골격의 발굴 및 형광바이오 프로브의 디자인에 관련된 연구를 서술하였다. 형광을 나타내는 새로운 중심골격인 pyrazolo[1,5-*a*]pyridine-fused pyrimidine 을 발견하고 이를 Fluoremidine(FD)라 명명하였다. FD 유도체들을 은촉매하에서의 연속고리화 반응을 통하여 합성하였으며, 화합물들의 광물리적 특성을 체계적으로 분석하였다. 그 결과, R^1 과 R^2 위치에 N,N-dimethylamino group 이 형광밝기와 발광파장에 영향을 준다는 것을 밝혀냈다. 또한 R^3 위치의 아세틸화를 통하여 발과파장의 장파장을 유도할 수 있었다. FD 유도체중 하나인 FD13 이 solavtochromism 과 함께 소수성 환경에서 형광밝기가 극적으로 증가되는 현상을 발견하였다. 이러한 특성을 이용하여 세포내 지방방울을 선택적으로 염색하는 실험적 결과를 확인함으로써 지방방울의 시공간적인 변화를 관찰할 수 있는 새로운 형광바이오프로브를 발굴하였다.